Estimation of Biophysical Parameters of Tropical Forest Using Optical and LiDAR Remote Sensing Techniques: A Case Study from Western Ghats of India

Thesis Submitted to the

Cochin University of Science and Technology

in Partial Fulfilment of the Requirements for the Degree of

Doctor of Philosophy

in

Environmental Science

Under the Faculty of Environmental Studies

By

INDU.I

REG. NO. 5054

SCHOOL OF ENVIRONMENTAL STUDIES

COCHIN UNIVERSITY OF SCIENCE AND TECHNOLOGY,

KOCHI-682022, KERALA, INDIA

March 2019

"Estimation of Biophysical Parameters of Tropical Forest Using Optical and LiDAR Remote Sensing Techniques: A Case Study from Western Ghats of India"

Ph.D. thesis in the field of Environmental Science

Author:

Indu I
Research scholar,
School of Environmental Studies,
Cochin University of Science and Technology,
Kochi-682 022, Kerala, India.
email: indupvm@gmail.com

Supervising Guide:

Dr M.V. Harindranathan Nair,
Associate Professor,
School of Environmental Studies,
Cochin University of Science and Technology,
Kochi-682 022, Kerala, India.
email: harinathses@gmail.com

Co Guide:

Dr. R. Jaishanker,
Professor,
C V Raman Laboratory of Ecological Informatics,
Indian Institute of Information Technology & Management – Kerala,
Technopark Campus, Kariavattom (PO),
Thiruvananthapuram-695 581, Kerala, India.
email: jrnair@gmail.com

March 2019

The fire of Knowledge burns all karmas into ashes - Bhagavat Gita

Dedicated to my respected teachers, beloved family and dear friends

Certificate

*This is to certify that this thesis entitled "**Estimation of Biophysical Parameters of Tropical Forest Using Optical and LiDAR Remote Sensing Techniques: A Case Study from Western Ghats of India**" is a bona fide record of research carried out by Mrs. Indu. I, Reg. No: 5054, under our guidance, in partial fulfilment of the requirement of the degree of Doctor of Philosophy in Environmental Science under the Faculty of Environmental Studies, Cochin University of Science and Technology and that no part of this work has previously formed the basis for the award of any degree, diploma, associateship, fellowship or any other similar title or recognition. All the relevant corrections and modification suggested by the audience during the pre-synopsis seminar and recommended by the Doctoral Committee of the candidate has been incorporated in this thesis.*

Dr. M.V Harindranathan Nair,
Associate Professor & Supervising Guide,
School of Environmental Studies,
Cochin University of Science and Technology,
Kochi -22

Dr. R. Jaishanker,
Professor & Co- Guide,
C V Raman Laboratory of Ecological Informatics, Indian Institute of Information Technology & Management – Kerala,
Thiruvananthapuram 695 581

Place: Kochi
March 2019

Declaration

I hereby declare that the thesis entitled "**Estimation of Biophysical Parameters of Tropical Forest Using Optical and LiDAR Remote Sensing Techniques: A Case Study from Western Ghats of India"** is based on the original work done by me under the guidance of Dr. M.V Harindranathan Nair, Associate Professor, School of Environmental Studies, CUSAT and under the co-guidance of Dr. R. Jaishanker, Professor, Indian Institute of Information Technology & Management -Kerala (IIITM-K), Thiruvananthapuram in partial fulfilment of the requirement of the degree of Doctor of Philosophy, under the Faculty of Environmental Studies, Cochin University of Science and Technology and that no part of this work has previously formed the basis for the award of any degree, diploma, associateship, fellowship or any other similar title or recognition.

Kochi-22, **Indu I**
March 2019

Acknowledgement

All acclamation and appreciation are for Bhagavan Narayana who is the creator of the universe and bestowed the human with knowledge and wisdom to search for its secrets. This thesis is the result of the support of some people and organizations whom I believed to be different forms of Bhagavan. Their roles and contributions throughout my research are highly appreciated. This column is dedicated to all of them.

I am expressing my utmost gratitude to my supervising guide Dr. M V Harindranathan Nair, Associate Professor, School of Environmental Studies, Cochin University of Science and Technology (CUSAT), for guiding my work, giving critical and constructive comments and corrections of the manuscripts within a short time. I am indebted to his immense guidance and encouragement, and he is always optimistic about my work which constantly boosts my confidence. I am expressing my sincere thanks to sir, for always there to motivate, support and guide me with great affection and positivity throughout my Ph.D.

My utmost gratitude is extended to my co-guide Dr. Jaishanker. R. Nair, Professor, C V Raman Laboratory of Ecological informatics, Indian Institute of Information Technology and Management-Kerala (IIITMK) for his guidance, valuable suggestions, motivation and a keen interest in my work. I am deeply indebted to him for the positive attitude, the prompt responses, critical comments on the manuscripts and continuous support. I am expressing my sincere thanks to sir, for always there with his valuable guidance and immense support throughout my Ph.D.

I am expressing my sincere gratitude for the guidance, support, encouragement, patience, and blessings of Dr. Rama Rao Nidamanuri, Associate professor, Indian Institute of Space Science and Technology (IIST), Thiruvananthapuram. I cannot thank him enough and will always remember the incredible support all through by spending countless hours on my research and revising my manuscript very patiently and carefully. I am also expressing my gratitude to him, for providing the data sets (Terrestrial Laser Scanned LiDAR data, AVIRIS-NG imagery and the required ground measurements for the study site) for the research.

Sincere thanks to the School of Environmental Studies, Cochin University of Science and Technology, for providing me with facilities for carrying out the research. I am also thankful to Dr. V. Sivanandan Achari, Director, School of Environmental Studies (SES) for the academic support, encouragement and the facilities provided to carry out the research work at the Institute. I express my profound gratitude to Dr. Santhosh K. R., Associate

Professor, Department of Atmospheric Sciences, CUSAT, for his valuable suggestions as a Doctoral Committee member as well as the subject expert. A special thanks to Dr.Rajathy Sivalingam, Associate Professor, for her generosity, kindness, and support showered upon me for the last three years when she was the director by motivating and giving me the insight to finish the research in time. Sincere gratitude to, Dr. E.P. Yesodharan, Dr. Suguna Yesodharan, Dr. M. Anand, Dr. Ammini Joseph and Dr. I S Bright Singh for their encouragement and support during this Ph.D. I express my thanks to Professor V.P.N Nampoori, School of Photonics CUSAT, for rendering the research methodology classes. Sincere thanks to my colleagues Ms. Anjana N. S, Mr. Sajith, Dr. Chitra S V, Mr. Amarnath and to my friends Samitha K A, Chandini P K, Vidhya, Ambily., Vijesh, Rajeswari, Gayatri and Balamurali who are the research scholars at CUSAT. Sincere thanks to all staff members of SES, Librarian of SES, administrative staffs and librarian of CUSAT.

I am expressing my acknowledgment and thanks to Kerala State Council for Science Technology and Environment (KSCSTE) for funding and supporting the research in the form of fellowship. Sincere thanks to Dr. Sarika A R, Scientist, KSCSTE, for all the support.

I acknowledge the facilities provided by Indian Institute of Information Technology and Management Kerala (IIITMK). I am expressing my deep sense of gratitude to Prof. Saji Gopinath, Director, IIITMK, Dr. Saroj Kumar V, Scientific Officer and my colleagues Mr. Sooraj N P, Ms. Athira K, and Mr. Sajeev C Rajan of C V Raman Laboratory of Ecological informatics. Sincere thanks to my friends Aiswarya, Anitha, Vidya Vinodini, Resmi and Aparna, all staff members and librarian of IIITMK. My sincere thanks to Mr. Radhakrishnan T, Assistant Professor, IIITMK for the support.

I acknowledge the facilities provided by the Department of Earth and Space Sciences, Indian Institute of Space Science and Technology (IIST), for providing me with facilities and the data necessary for the research. Sincere thanks to Dr. V K Dadhwal, Director, IIST for giving me all the support. I am deeply indebted to Dr. Ramiya A M, Assistant Professor for her constant support, encouragement. Special thanks to Manohar Kumar, Divya and Aswathy and all other staffs of Department of Earth and Space Sciences, IIST. Special thanks to Dr. Sooraj R and Dr. Vineeth B S, Assistant Professors of Dept of Avionics, IIST for all their support and encouragement.

Special thanks to the United States Geological Survey (USGS) and National Snow and Ice Data Center (NSIDC) for providing the data sets (Landsat ETM+, Sentinel 2, Landsat 8 OLI and GLAS data) for the research. Special thanks to Mr. Greg Deemer and Mr. Sam O' Donnell from NSIDC user services, the University of Colorado for clarifying my doubts regarding GLAS data and by sharing good literature. I am expressing my thanks to

Dr. J B Sharma, Professor, University of North Georgia and Dr. Sagar S Deshpande, Assistant Professor, Ferris State University for their motivation and encouragements. Special thanks to Mr. Ravichandran Kaushika and his wife Mrs. Vijayalakshmy for their friendship and support. Sincere thanks to Dr. A. Sabu, Associate Professor, Kannur University, Dr. Suresh George, Associate Professor, Coventry University, UK and Dr. G.Rajasekhar Assistant Professor, the University of Madras for their support and encouragement. Special thanks to my friends Ujjwal Singh and Irshad for their support.

Special and sincere thanks to two important persons, Mrs. Vijayalakshmy for her warmth, friendship, encouragement, blessings, and hospitality during this Ph.D. and Mrs. Mini Shankar, for always welcoming, motivating, blessing and encouraging me to finish my Ph.D. in time.

Special thanks to Syam lal and Binoop Kumar of Indu photos for the DTP and binding of the thesis in time with perfection and sincerity.

I am expressing my deepest gratitude to my parents, brother, and parents in law for their encouragement, blessings, and support. The utmost affection, prayers and immense blessings of Sasikala, gives great strength to me. Special thanks to my friends Sudeesh M, Madhanan Kumar and Sanish Kumar for their support. Deepest gratitude to my spiritual motivator and dearest friend Suneesh M for his continuous encouragement and motivation.

Finally, I am much obliged to my beloved husband Pradeep V M, who is my dearest friend and my loving son Siddharth P for their great support throughout my life. I would also like to express my heartfelt appreciation for their company, tolerance and a great help during this learning experience. I thank him and my little son for sitting next to me and supporting me, and they sacrificed the most so that I can complete my Ph.D.

Finally, but foremost to Bhagavan Narayana, who is always with me in the form of all the above loving persons to complete the task assigned to me.

Indu I

Abstract

Periodic estimation of biophysical parameters is important for understanding the functioning and productivity status of forest ecosystems. Remote sensing methods using both multispectral and hyperspectral imagery has been traditionally applied for broad-scale characterization of the forest ecosystem. Some of the successful applications of multispectral imagery include identification of forest types, assessment of forest health status, landscape-level biodiversity etc. Given the contemporary demands of governments to make the forest inventory dynamic and at high resolution, reflecting the actual tree species diversity and biomass as part of the carbon sequestration, it is necessary that forest ecosystem is characterized with emphasis on the vertical structure of forest tree stands. Due to the spatial sampling and the operation of sensors in the optical electromagnetic spectrum, multispectral remote sensing data is not a reliable source for characterizing vertical structural attributes of the forest ecosystem. However, multispectral remote sensing technology is very reliable for species discrimination and biophysical characterization of the forest ecosystem. LiDAR (Light Detection and Ranging) is an evolving remote sensing technology which has the capability to provide base data on the vertical structural attributes of landscapes. The discrete LiDAR pulses which can penetrate through the gaps between the canopy can also be helpful in addressing the type and spatial distribution of forest undergrowth. By its virtue, LiDAR remote sensing can reliably offer the ability for the structural characterisation of forest ecosystem. However, discrete LiDAR remote sensing has serious limitations in providing discriminating ability to forest species characterisation and tracking the biophysical attributes which depend on the interaction between optical electromagnetic radiation and various biophysical plant pigment at the leaf level. A comprehensive biophysical and structural characterisation of forest ecosystem, therefore, requires combined usage of optical and LiDAR remote sensing data.

There have been a good number of studies on the combined use of optical and LiDAR point cloud in a typical homogeneous forest ecosystem globally. However, the potential of this combination of optical and LiDAR point cloud for structural, biophysical characterization in a complete forest ecosystem such as

Western Ghats of India has not been addressed. Therefore, this study examines the potential of optical imagery and spaceborne LiDAR point cloud for structural as well as biophysical characterization of two important forest ecosystem in Western Ghats of India.

Common to many remote sensing applications of forest inventory surveys, field measurements of various tree attributes are a time consuming and exhausting work in forestry. Users often require operating multiple instruments at each measurement site for the collection of different types of data. While these exercises are manageable in the case of small scale forestry, it is proved to be expensive and time-consuming for covering large sites of forestry. Terrestrial Laser Scanner (TLS), a LiDAR instrument which is operating on ground-based platform, which can provide 3D LiDAR point cloud, is emerging as a promising tool for acquiring survey quality data on various stand and tree level attributes. This data from TLS, in principle, can be an alternative source for the collection of reference data simultaneously and graphically across large forest landscape. However, there are no algorithm available for the direct interpretation or processing of TLS data for the estimation of tree parameters such as Leaf Area Index (LAI).

The specific objectives of this study are 1) estimation of biophysical parameters across Mudumalai and Sholayar forest by the integration of spaceborne LiDAR data and multispectral imagery 2) 3D tree reconstruction and biophysical parameter estimation in Mudumalai forest using Terrestrial Laser Scanner and development of an algorithm for the direct estimation of LAI from TLS point cloud and 3) estimation of biophysical parameters from AVIRIS hyperspectral data by integration with LiDAR point cloud.

The methodology used in the research includes pre-processing of the optical imagery, both multispectral (Landsat ETM+, Landsat-8 OLI, Sentinel-2) and hyperspectral (AVIRIS-NG), and retrieval of parameters from both spaceborne (ICESat GLAS) and Terrestrial Laser Scanner LiDAR point cloud. From the spaceborne GLAS point cloud, Digital Elevation Model and Digital Surface Model for two regions are derived, thereby obtaining the Canopy Height Model. Various spectral indices and biophysical parameters are obtained by combining the optical multispectral and hyperspectral imagery at the feature

level. Classification and modeling of various structural and biophysical parameters (biomass, canopy height, canopy density, Leaf Area Index, Diameter at breast height) have been successfully done using the combined data. Based on spatial variation and correlation of the geometric attributes from LiDAR point cloud and optical imagery, understory vegetation height is also estimated. The results obtained are validated using field measurements acquired simultaneously and using various statistical metrics. A very strong correlation between estimated and measured biophysical parameters has been observed. The results indicate strong correlation (R^2= 0.98, R^2=0.97) for the canopy height, (R^2= 0.97, and R^2=0.96) for the biomass with the ground measurements of Sholayar and Mudumalai forest region respectively.

Similarly, using the combination of Sentinel-2 and LiDAR point cloud, the strong correlation for biophysical parameters is obtained. Combining hyperspectral imagery with LiDAR point cloud, a strong correlation is obtained on validation with ground measurements. The height of understory vegetation ranging from 1 m to 5 m which is estimated from LiDAR point cloud is comparable with the field estimated height reported in these forests. The proposed algorithm for the direct estimation of LAI seems to offer stable performance when compared with the field measurements values. The key features of the research include the potential to estimate understory vegetation height using spaceborne LiDAR point cloud and the direct estimation of LAI by the newly developed algorithm from TLS LiDAR point cloud data which have not yet been explored. Apart from these, the understory forest ecosystem can be studied using the fused data sets, whereas the height of the understory can also be estimated. The overall study offers prominent application of LiDAR and optical remote sensing including hyperspectral data for effective retrieval of biophysical and structural parameters of the forest ecosystem in Western Ghats of India.

Contents

List of Tables

List of Figures

Abbreviations

3D	Three Dimensional
AVHRR	Advanced Very High Resolution Radiometer
AVIRIS-NG	Airborne Visible and Infrared Imaging Spectrometer-Next Generation
CHM	Canopy Height Model
DBH	Diameter at Breast Height
DEM	Digital Elevation Model
DSM	Digital Surface Model
DVI	Difference Vegetation Index
ENVI	Environment for Visualizing Images
ESA	European Space Agency
EVI	Enhanced Vegetation Index
FAO	Food and Agricultural Organisation
FCC	False Colour Composite
FLAASH	Fast Line-of-sight Atmospheric Analysis of Spectral Hypercubes
FSI	Forest Survey of India
GDVI	Green Difference Vegetation Index
GLAS	Geoscience Laser Altimeter System
GLONASS	Globalnaya Navigazionnaya Sputnikovaya Sistema/Global Navigation Satellite System
GNDVI	Green Normalized Vegetation Index
GPS	Global Positioning System
GRVI	Green Ratio Vegetation Index
GSD	Ground Sampling Distance
GSFC	Goddard Space Flight Centre
ICESat	Ice Cloud and land Elevation Satellite
IDL	Interactive Data Language
IIST	Indian Institute of Space Science and Technology
IMU	Inertial Measurement Unit
ISRO	Indian Space Research Organisation

JPL	Jet Propulsion Laboratory
LAI	Leaf Area Index
Landsat 7 ETM+	Landsat Enhanced Thematic Mapper Plus
Landsat-8 OLI	Landsat Operational Land Imager
LiDAR	Light Detection and Ranging
LVIS	Laser Vegetation Imaging Sensor
MODIS	Moderate Resolution Imaging Spectroradiometer
MSI	Multispectral Instrument
MSI	Moisture Stress Index
NASA	National Aeronautics and Space Administration
NDII	Normalized Difference Infrared Index
NDVI	Normalized Difference Vegetation Index
NDWI	Normalized Difference Water Index
NGAT	NSIDC GLAS Altimetry Elevator Extractor Tool
NSIDC	National Snow and Ice Data Centre
PCL	Point Cloud Library
PSD	Point Spatial Density
QUAC	Quick Atmospheric Correction
RBF	Radial Basis Function
REEVI	Red Edge Enhanced Vegetation Index
RENDVI	Red Edge Normalized Difference Vegetation Index
RERVI	Red Edge Ratio Vegetation Index
RTM	Radiative Transfer Model
RVI	Ratio Vegetation Index
SAVI	Soil Adjusted Vegetation Index
SLICER	Scanning LiDAR Image or Canopies by Echo Recovery
SNAP	Sentinel Application Platform
SPOT	Satellite Pour I'Observation de la Terre
SVM	Support Vector Machine
SWIR	Short Wave Infra-Red
T/P	TOPEX/Poseidon
TLS	Terrestrial Laser Scanner

ToA	Top of Atmospheric Reflectance
USGS	United States Geological Survey
VCCS	Voxel Cloud Connectivity Segmentation
VNIR	Very Near Infra-Red
WGEEP	Western Ghats Ecology Expert Panel
WGS	World Geodetic System

Chapter 1

GENERAL INTRODUCTION

Contents

1.1 Theme Introduction

Forests, the lungs of our planet and the green gold of a country are essential to life on Earth. Forests play a vital role in the environment by releasing oxygen, by locking up the vast amount of carbon, controlling the water cycle, providing sustenance, fuelwood, medicines and maintenance of biodiversity. The epics *Yajurveda*, *Matsya Purana*, and *Varaha Purana*, depicted the significance of forests which composed of the sayings '*one tree is equal to ten sons',* and in *Charaka Samhitha*, it is stated that 'destruction of forests is taken as the destruction of the state.' The word forest has been derived from the Latin word *Floris*, which means outside and the United Nation's Food and Agricultural Organisation (FAO) defined forest as all lands bearing vegetation dominated by trees of any size, exploited or unexploited, capable of producing wood or other forest products. Forests cover about one-third of the land area of the earth, and nearly 50% is tropical forests. In India, the total forest and tree cover is 21.54 %

of the geographical area of the country (India State of Forest Report 2017 -Forest Survey of India). The forest cover has been classified based on the tree canopy density into very dense, moderately dense and open forests. The density class wise proportion of forest is depicted in Figure 1.1. The predominant forest types of India mainly comprise of tropical dry deciduous and tropical moist deciduous and the distribution of forest types across India are tropical moist, tropical dry, subtropical, temperate and subalpine forests (Reddy et al., 2015).

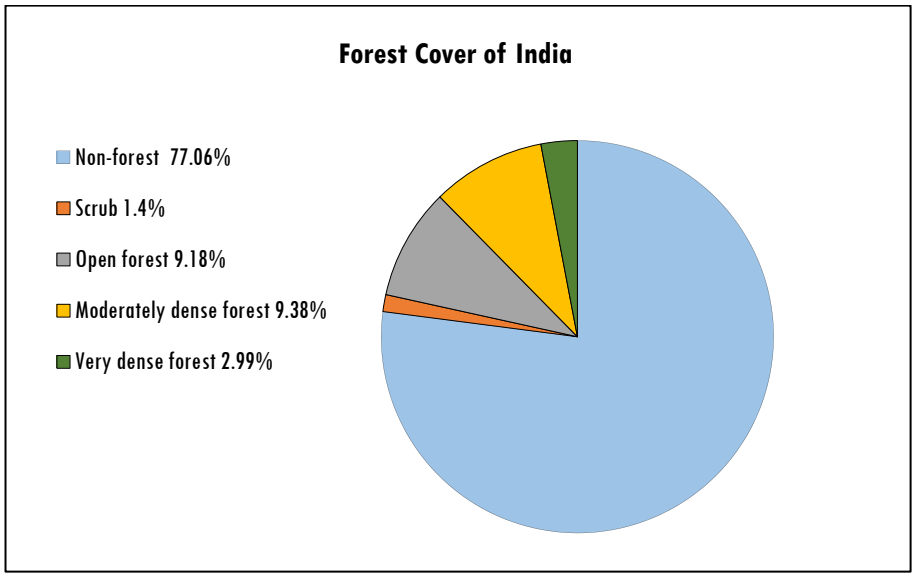

Figure 1.1: Forest cover of India (Source: State of Forest Report 2017 - Forest Survey of India)

Western Ghats of India is one of the unique biological hotspot regions of the world and is an area of high level of biodiversity. The Western Ghats are characterized by a highly complex and heterogeneous forest ecosystem with rich biodiversity. The forest regions include a diversity of ecosystems with a range of woody and nonwoody tree species, stand quality, structural evolution and stand diversity as shown in Figure 1.2. The Western Ghats comprise of tropical wet evergreen forest with tree species like Macaranga peltata, Terminalia paniculata, Knema attenuata, Mesua ferrea, Artocarpus

hirsutus, etc, (Reddy et al., 2015). Forest management practices include the description of condition and dynamics of forests ecosystems described by a set of general characteristics including structural and biophysical parameters (Franklin et al., 1986). Given the well-defined roles of regional governments for dealing with climate change, periodic monitoring of forests and understanding the structural and biophysical parameters are crucial for effective management of forest stocks. The government has been making a lot of efforts and initiatives to mark the ecologically sensitive areas in the Western Ghats (Kasturirangan et al., 2013). However, the actual ecological regions to be labeled as ecologically sensitive depends upon the existence of the functional forest stands and associated ecological system from horizontal and vertical spatial perspectives. Assessment of this horizontal, as well as vertical perspective of a range of forest ecosystem at the stand level, requires spatially continuous data discriminating the stand and the biophysical attributes of trees at medium to high spatial resolution.

Figure 1.2: Western Ghats' forests with thick canopy and understory

Biophysical parameters are direct indicators of the quality, composition and are necessary for monitoring of the forest ecosystem. Widely studied forest structural attributes are grouped under forest stand elements like foliage, canopy cover, tree diameter, tree height, stand biomass, tree species, overstory vegetation, foliage density, Diameter at Breast Height (DBH), height of overstory, biomass, standing volume, shrub cover, total understory cover, etc, (McElhinny et al., 2005). The structural features of the forest stand are useful for describing the forest ecosystem complexity. The quantification, mapping, monitoring and the estimation of forest parameters are now vital issues due to the importance of forest conservation, and also because the biomass is a renewable energy source in many countries of the world. The estimation of forest parameters is a challenging task, especially in areas with complex stands and varying environmental conditions and hence requires accurate and consistent measurement methods. In order to conserve the forest resources and for utilizing the resources effectively, it is essential to have detailed knowledge of its distribution, abundance, and quality. Estimation of biophysical parameters plays a significant role in forest management and practices. Ecological function and carbon storage capacity of forests are significantly related to biophysical parameters. Spatio-temporal assessment of biophysical parameters gives the possibility of understanding the spatial, temporal and climatological aspects of the forest ecosystem.

1.2 Need for Remote Sensing Methods

Estimation of biophysical parameters over large forest areas by traditional methods is relatively tedious, expensive and is often marred by inaccessibility in mountainous terrains. Various ground-based instruments used for the estimation of parameters include calipers, diameter tapes, biltimore sticks, hypsometer, etc. However, they are limited by spatial

coverage, speed, time lag, and availability of skilled manpower for data interpretation. Traditional methods lead to non-probabilistic surveys and yield unrepresentative and biased samples. Therefore, it is necessary to have an effective and accurate method for biophysical parameters' estimation. Also, in India, there is a lack of national spatial databases including variations of forest cover and natural resources at regular intervals (Roy et al., 1996). With the advent of improved measurement capabilities and technologies, particularly remote sensing, there is potential to improve the forest parameter estimation, which can overcome the limitations of traditional in situ and aerial measurements. The use of remote sensing tools as an alternative to ground surveys ensure the possibility of sustainable of forest management practices.

Aerial photography is the oldest form of remote sensing frequently used for assessment of forests (Gillies and Leckie 1996), but is limited by film properties, and also is expensive, time-consuming and inconsistent. Remote sensing can overcome jurisdictional and physical impediments in the large area monitoring from the ground and can provide a synoptic perspective over large forest areas as well as frequent revisits can ensure the monitoring of temporal and spatial changes (Peterson et al., 1999). Also, remote sensing technology can offer a multi-layered data archive that can be utilized based on the information needs of the users. Enhanced resolutions enable the users to extract more spatial, spectral and temporal attributes of forests. Remote sensing is a powerful tool for acquiring information related to logging, mining and extracting the amount of degradation using specific algorithms by the integration of various sensors (Pithon et al., 2013). The remote sensing has the potential to provide cost-effective estimates of biomass compared to the labor-intensive, costly and time-consuming traditional techniques (Timothy et al., 2016).

1.3 Applications of Multispectral and Hyperspectral Remote Sensing Data

Remote sensing technology has a high potential for exploring the forest details. Multispectral remote sensing has been explored extensively for biophysical characterization of forests across various sites (Chen et al., 1996; Wudler, 1998; Cohen and Goward, 2004) and has been extensively used for measuring the horizontal structure, spatial distribution of forest canopies, stress, forest community delineation and to a limited extent, biomass (Reese et al., 2002; Lillesand et al., 2014; Roberts et al., 2007; Dube and Mutanga, 2015; Karlson et al., 2015; Gao et al., 2016). Examples of various multispectral imagery (Landsat, Sentinel) over different regions of the Western Ghats forests are given in Figure 1.3.

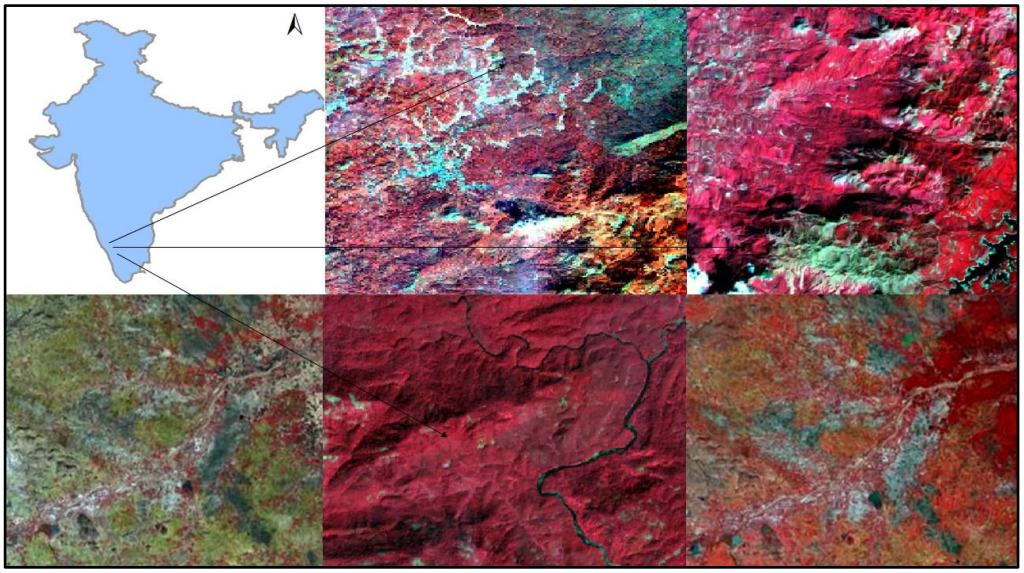

Figure 1.3: Multispectral imagery: Landsat-8 OLI, IRS LISS III, Sentinel-2, Landsat ETM+ over different regions of the Western Ghats forests, India.

Several studies show that multispectral remote sensing data can be used to

obtain some biophysical attributes at local to global scales (Wang et al., 2005; Dube and Mutanga 2015; Cohen et al., 2001). Most of these operational products use data from coarse resolution satellite sensors such as MODIS, AVHRR, SPOT-Vegetation, etc., which provide standard products available at various scales on a daily, weekly or monthly basis.

1.4 Limitations of Multispectral Data

Global biophysical products from multispectral data, which are very useful in understanding the forest ecosystem and climate parameters at national to global scale, are very limited in explaining the forest composition, spatial complexity, biophysical condition at a scale which enables operational management of forest ecosystem. Owing to this, there has been a renewed interest in the use of moderate resolution multispectral data for forest biophysical characterization taking the benefit of the evolving complementary active remote sensors. The forest biophysical parameters which are mainly driven by the physical or chemical composition of forest species can be retrieved relatively successfully from moderate resolution multispectral data. However, the biophysical parameters which are influenced by the vertical structure of the stands cannot be successfully retrieved from some multispectral data. Saturation of multispectral vegetation indices for a higher value of LAI is widely reported (Waring et al., 1995; Carlson and Ripley, 1997; Turner et al., 1999). Biophysical parameters such as biomass and canopy density are highly influenced by the vertical structure of forests stands.

Multispectral data are sensitive to the composition of spatial distribution and leaf level electromagnetic radiation of plants, and hence estimation of biophysical parameters, which are indications of plants' vertical structure cannot be estimated directly with multispectral data at the required

spatial scale (Lefsky et al., 1998; Foody et al., 2001; Hudak et al., 2012). Understory vegetation forms an integral part of land covers in a complex forest ecosystem such as the Western Ghats. A range of plant species valuable to maintain forest soil ecology, and species which are detrimental to the forest and soil ecology, constitute the forest undergrowth. On the one hand, several plant species which include economically valuable medicinal plants and other edible herbs are widely distributed across the Western Ghats' forest regions. On the other hand, a substantial portion of forest undergrowth is now occupied by invasive plant species causing enormous environmental and ecological damage in the Western Ghats forest regions. Information on the spatial distribution and species composition of the forest undergrowth, despite complementary for understanding the quality of forest ecosystem, has not been addressed using multispectral remote sensing. This can be attributed to the lack of penetration ability of optical signal through thick canopies. In general, multispectral remote sensing over the forest ecosystem emphasizes only overgrowth in the forest ecosystem as the optical signals cannot penetrate through complex and thick canopies of trees. The spatial aggregation of reflectance spectra in image pixels are weighted spatial aggregates of materials present within the instant field of view of the sensor is also a drawback.

1.5 Potential of LiDAR Point Cloud

The evolution of active remote sensing technology, LiDAR apart from high-resolution microwave remote sensing, has paved the way for theoretical possibility of direct estimation of the vertical structure of forests ecosystem. LiDAR is the acronym for Light Detection and Ranging. LiDAR mainly works under the principle similar to electronic distance measuring instruments, working on the principle of laser ranging in which a continuous or discrete laser pulse fired from a transmitter is reflected and is captured by a receiver.

The distance between the transmitter and the reflector (natural objects) is taken as the time taken for the laser pulse to travel (Bachman 1979, Young 1986). A LiDAR instrument consists of the laser scanner (high energy and directional optical pulses) coupled with a receiver and scanning system with specialized Global Positioning System (GPS) receivers and an integrated system of differential GPS and, inertial measurement units which generate position and orientation. The scanning patterns of the LiDAR systems can be zigzag, parallel or elliptical. The most important platforms for the LiDAR measurements are terrestrial, aerial and satellites. The incident laser pulses interact with the earth features and are reflected, which are received by the receiver unit. The time of travel gives the distance of the object from the instrument and thereby obtaining the coordinates of the object. Figure 1.4 shows the working principle of LiDAR.

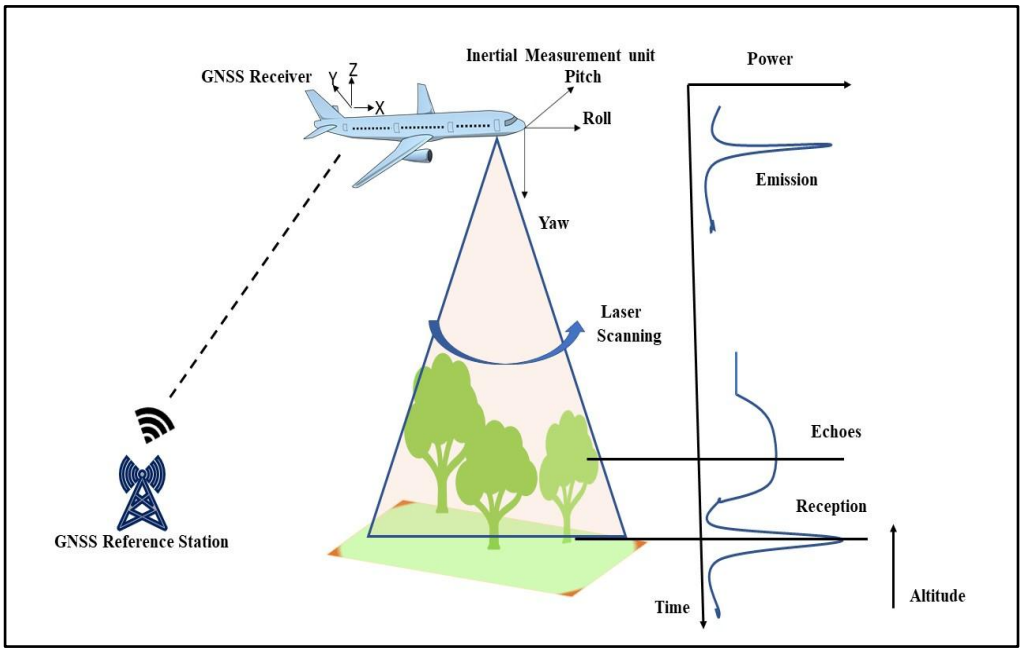

Figure 1.4: Working principle of LiDAR

Multiple returns of LiDAR pulses are shown in Figure 1.5. When the laser pulse hits the target trees, the first return is the most significant return, and in this case, the coordinates of the top of the tree are considered. The height of the tree can be calculated by capturing the first and last returns. In the cases of the thick canopy, last return may not be from the ground.

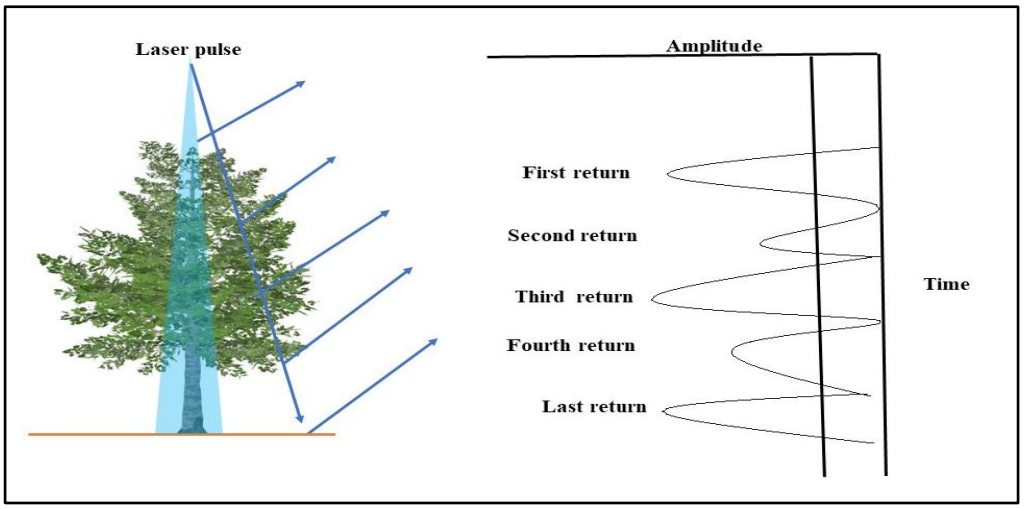

Figure 1.5: Example of multiple returns from a tree

LiDAR remote sensing is a very promising technology for direct estimation of structural parameters of forests. Unlike optical remote sensing, LiDAR can penetrate through the plant canopy and thus enable the study of undergrowth vegetation of the forest ecosystem. Various forest structural parameters - canopy height, canopy volume, diameter, and even stand level measurements can be estimated using LiDAR remote sensing data. LiDAR data is generally called discrete points, and the data is often termed as a point cloud. Several studies have been reported on the estimation of the structural parameters of forests using airborne and space-borne LiDAR point cloud. Lefsky (2002a) has addressed the direct retrieval of forest structural characteristics using airborne LiDAR point cloud. LiDAR point cloud can be

used for the identification of forest structural variables (Zimble et al., 2003; Anderson et al., 2005) and crown diameter (Dean et al., 2002). Various forest landscape parameters such as tree height (Eggleston 2001; Mc Combs et al., 2003; Popescu and Wynne 2004), average stand height (Naesset 1997a; Young et al., 2000; Andersen et al., 2005), canopy cover, timber volume estimates (Naesset 1997b, Means et al., 2000; Parker and Evans 2004), forest inventory, forest structural characteristics and forest visualisation (Fujisaki et al., 2003; Mitchell 2004; Fujisaki 2005) have been successfully retrieved using LiDAR point cloud.

1.6 Need for the Integration of LiDAR Point Cloud and Optical Imagery

Despite its promising results in estimating structural and stand level parameters of forest species, LiDAR point cloud is devoid of spectral information which is complementary and crucial for understanding the biophysical spectral characteristics of plant species. Recent developments in the approaches of remote sensing for forest ecosystem studies suggest integrated analysis of multispectral and LiDAR data to effectively estimate the structural and biophysical parameters at a spatial scale commensurate with the spatial complexity of the forest ecosystem. These studies report successful results, but they are found to be site specific and are not appropriate in a complex forest ecosystem like that of Western Ghats. Despite very successful in integrating LiDAR point cloud and multispectral data for biophysical characterization, most of the existing studies are done in the local forests which are of pine, dry deciduous in nature and tropical in nature towards higher latitudes.

Several studies report the potential of integration of optical remote sensing and LiDAR data for an improved level of accuracy (Ghassemian et al., 2016; Hajj et al., 2017). By combining airborne LiDAR and Landsat imagery, aboveground biomass was accurately estimated in forest and woody ecosystem (Wu et al., 2016). Small footprint LiDAR point cloud combined with multispectral data has also been used for estimating plot level volume and biomass in deciduous and pine forests (Popescu et al., 2004). These studies report accurate results, but they are found to be site specific and not appropriate in complex forest ecosystems such as Mudumalai and Sholayar forest regions of Western Ghats of India. Further, the studies which have fused LiDAR point cloud and multispectral data for the estimation of biophysical measurements have been done for forests which are of pine, dry deciduous.

The forest composition and the structural characteristics of a highly productive yet a global biodiversity hotspot, Western Ghats of India are complex by species composition, terrain nature, and human interaction and influence. The nature of forest ecosystem in the Mudumalai and Sholayar regions of the Western Ghats of India is characterized by a large number of woody species, nonwoody species, shrubs, and plantations. Stand-level estimation of the structural and biophysical parameters is obligatory in the case of such forest regions. Estimation of the structural and biophysical parameters at a stand level for Western Ghats regions of India has not been reported yet. The potential of integrating multispectral data with space-borne LiDAR point cloud for estimating biophysical parameters in the Western Ghats regions of India has not been explored yet. Further, there are no studies which report on the possibility of height estimation of understory vegetation using LiDAR point cloud remote sensing data.

The presence and impact of many exotic plants like Lantana Camera, elephant browse plants and other grass species on understory vegetation is evident in the Western Ghats region of India. The exotic plants have a significant impact on the growth of the different species of flora and fauna which may even stop the tree regeneration. Lantana is found to be abundant in areas with higher light availability at ground levels. These plants may significantly affect the plant species assemblage as well as tree community. Understory herbaceous plants thus prove to play an important part in the biodiversity of Western Ghats. By estimating the growth of the plants such as Lantana, forest managers can identify high-risk zones that should be monitored intensively.

This study explores the potential of LiDAR point cloud in estimating the height of understory vegetation, which will help to understand the nature of the species growing in these forests.

1.7 Role of Ground Truth Measurements for Forest-Traditional Ways

Generally, a lot of extensive field measurements are required for monitoring the forest ecosystem and estimating the multiple forest parameters including height, DBH, basal area, Leaf Area Index (LAI), and canopy cover. Usually, large scale monitoring of forests requires extensive time and spatial extent. In the case of a large tropical forest area, each sample is characterized by a variety of tall, medium and small tree species along with thick understory vegetation. Depending upon the parameters of measurements, several instruments must be operated simultaneously to capture different parameters at the sites (Figure 1.6).

Figure 1.6: Requirement of multiple instruments for ground truth measurements (Source: Google)

In addition to time, logistical complexity and accessibilities, the operation of multiple field equipment is a complicated job for acquiring in situ forest canopy properties. For example, measurement of LAI using non-harvesting litter traps and destructive sampling is time-consuming and labor-intensive when the study area is large. Leaf area measurement tools such as hemispherical photography, plant canopy analyzer, LAI -2000 plant canopy analyzer, Accupar Ceptometer, can measure leaf properties with high speed and ease but are limited by factors such as woody -to -total area ratio, leaf clumping and illumination conditions. Remote sensing technologies have attempted measurements of the spatial distribution of LAI using the spectral responses from both aerial and satellite sensors. Landsat-8 OLI and Landsat-7 ETM + are compared for estimating LAI by Radiative Transfer Models (RTM) and spectral indices based models in which the RTM proved to have higher accuracy (Masemola et al., 2016; Quan et al., 2017). Fine resolution hyperspectral imagery has also been used to retrieve LAI (Richter et al., 2008;

Darvishzadeh et al., 2011). However, these methods are limited by factors such as sensor characteristics, atmospheric constraints, overlapping and clumping of leaves related to inclination and azimuth. In addition, most of the existing methods are based on empirical relations between vegetation indices such as NDVI and parameters of interest. However, the vegetation indices values saturate after the accumulation of a certain amount of biomass in the case of the dense canopy environments (Huete et al., 1997; Mutanga & Skidmore, 2004). Other cases which use allometric relations, where the LAI is estimated based on DBH and height, are also limited by the saturation effects of indices. As a result, biomass estimates based on the spectral indices and estimation of LAI is often erroneous (Weiss et al., 2004; Lu, 2006)

1.8 Potential of using Terrestrial Laser Scanner for acquiring Ground Truth Data

An instrument or approach which can provide high-quality field data estimates on multiple forest sites and tree stands is highly useful for acquiring a vast amount of field measurements across length and breadth of tropical forests. Here comes the role of the high-resolution terrestrial laser scanner, which has the potential to acquire a response from individual tree components to plot level, capturing the spatial and geometrical distributions of leaves, branches, and trees over several hundreds of square meters of forest area. Therefore, an approach which can model tree and plot parameters which form part of field measurements will have the potential to replace the use of traditional equipment for in situ measurements and enhance the speed of acquiring in situ measurements. Terrestrial Laser Scanner (TLS) is an active remote sensing technology that offers a potential solution for estimating various tree parameters by rapidly extracting extremely dense three-

dimensional structural data of forests. TLS scans an object by emitting laser pulses and recording the subsequent intensity of the return signals which is reflected (Figure 1.7).

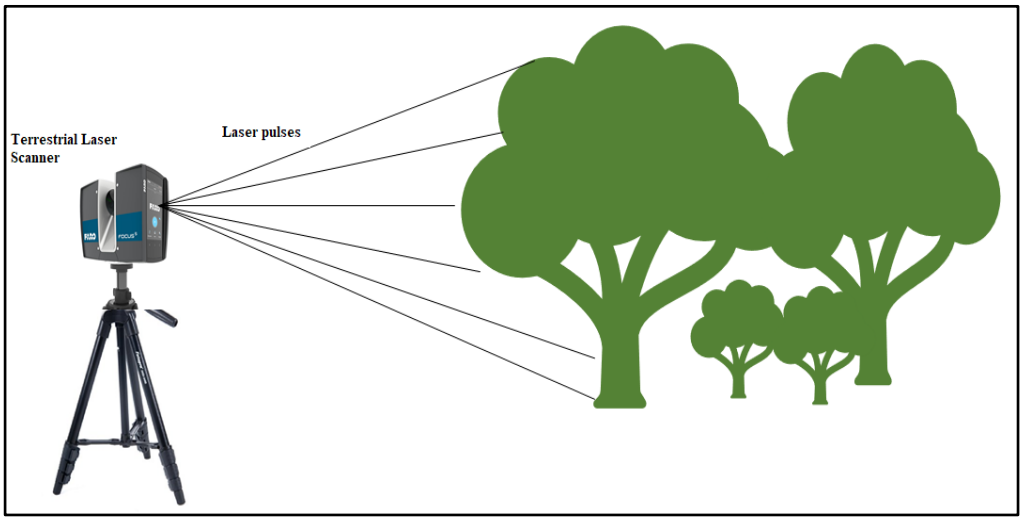

Figure 1.7: Working principle of Terrestrial Laser Scanner

The dense leaf point cloud from TLS extracts the tree properties even at leaf level. The structural properties of leaves are obtained from the multi-viewpoint cloud of leaves. TLS provides point cloud which contains almost all returns recorded from leaves enabling the retrieval of leaf-spatial properties. High-resolution TLS point cloud has the potential to acquire responses from individual leaf to plot level, thereby capturing the spatial and geometrical distribution of leaves, branches, and trees over several hundreds of square meters area. TLS can model tree and plot parameters, which form part of field measurements and have the potential to replace the use of traditional equipment for acquiring in situ measurements and enable rapid acquisition of in situ measurements. For long term sustainable forest management and in understanding multifunctional forest dynamics, accurate estimates of forest structural parameters are critical. In the case of dense and complex forest

ecosystems, the variability, and diversity in the distribution of trees are predominant. Discrimination and delineation of individual trees is a challenge in the heterogeneous forests since multi-layered canopies have the crowns connected and immensely clumped. Detailed structural information such as height, Diameter at Breast Height(DBH), crown measurements of individual trees and crown width play critical roles in obtaining and validating biomass, carbon budget, and biogeochemical cycles, which are essential for sustainable forest management and practices.

Three-dimensional reconstruction of trees is significant in forest management for representing the complexity of the physical structure of trees, tree architecture, topological relationship between tree entities, geometry, and spatial display. The automatic 3D modeling of tree structures and branches is an indispensable technology for effective forest structural measurements including height, diameter, width, area, biomass, volume and to visualize the trees in virtual 3D space (Omasa et al., 2008; Bournez et al., 2017). Capturing real world trees for 3D reconstruction is an interesting and challenging task due to the geometrical complexity of the leaves and branches. In forestry, tree geometry is crucial for taking harvesting decisions and yield estimations. Instead of taking direct measurements of the trees, the 3D model of a tree can give geometric measurements accurately, quickly and automatically (Rosell et al., 2009; Huang et al., 2011; Cote et al., 2011).

In this study, an attempt has been made to develop an approach using TLS point cloud for three-dimensional modeling and reconstruction of trees and proposes an algorithm for direct estimation of LAI, intended to use as a substitute for manual field data measurements in the modeling of forest stand parameters. The thesis presents a method for direct estimation of the LAI from the reconstructed individual trees in the chosen tropical forest. The algorithm

introduced provides an approach for estimating LAI using point spacing, the height of the tree and the point density. The estimated LAI, when compared with the ground measurements offers a good correlation validating the applicability of the proposed algorithmic approach for LAI estimation in tropical forests which are characterized by thick understory and a complex heterogeneous environment. The novelty of this approach is the introduction of point spatial density algorithm for the estimation of LAI from reconstructed individual trees. Individual trees are reconstructed based on segmentation algorithms implemented from point cloud library so that three-dimensional modeling of the trees with high precision can be successfully achieved. The individual tree crown points along with the trunk points can be extracted by implementing segmentation approaches which explicitly model each tree in the forest.

1.9 Significance of the Study

The integration of satellite multispectral remote sensing data with LiDAR point cloud provides opportunities to capitalize upon the unique characteristics of both passive and active remote sensing systems. To reduce the cost limitations currently associated with large-area acquisitions of LiDAR point cloud, recent studies have suggested on the integration of LiDAR point cloud with optical remotely sensed data for estimating canopy structure (Hudak et al., 2002; Hu et al., 2016). Limited research has been conducted to combine LiDAR point cloud with other optical remote sensing data to estimate LiDAR-derived forest structure using non-parametric machine learning algorithms. Support Vector Machine (SVM) models can achieve better performance than multiple regression for estimating canopy height and above-ground biomass. This study aims at addressing this important methodology

aspect for estimation of forest parameters using the medium to coarse resolution space-borne LiDAR and multispectral data.

For acquiring extensive in situ forest canopy properties in the large area forest ecosystem, several instruments need to be operated at the same time, which is a strenuous job. An instrument or approach which can provide field data quality estimates on multiple forests site and tree measurements simultaneously is highly helpful in acquiring a vast amount of field measurement data across the length and breadth of the study area. High-resolution TLS point cloud has the potential to acquire a response from individual leaf to plot level thereby capturing the spatial, and geometrical distribution of leaves, branches, and trees over several hundreds of square meters area in a single scan. TLS can model, tree and plot parameters which form part of field measurements and have the potential to replace the use of traditional equipment for in situ measurements and speed of the in situ measurements. In this study, an attempt has been made to develop an approach using TLS data for three-dimensional modeling and reconstruction of trees and an algorithm for direct estimation of LAI intended to use as a substitute for field data measurements in the modeling of forest stand parameters.

The estimation of the biophysical parameters by integration of LiDAR point cloud with high resolution airborne hyperspectral imagery AVIRIS-NG narrow band features can offer enhanced spectral information on integration with LiDAR point cloud.

1.10 Objectives of the Work

The work attempts to estimate biophysical parameters using optical and LiDAR point cloud in Mudumalai and Sholayar reserve forests of Western Ghats of India. The main objectives of the research are summarized below

I. Estimation of biophysical parameters by the integration of spaceborne LiDAR point cloud and multispectral imagery.

   The work relevant to this objective is organized as being composed of the activities involving: -

   a) pre-processing of spaceborne LiDAR data and multispectral data,
   b) development of the canopy height models from the spaceborne LiDAR point cloud,
   c) delineation of structural parameters from LiDAR point cloud,
   d) integration of the data sets from active and passive sensors, and
   e) extraction of biophysical parameters from the integrated data sets.

II. 3D tree reconstruction and biophysical parameter estimation in Mudumalai forest using Terrestrial Laser Scanner (TLS).

   The work relevant to this objective is organized as being composed of the activities involving: -

   a) pre-processing of the TLS point cloud,
   b) segmentation based three-dimensional reconstruction of trees,
   c) extraction of structural metrics from the reconstructed trees,
   d) estimation of LAI by multivariate regression of structural metrics,

e) estimation of LAI by proposing a new algorithm called Point Spatial Density (PSD) algorithm.

III. Estimation of biophysical parameters from AVIRIS-NG hyperspectral data by integration with LiDAR point cloud.The work relevant to this objective is organized as being composed of the activities involving: -

a) pre-processing of the AVIRIS-NG imagery,

b) integration with LiDAR data sets,

c) extraction of biophysical parameters from the integrated data sets,

1.11 Salient Features of the Work

- Attempted estimation of the height of understory vegetation with LiDAR point cloud in heterogeneous forests.
- The integration of spaceborne LiDAR with multispectral imagery which enhances the accuracy of forest structural and biophysical characterizations.
- Proposed a new algorithm named Point Spatial Density algorithm (PSD) for the direct estimation of LAI from TLS point cloud.
- Three-dimensional reconstruction of individual trees using terrestrial laser scanned data.
- Biophysical characterization using hyperspectral imagery in the tropical forests and integration with LiDAR for parts of Western Ghats.

1.12 Organisation of the Thesis

The thesis is organized into six chapters

Chapter 1 General Introduction

Chapter 2 Literature Review

Chapter 3 Study Area and the Materials Used

Chapter 4 Methodology

4.1 Estimation of biophysical parameters by the integration of spaceborne LiDAR point cloud and multispectral imagery.

4.2 The biophysical parameter estimation in Mudumalai forest region using Terrestrial Laser Scanner. (TLS).

4.2.1 Three-dimensional reconstruction of trees and the estimation of LAI from structural metrics using segmentation of Terrestrial Laser scanner point cloud.

4.2.2 Direct estimation of LAI of tropical forests using Terrestrial Laser Scanner LiDAR point cloud.

4.3 Estimation of biophysical parameters from AVIRIS-NG hyperspectral data by integration with GLAS LiDAR point cloud.

Chapter 5 Results and Discussion

Chapter 6 Summary and Conclusion

*****

Chapter 2

LITERATURE REVIEW

Contents

Estimation of forest structural attributes is important in planning regional to national level forest management practices and is useful in providing a baseline database for modeling global climate change and ecosystem dynamics. Numerous approaches and data sources have been used to estimate biophysical parameters. In this chapter, earlier studies related to the estimation of biophysical parameters by the traditional methods, multispectral and hyperspectral remote sensing, and their limitations are described. Use of spaceborne and terrestrial LiDAR in forestry, as well as applications of multispectral and hyperspectral imagery, are also detailed. This chapter elucidates different methods of conventional forest mensuration along with the advantages and limitations of conventional techniques. The limitations of the conventional techniques lead to the development of most advanced technologies including photogrammetry, remote sensing, LiDAR, etc. The integration of the advanced technologies along with conventional field measurements can be used for the accurate and effective measurement of the forest parameters. The limitations of optical remote sensing in the estimation of forest structural parameters lead to the application of LiDAR in forest

mensuration. The need for the active remote sensing along with the integration of LiDAR with remote sensing imagery is well demonstrated in this review.

2.1Introduction

Biophysical parameters play an important role in determining characteristics, classification as well as the condition of the forest resources, which can lead to effective forest management based on forest ecology. Acquisition of accurate biophysical parameters is crucial for forest inventory studies, habitat analysis and biophysical modeling in the forest research. The quantification, mapping, monitoring, and estimation of forest parameters are central issues in forest conservation. Biomass is a renewable energy source in many countries. The estimation of forest parameters is a challenging task, especially in areas with complex stands and varying environmental conditions which require accurate and consistent measurement methods. For conserving forest resources and utilizing them effectively, it is vital to have detailed knowledge of its spatial distribution, abundance, and quality.

A description of the application of optical remote sensing and its limitations for extracting structural attributes is included in the following sections. The application of LiDAR point cloud compared with optical imagery for biophysical-structural attributes as well as the need for integration of optical and LiDAR point cloud is also described. The literature also focuses on the need for the terrestrial laser scanner in the case of ground measurements and its application for estimating biophysical parameters in heterogeneous forests such as the Western Ghats.

2.2 Traditional Methods for Biophysical Parameters' Estimation

The measurements of trees and forests coverage, in general, are essential for the effective utilization of forest resources as well in

understanding the development and growth of the forests. Several traditional methods are used for estimating forest parameters such as canopy height, diameter, biomass and canopy cover. For measuring canopy heights, laser range finder, clinometer, measuring tape, pole, simple distance prism, etc. are usually used (Clark & Clark, 2001; Chave, 2005; Larjavaara and Muller-Landau, 2013). These methods require skilled, motivated and experienced human resource for measurements (Goodwin, 2004). Traditional methods of forest parameter estimation are effective in case of limited forest area, but cannot be applied in large scale forest inventory which requires a periodic update of forest data. They are too expensive, time-consuming and cannot cover the entire and remote forests.

For measuring the diameter, instruments like dendrometer (Yoda et al., 2000), tree calipers, tape, biltmore stick, and relaskop are usually used in the field but the main concerns are based on the accuracy, economy, and efficiency (Rhody, 1975). However, when the results are validated, it is indicated that there are statistically significant variations in other related parameters including tree volume (Binot et al., 1995; Parker and Matney 1999). Forest characteristics and measurement distance play a key role in remote diameter measurement accuracy (Weaver et al., 2015). By using cross-sectional photogrammetric and densitometric methods, canopy profiles can be estimated (Maclean and Martin, 1984). The limitations of conventional methods of forest mensuration and the need for proper integration of traditional measurement methods with current technologies are well reviewed by Van Laar & Akca, 2007. In some studies, field methods for sampling tree heights for tropical forest biomass by testing different strategies of sampling trees' top produce locally derived models (Sullivan et al., 2018). Growing stock variation in pure coniferous forest types of Garhwal Himalaya of

Uttarakhand using growing stock estimation method provides valuable information about stand biomass and carbon flux (Dimri et al., 2014). Biomass can be estimated by means of direct methods which involve harvesting of all the tree components and measurements of the weight of trees (Singh et al., 1975, Bonham, 1989; Brummer et al., 1994; Nelson et al., 1999; Hashimotio et al., 2000; Lodhiyal and Lodhiyal, 2003; Ravindranath and Ostwald, 2008; Devi and Yadava, 2009; Vashum and Jayakumar, 2012). But this method is time-consuming, destructive and costly. Biomass estimation can also be done by non-destructive methods using allometric equations (Brown et al., 1997; Hughes et al., 1999; Aboal et al., 2005). This method is species specific and is not generalizable.

2.3 Remote Sensing Technology for the Biophysical Parameters' Estimation

Estimation of large area biophysical parameters by traditional methods including ground-based methods is relatively tedious. Field-based inventory is limited by the inassessibility in large remote areas and the extreme demand of time as well as cost. In the case of forestry, strategic and operational planning is required for obtaining information on forest resources and management practices. Traditional forest inventories which can extend only to some limited spatial coverage are designed to obtain information associated with timber harvesting and restricted only to few locations (White et al., 2016). However, the accuracy and consistency of the measurements and interpretations along with the high cost of the traditional field inventories are a common challenge (Tomppo et al., 2010). In order to characterise the quality and quantity of forests including stand structure, productivity, and composition of the forest ecosystem, consistent and enhanced information is vital for developing and

improving the management strategies related to biodiversity, forest health and biophysical parameter estimations (Listopad et al., 2015; Alam et al., 2014; White et al., 2016). The role of remote sensing technologies is significantly increasing in the case of forest inventories and practices since they can provide enhanced information directly or indirectly as well as collecting forest resource information with high spatial accuracy which can enable tactical, strategic and operational forest planning and management (Brosofske et al., 2014; White et al., 2016). Figure 2.1 illustrates multispectral and hyperspectral sensors along with the imagery of each sensor.

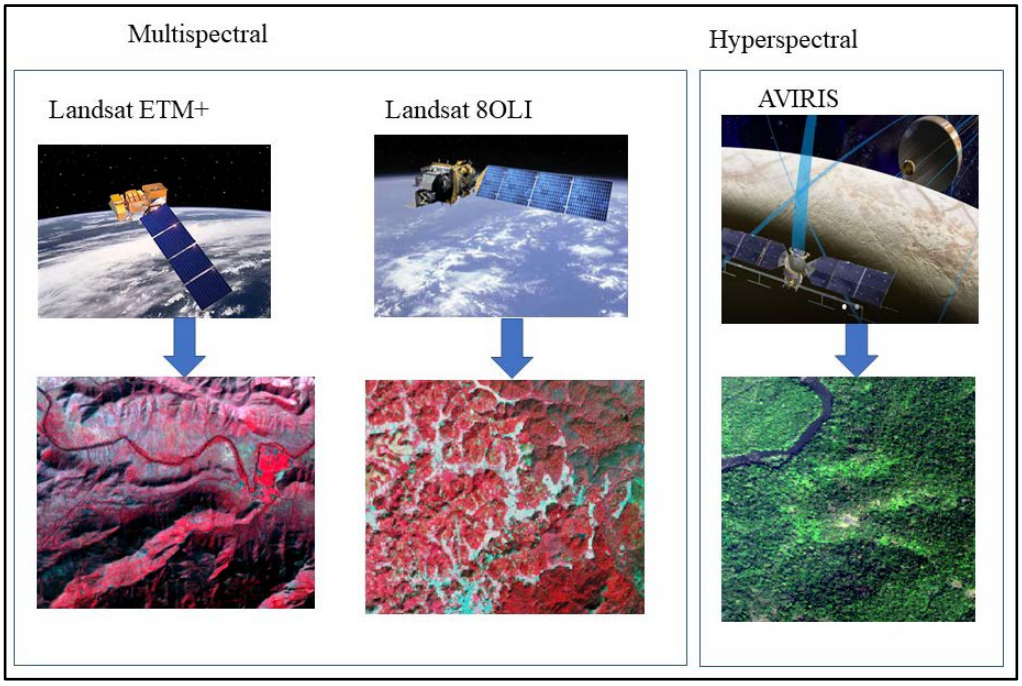

Figure 2.1: Multispectral and Hyperspectral Remote Sensing (Images of sensors credit: NASA)

Role of optical remote sensing including both multispectral as well as hyperspectral imagery in various studies for the estimation of biophysical parameters is elucidated in the following sections.

2.3.1 Role of Multispectral Imagery

Multispectral remote sensing has been explored extensively for biophysical characterization of forests across various sites (Chen et al., 1996; Wulder 1998; Cohen and Goward, 2004). Moderate-resolution multispectral remote sensing data such as Landsat ETM+, Landsat-8 OLI has been widely used for measuring the horizontal structure and distribution of forest canopies, stress, forest community delineation and to a limited extent biomass (Reese et al., 2002; Roberts et al., 2007; Lillesand et al., 2014; Dube and Mutanga 2015; Karlson et al., 2015; Gao et al., 2016). Several studies show that multispectral remote sensing data can be used to obtain some biophysical attributes at local to global scales. Landsat imagery has been widely used in assessing forest health, forest phenology, estimating Net Primary Productivity (NPP), timber volume, etc. (Cohen et al., 2001; Dymond et al., 2002; Hansen et al., 2002). High-resolution multispectral sensors like Quickbird, Ikonos, and SPOT-5 allow detailed spatial-geometrical analysis of forest parameters (Wang et al., 2004; Kosaka et al., 2005). For example, forest health assessment using spectral and textural information extracted from SPOT-5 satellite images (Meng et al., 2016) has been well reported. Most of the operational products use data from coarse resolution satellite sensors such as MODIS, AVHRR, SPOT- Vegetation which provide standard products available at various scales on a daily, weekly or monthly basis. For example, MODIS/ Terra MCD15A2H version 6 MODIS provides Leaf Area Index, MYD13A1 MODIS provides vegetation indices on a pixel basis. Even though these global biophysical products are very useful in understanding forest ecosystem and climate influences, they are very limited in explaining the forest composition, spatial complexity, biophysical condition at a scale which corresponds to local to sub-regional level management of forest ecosystem, especially when the

landscape complexity is very heterogeneous. Owing to this, there has been a renewed interest in the use of moderate to high-resolution multispectral data for forest biophysical characterization and taking the benefit of the evolving complementary active remote sensors.

2.3.2 Role of Hyperspectral Imagery

Hyperspectral data has the potential to improve the applicability of optical remote sensing in complex forest ecosystems and identification of individual tree species along with fine spectral and spatial details (Goetz and Landauer, 1979; Tong et al., 2014). Several studies have reported the application of hyperspectral imagery in forestry (Martin et al., 1998; Zarco et al., 1999; Townsend et al., 2003; Clark et al., 2005; Anderson et al., 2008; Belgiu and Drăguț, 2016). Narrow-band spectral indices which are sensitive to both chlorophyll content and canopy structure are useful in understanding whether the forests are healthy or stressed, forest decline, and for modelling forest nitrogen content, and leaf development (Rock et al., 1988; Miller et al., 1991; Sampson et al., 2003; Zhang et al., 2008; Wang et al., 2018). Hyperspectral remote sensing sensors record spectral reflectance in very narrow spectral bands typically 200 or more bands at a bandwidth better than 10 nm thus obtaining contiguous reflectance bands for every pixel in the scene (Govender et al., 2007).

Hyperspectral remote sensing successfully generates species level maps with high spatial heterogeneity and species diversity with tree species identification. However, their application in heterogeneous forests such as the Western Ghats is limited since they fail to discriminate structural parameters of different tree species. The forest region is characterized by a large number of trees with different species, age and a high degree of structural

heterogeneity. In the Western Ghats region, more comprehensive information regarding the structural discrimination of species as well as spectral parameters is needed for identifying tree species. Ability to discriminate understory vegetation species from overstory clumped groups with varying tree heights, crown widths, multiple treetops and different degrees of canopy overlaps are difficult using hyperspectral imagery in these types of the forest ecosystem. Vertical canopy profile of trees is very important for assessing the structural characteristics of individual trees of the forest ecosystem.

2.4 Role of LiDAR Point Cloud for Understanding Vegetation Height

Understory vegetation forms an important part of land covers in a complex forest ecosystem such as the Western Ghats. A range of plant communities – grasses, bushes, shrubs, scrubs forms the forest undergrowth. On the one hand, several plant species which form the undergrowth include economically valuable medicinal plants, and other edible herbs are widely distributed across the Western Ghats' forest regions. On the other hand, a substantial portion of forest undergrowth is now occupied by invasive plant species causing substantial environmental and ecological damage in these forest regions. Information on the spatial distribution and species composition of the forest undergrowth, despite complementary for understanding the quality of forest ecosystem, has not been addressed using multispectral remote sensing. This can be attributed to the lack of penetration ability of optical signal through thick canopies. In general, multispectral and hyperspectral remote sensing over forest ecosystem emphasize only the overgrowth, as the optical signals cannot penetrate through elaborate and thick canopies of trees and also because multispectral image pixels are weighted spatial aggregates of

materials present within the instant field of view of the sensor. Thanks to the inherent canopy penetration ability of LiDAR remote sensing, it is in principle possible to study the spatial distribution and structural attributes of forest undergrowth. This, in turn, estimates the presence and impact of many invasive understory vegetation species. In the case of the highly complex biodiverse heterogeneous forests of Western Ghats, GLAS data is yet to be utilized. The novelty of this study is the application of the large footprint spaceborne waveform LiDAR data in the complex environment of Western Ghats' forest ecosystem. Availability of GLAS ICESat data without any cost increases the future applicability of this approach.

While the forest biophysical parameters, which are mainly driven by the physical or chemical composition of forest species can be relatively successfully retrieved from moderate resolution multispectral data, the biophysical parameters influenced by the vertical structure of the stands, cannot be retrieved from some multispectral data, particularly parameters such as biomass, canopy density, etc. Multispectral data is sensitive to the composition of spatial distribution and leaf level electromagnetic radiation of plants, estimation of biophysical parameters which are an indication of plants' vertical structure cannot be estimated with multispectral data at the required spatial scale and accuracy.

The evolution of active remote sensing technology LiDAR has paved the way for estimation of the vertical structure of forests ecosystem, which is very promising in the direct estimation of structural parameters with the three-dimensional structure of forests. Unlike optical remote sensing systems, LiDAR pulses have the ability to penetrate through gaps in tree canopy and interact with soil, and under tree surface covers thus enabling the study of undergrowth vegetation of the forest ecosystem.

Direct estimation of forest structural parameters including canopy heights, canopy volume, diameter, and even stand level measurements can be estimated using LiDAR remote sensing data. Several studies have been done based on the estimation of the structural parameters of forests using LiDAR point cloud. LiDAR point cloud can be used for the identification of forest structural variable by the direct retrieval of LiDAR structural characteristics including crown diameter, canopy height, DBH, etc (Zimble et al., 2003; Andersen et al., 2005; Dean et al., 2002). LiDAR point cloud can also help to develop three-dimensional structure of forest and estimation of tree height, canopy cover, crown width, canopy density, etc (Eggleston, 2001; McCombs et al., 2003; Andersen et al., 2005, Means et al. 2000; Fujisaki et al., 2003) can be accurately done.

2.4.1 Types of LiDAR

For forestry applications, based on the type of information collected from laser returns, LiDAR sensors can be categorized into the discrete return and continuous, or waveform LiDAR. LiDAR sensors again can also be categorized based on the size of the footprint of pulses or the sampling patterns (Dubayah and Drake, 2000; Lefsky et al., 2002a; Lim et al., 2003). The sampling method of a three-dimensional structure of forests by laser systems are of two types, vertical sampling which depends on the number of range samples recorded and horizontal sampling which depends on the number and area of footprints.

Discrete return LiDAR with small footprints (10-30 cm) which represents the surface objects as discrete points, have various applications in forestry (Lim et al., 2003; Naesset et al., 2004; Wulder et al., 2008; Evans et al., 2009; Latifi et al., 2012; Maltoma and Packalen, 2014). In the case of

discrete return LiDAR, most commonly 3-5 returns are possible and record the pulses as separate returns with dense distribution (Flood and Gutelis, 1997; Wehr and Lohr, 1999; Baltsavias, 1999; Lefsky et al., 2002a). Most of the discrete return LiDAR systems are capable of estimating biophysical parameters with high accuracy (Naesset et al., 2004; Goodwin et al., 2006; Hopkinson and Chasmer, 2007; Magnusson et al., 2007; Orka, 2011). The discrete return LiDAR does not provide full details of trees' vertical distribution. However, the full waveform system records the entire return signal as a continuous waveform, thereby giving complete information on canopy structure. Common waveform LiDAR systems are Scanning LiDAR Image or Canopies by Echo Recovery (SLICER), Laser Vegetation Imaging Sensor (LVIS) (Blair et al., 1999), and Geoscience Laser Altimetry System (GLAS) (Shcutz et al., 2005). Full waveform LiDAR system records the entire backscattered optical intensity at regular intervals (Pirotti et al., 2014). Due to large footprint (varying from 8 m to 70 m), the point cloud covers large areas and thus canopy structure modeling is more efficient (Harding et al., 1994; Means et al., 2000; Lefsky et al., 1999; Dubayah et al., 2000; Harding et al., 2001; Parker et al., 2001).

2.4.2 Airborne LiDAR and Spaceborne LiDAR

Airborne discrete return LiDAR systems are found to be capable of predicting the forest canopy height and structural parameters with high accuracy (Harding and Carabajal, 2005; Popescu and Zhao, 2008). Airborne and spaceborne LiDAR systems are illustrated in Figure 2.2.

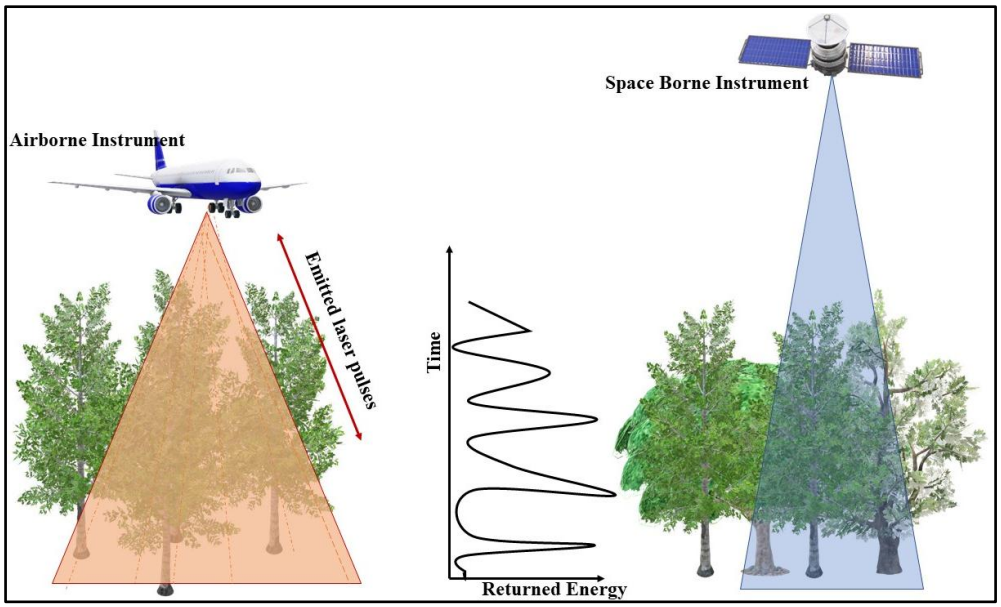

Figure 2.2: Airborne LiDAR and Spaceborne LiDAR systems

Despite being very successful in forests' three-dimensional structural measurements, applications of airborne LiDAR systems are limited to some extent because of the high cost of acquisition, limited spatial coverage and lack of processing expertise (Renslow et al., 2000; Wulder et al., 2003; 2008; McInerney et al., 2010). Airborne discrete LiDAR is found to segment overstory trees with 87% accuracy and understory trees with 67% (Hamraz and Contreras, 2017). The processing time of the voluminous data is also found to be very high and is suitable only for a small and localized area (Duncason et al., 2010).

In many cases, airborne LiDAR systems are discrete and are not capable of providing a better vertical representation of canopies. Several studies have addressed these limitations (Harding et al., 2001; Lovell et al., 2003). It is found from earlier studies that most of the LiDAR systems can retrieve only the local and regional scale of vegetation height measurements. To overcome the limitations of cost as well as spatial coverage of the discrete return data, freely available satellite-based LiDAR point cloud with global coverage can contribute a significant role. The large footprint full waveform

LiDAR system is capable of recording canopy and subcanopy. Whereas in the case of discrete returns LiDAR systems, only a portion of the canopy is recorded. Full waveform LiDAR systems with large footprint can provide subcanopy details including height with good accuracy and reduced bias (Naesset, 1997a). In some cases, airborne full waveform LiDAR has been used for three-dimensional segmentation and classification of single trees with an overall classification accuracy of about 95% (Reitberger et al., 2009). Airborne full waveform LiDAR gives better representations of the forestry compared to discrete return LiDAR, but systematic errors occurs based on the accuracy of IMU/GPS systems, wind strength, etc. (Park et al., 2014).

Geoscience Laser Altimeter System (GLAS) is the first spaceborne LiDAR on board the Ice Cloud and Land Elevation Satellite (ICESat) mission, launched on January 13, 2003. It can digitize the backscattered waveform. GLAS is the first polar orbiting sensor which combines high precision surface LiDAR with a sensitive dual wavelength cloud and aerosol LiDAR (Wang & Dessler, 2006). The operation of the ICESat GLAS is shown in Figure 2.3.

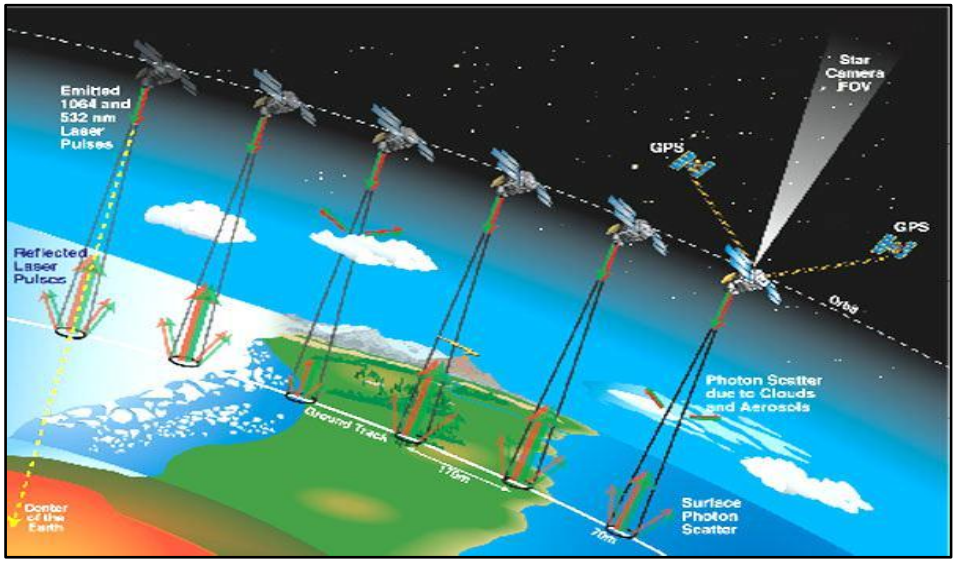

Figure 2.3: ICESat in orbit sending down its laser pulse earthward (Image credit: NASA)

GLAS offers global coverage by carrying three lasers orbiting at 600 km and transmits short pulses of infrared (1064 nm) and visible green (532 nm) light at a rate of 40 Hz (Zwally et al., 2002). The diameter of the GLAS footprint is 70 m with 172 m spacing. GLAS point cloud is found to have horizontal and vertical accuracies of 3.7 m and 10 cm respectively (Bae & Schutz, 2002; Abshire et al., 2005). ICESat provides 15 GLAS datasets intended for different applications. Even though GLAS was originally designed to measure the changes in polar ice, it can be used to measure forest canopy heights and biomass (Schutz et al., 2005). Several studies have addressed the applications of GLAS point cloud (Chauve et al., 2008; Reitberger et al., 2008; Rowe, 2013).

ICESat/GLAS is capable of measuring the 3D information of forest at a global scale (Sun et al., 2004; Chen, 2010; Lefsky, 2010; Mahoney et al., 2016). GLAS can provide an accurate estimation of forest height and biomass as well as quantify the forest growth rate (Lefsky et al., 2002b; Rosette et al., 2008; Sun et al., 2008; Chi et al., 2017; Hajj et al., 2017; Liu et al., 2017). The study of global forest height using satellite laser altimetry data and the combined use of other remote sensing data has received increased attention nowadays (Yu et al., 2015; Wang et al., 2016). GLAS point cloud has been used successfully for estimating the surface elevation with high accuracy and that also helps to generate vegetation height models and biomass estimates (Lefsky et al., 2005; Schutz et al., 2005; Wang et al., 2011; Luo et al., 2013; Baghdadi et al., 2014). GLAS point cloud can accurately estimate canopy height as well as the forest structural properties (Lefsky et al., 2007; Bourdreau et al., 2008; Chen 2010; Saatchi et al., 2011; Hayashi et al., 2013; Tao et al., 2016). Hayashi et al., 2013, developed an approach for measuring

the forest canopy height using GLAS point cloud integrated with other LiDAR point cloud. GLAS LiDAR point cloud is freely assessable and globally available. GLAS point cloud can provide good prediction even for high biomass values and can be used to produce global canopy height maps (Lefsky 2010, Simrad et al., 2011; Peterson and Nelson 2014).

However, it is clear from the literature that most of the applications of GLAS data in forests regions have been made where the nature of forests is pine, deciduous or plantation types and was found to be site specific. The nature of forests in the Western Ghats is highly heterogeneous, characterized by a large number of woody, nonwoody species, shrubs, small plantations along with significant understory vegetation and is depicted in Figure 2.4.

Figure 2.4: Difference between the heterogeneous forests of the Western Ghats and other homogenous (Source: Google) forests

2.5 Need for the Integration Approach

Despite its promising results in estimating structural and stand level parameters of forest species, LiDAR point cloud is devoid of spectral information which is crucial for discriminating and assessing the spectral biophysical characteristics of plant species. Recent developments in the approaches of remote sensing of forest ecosystem studies suggest integrated analysis of multispectral and LiDAR point cloud so as to effectively estimate structural and biophysical parameters at a spatial scale commensurate with the spatial complexity of forest ecosystem. Several studies indicate the potential of the integration of optical remote sensing and LiDAR point cloud for improved accuracy in tree species discrimination (Ghassemian, 2016). By combining airborne LiDAR point cloud and Landsat imagery, aboveground biomass has been accurately estimated in woody forest ecosystem (Wu et al., 2016). The application of LiDAR point cloud can be combined with optical imagery to produce data products which can further be used for deriving various parameters in forest ecosystem (Liu et al., 2016). Small footprint LiDAR point cloud combined with multispectral data has been used for estimating the plot level volume and biomass in deciduous and pine forests (Popescu et al., 2004). These studies report successful results, but they are found to be site specific and are not appropriate in complex mixed forest ecosystems such as Mudumalai and Sholayar forest regions of Western Ghats of India. Moreover, many of the existing studies have been done in forest ecosystems which are mainly of pine, dry deciduous in nature.

The forest composition and structural characteristics of highly productive and biologically diverse ecological systems of Western Ghats of India are entirely different. The nature of the forest ecosystem in the

Mudumalai and Sholayar forest regions of Western Ghats of India is often characterized by a large number of woody species, non-woody species, shrubs, plantations, etc. Stand-level estimation of structural and biophysical parameters has often been demanded for climate and carbon monitoring activities of governments. There has been no study performed on the integrated analysis of multispectral data with spaceborne LiDAR for estimating the biophysical parameters and structural parameters in the Western Ghats regions of India.

Extensive spatial distribution of many exotic plants like Lantana Camera, elephant browse plants and other grass species as understory vegetation in the Western Ghats region of India has been reported (Ramaswami and Sukumar, 2011; Prasad, 2010; Hiremath and Sundaram, 2013). There are no earlier studies which have mapped the distribution or estimating the height profile of understory vegetation. Exotic plants have a significant impact on the growth of different species of flora and fauna which may stop tree regeneration. Lantana is found to be abundant in areas with higher light availability at ground levels. These plants may significantly affect the changes in the plant species assemblage as well as tree community. Understory herbaceous plants thus prove to play an important part in the biodiversity of Western Ghats. Understanding the growth of the plants such as Lantana, forest managers can identify high-risk zones that should be monitored intensively. This thesis has explored the potential of LiDAR point cloud for estimating the height of understory vegetation thereby indicating the nature of the species growing in these forests.

2.6 Need for Terrestrial LiDAR Point Cloud for Biophysical Parameter Estimation

Usually, national/regional level monitoring of forest requires in situ measurements, often called forest mensuration with extensive spatial coverage at multiple time intervals. In the case of large tropical forests, each forest sampling site is characterized by a variety of medium, tall and small tree species along with thick understory vegetation. Generally, a lot of field measurements are required for monitoring the forest ecosystem and estimating multiple forest parameters such as height, DBH, basal area, LAI, canopy cover, etc. Depending upon the parameters of interest, several instruments must be operated simultaneously at each measurement sites. In addition to time, logistical complexity and accessibilities, the operation of various field equipment is a complicating job for acquiring in situ forest canopy properties. An instrument or approach which can provide high quality field data on multiple forest sites and tree measurements are highly useful in the case of tropical forests (Figure 2.5). Here comes the role of high-resolution Terrestrial Laser Scanner (TLS), which has the potential to acquire a response from individual leaf to plot level capturing the spatial and geometrical distributions of leaves, branches, and trees over several hundreds of square meter area. Therefore, an approach which can model tree and plot parameters which form part of field measurements will have the potential to replace the use of traditional equipment for in-situ measurements and speed of the in-situ measurements. In this study, an attempt has been made to develop an approach for 3D modeling and reconstruction of trees as well as proposing an algorithm for direct estimation of LAI intended to use as a substitute for measured field data in the modeling of forest stand parameters.

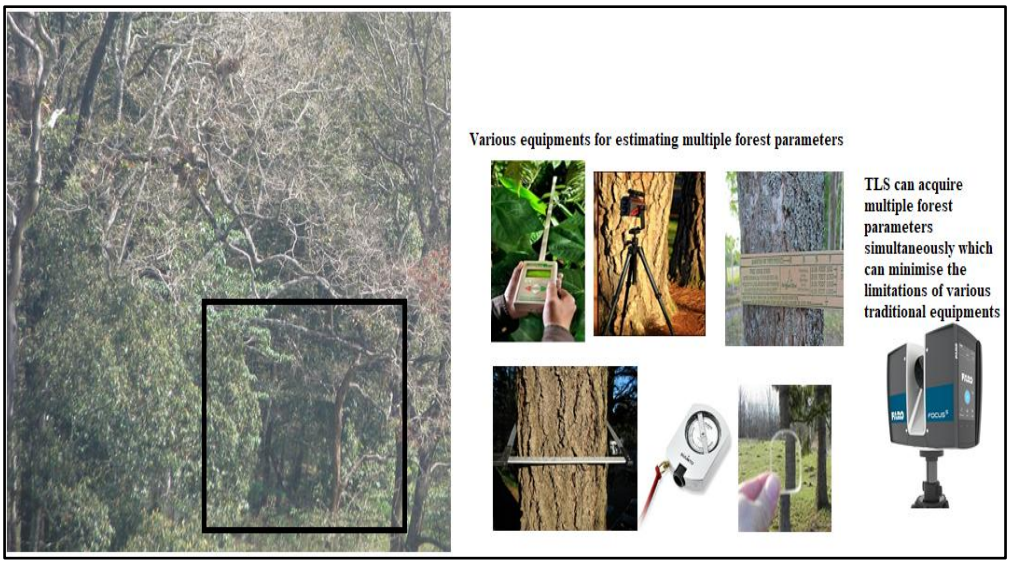

Figure 2.5: Application of TLS compared to the usage of other equipment (Equipment Images Source: Google)

Leaf Area Index (LAI) is one of the most important structural parameters to model many physical processes such as canopy photosynthesis, transpiration, carbon cycle, and nutrient cycle. It is defined as the total one-sided area of photosynthetic tissue per unit ground surface area (Watson, 1947; Lang, 1991; Chen and Black, 1992). LAI greatly varies with species and canopy structure and, the change in the LAI affects the stand productivity. It is a crucial parameter which characterizes the canopy-atmosphere interface and process-based ecosystem simulation models. Thus, periodic, accurate and effective measurement of LAI is crucial for forest managers, ecologists and global forest carbon modelers (Boegh et al., 2002; Luo et al., 2013).

The traditional method of LAI estimation by regression of tree height and DBH often leads to substantial overestimation or underestimation. Several studies have attempted retrieving LAI using TLS point cloud (Leblanc, 2002; Danson et al., 2014; Jupp et al., 2009). In some cases, LAI is estimated based on a 3D approach which needs direct manipulation of large point cloud

(Hosoi et al., 2006; Takeda et al., 2008; Antonarakis et al., 2010). The 3D point cloud is transformed into 2D raster for the estimation of LAI in several other cases (Danson et al., 2007; Zheng et al., 2013). There are specific approaches in which LAI estimates are based on voxel size in which accuracy may be affected (Clawges et al., 2007; Zheng and Moskal, 2012; Cifuentes et al., 2014; Liu et al., 2016), whereas in some instances, the sampling resolution is assumed to be constant for mitigating the accuracy problem (Hosoi and Osama, 2006; Seidel et al., 2012). The sampling resolution changes with the scanning distance. Other methods for estimating LAI include point quadrant analysis and algorithmic approaches like morphological transforms, local surface fitting algorithm and 3D convex hull algorithms (Wilson, 1965; Dornbusch et al., 2007; Raumouan et al., 2013; Olsoy et al., 2014). However, these approaches cannot reconstruct the trees and isolate them in detail along with branches and also the removal of noise effects including the occlusion effects is a challenge.

Terrestrial Laser Scanner, an active remote sensing technology offers a potential solution for estimating LAI by rapidly extracting extremely dense three- dimensional structural data of trees in a forest environment. The dense leaf level point cloud from TLS extracts the tree properties and leaves thereby providing leaf structural properties. The structural properties of leaves are obtained from the multi-viewpoint cloud of leaves. TLS provides point cloud which contains returns recorded from leaves enabling the retrieval of their leaf spatial -geometrical properties.

2.7 Chapter Conclusion

Past studies led to the perception that there is an urgent need for incorporating *state de art* technologies and techniques in forest studies like the integration of LiDAR and optical imagery, particularly in the case of heterogeneous forests as seen in the Western Ghats. The applications and the limitations of LiDAR and optical remote sensing data mentioned in the review indicate that the integrated approach can enhance information content for structural, biophysical characterization. The importance of terrestrial LiDAR point cloud as an alternative for field instruments for forest mensuration in the heterogeneous forest is also detailed in the review.

*****

Chapter 3

STUDY AREA AND MATERIALS USED

Contents

In order to fulfill the identified research objectives, two different protected reserved tropical forest regions of Western Ghats are considered as the study sites. This chapter gives a detailed description of the study sites- Mudumalai and Sholayar in the protected tropical forests in the Western Ghats of India. The data sets used for the study for each objective are also described. The software used for processing is also briefly explained.

3.1 Study Area

3.1.1 Western Ghats of India

The predominant forest types in India are tropical forests, of these, tropical dry deciduous and tropical moist deciduous are the most common types. The area selected for this study are the tropical forests in the Western Ghats. The Western Ghats extends from Tapti valley in north India to Kanyakumari in South India, and extends to a width of 210 km in Tamilnadu and narrows 48 km in Maharashtra. Western Ghats (Figure 3.1) lies between 8° 19’ 8” — 21° 16' 14” N and 72°56’24” — 78°19’40” E and is approximately 1,440 km long (WGEEP, 2011) and covers an area of 129037 square km. The average elevation is around 900 m, and the highest mountain peak is Anamudi (2695 m).

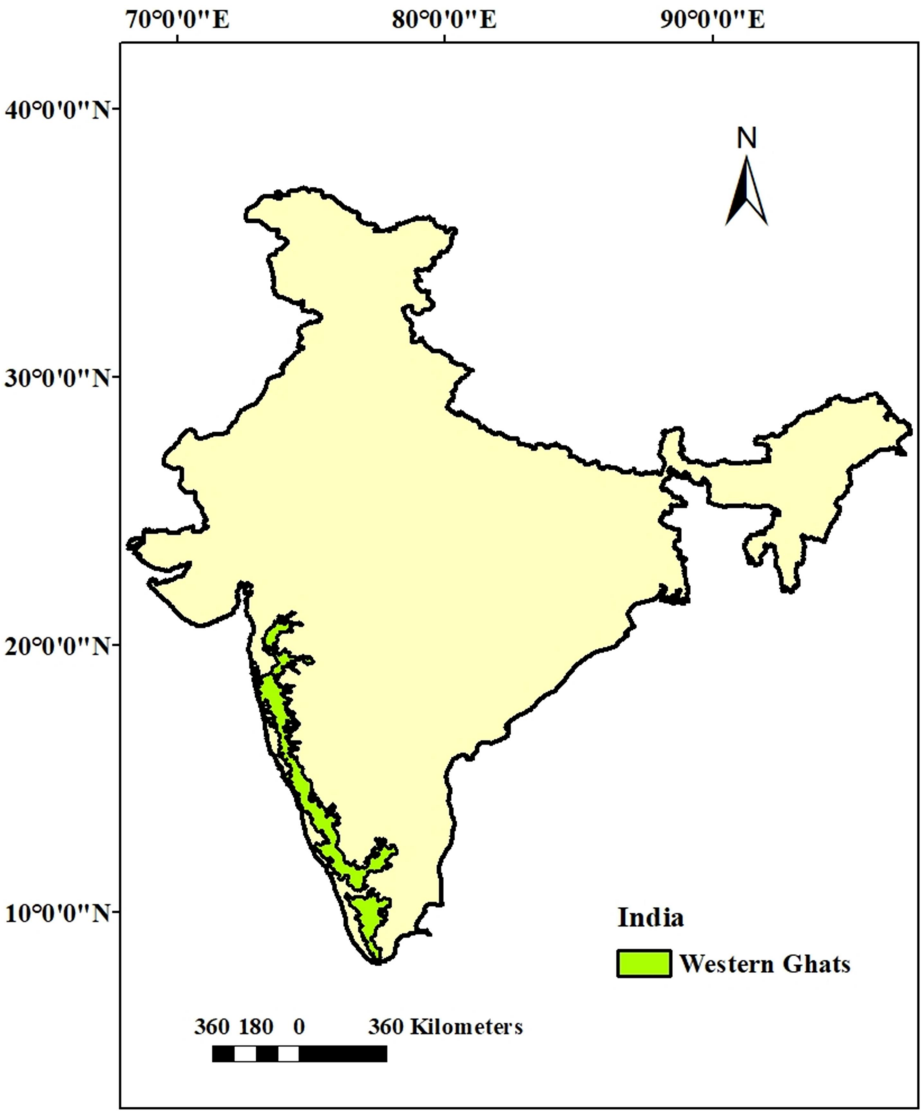

Figure 3.1: Location of Western Ghats

The Western Ghats are well known for the rich and unique assemblage of flora and fauna. Western Ghats region is one of the 25 global hotspots of biodiversity and one of the three mega centers of endemism in India. Western Ghats are known as Sahyadri in northern Maharashtra and Sahyaparvatam in Kerala. The Western Ghats include a diversity of ecosystems, biologically rich and biogeographically unique. The major forest types range from tropical

wet evergreen to montane grasslands and include numerous medicinal plants, important genetic resources such as wild varieties of fruits, grains, and spices. The Western Ghats also include unique shola ecosystem and savannas including peat bogs and Myristica swamps. The Ghats are home to about four thousand species of flowering plants, exotic varieties of plants. The climate in the Western Ghats is humid and tropical with an average annual temperature of 15 °C (59 °F). Annual rainfall ranges from 3000-4000 mm (Chandran et al., 2001).

The Western Ghats consist of four tropical and subtropical moist broadleaf forest ecoregions. Northern Western Ghats are dry at lower elevations and includes deciduous forests mainly Teak, at higher elevations, the northern Western Ghats are colder and wetter. Southern Western Ghats extend through the states of Kerala and Tamilnadu and comprise of wide varieties of flora and fauna, high level of endemism and about 15 percent is under protected area network. In higher elevation region, unique habitat types including wet evergreen forests and sholas are found. The Western Ghats are home to thousands of animal species including a variety of threatened species.

Understory vegetation forms an integral part of land covers in Western Ghats. A range of plant species valuable to maintain forest soil ecology, and some species which are detrimental to the forest and soil ecology, form the forest undergrowth. On the one hand, several plant species which include economically valuable medicinal plants and other edible herbs are widely distributed across the Western Ghats forest regions. On the other hand, a substantial portion of forest undergrowth is now occupied by invasive plant species causing substantial environmental and ecological damage in the Western Ghats forest regions. In order to encompass the range of diversity in the Western Ghats landscape, coverage of overstory and understory, two

different sites are selected which represents typical gradients in the terrain and general composition of overstory and understory of the forest ecosystem. The study site location consists of two different protected forest regions of the Western Ghats, namely Sholayar (368 km^2), and Mudumalai (411 km^2).

3.1.2 Mudumalai Reserve Forest

One of the study areas selected is Mudumalai forest in Tamilnadu state. Tamilnadu, the southernmost state of India, with an area 1,30,058 sq.km, shares the Western Ghats with the states of Kerala, Karnataka, Goa, Maharashtra, and Gujarat. Out of the 16 forest types in India (Champion and Seth,1968), Tamilnadu contains a maximum of 9 types ranging from wet evergreen forests to moist deciduous, dry deciduous, sholas, grasslands and scrub forest. Mudumalai forests located in between 11°43'37.17"N, 76°27'44.19"E and 11°22'56.03"N, 76°33'38.01"E covering an area of 411 square km is selected as one of the study areas, which lies in Niligiri district of Tamilnadu, about 150 km north west of Coimbatore city in Tamilnadu (Figure 3.2). The study area shares the boundary with Karnataka and Kerala states. The tropical semi-evergreen forest is seen in Mudumalai forest as per the forest report of Tamilnadu state, and the top canopy consists of Artocarpus, Dalbergia latifolia, Hopea parviflora, etc. The understorey vegetation consists of species of Actinoldaphne, Aglaia, Bischofia javanica, Drypetes, Symplocos, and the shrub species are mainly Glycosmis, Ixora, Lasianthus, Leea indica, Memecylon, Pavetta, Butea parviflora, Cynanchum tunicatum, Entada pursaetha, and other common species are Calycopteris floribunda, Dioscorea, Strychnos, Bambusa arundinacea and Ochlandra travancorica, etc. (Sukumar et al., 1992). Riparian vegetation is also found along the banks of rivers and streams in plains, where alluvial soil is deposited. The trees may be evergreen or deciduous depending on the region, and the characteristic species include

Azadirachta indica, Tamaridus indica, Albizia amara, Albizia lebbeck, Acacia ferruginia, Terminalia chebula, Gyrocarpus americanus, Morinda tinctoria, Ficus benghalensis, Semecarpus anacardium, Terminalia arjuna, Typha angustata, and Vitex leucoxylon. Tropical moist deciduous forests are also reported in Mudumalai region and the trees reach a height which ranges from 3 to 30 m. The most common trees are Bombax ceiba, Dillenia pentagyna, Mitragyna parviflora, Tectona grandis, Terminalia., Vitex, and Ziziphus xylopyrus. Cycas circinalis is occasional. Helicteres isora, Lantana camara, Aculeata, and Ziziphus oenoplia are common shrubs. The common climber is Ipomea, and the natural grass is Imperata cylindrica (Sukumar et al., 2004; Suresh et al., 1996; 2010). The annual rainfall varies from 700 mm to 1700 mm.

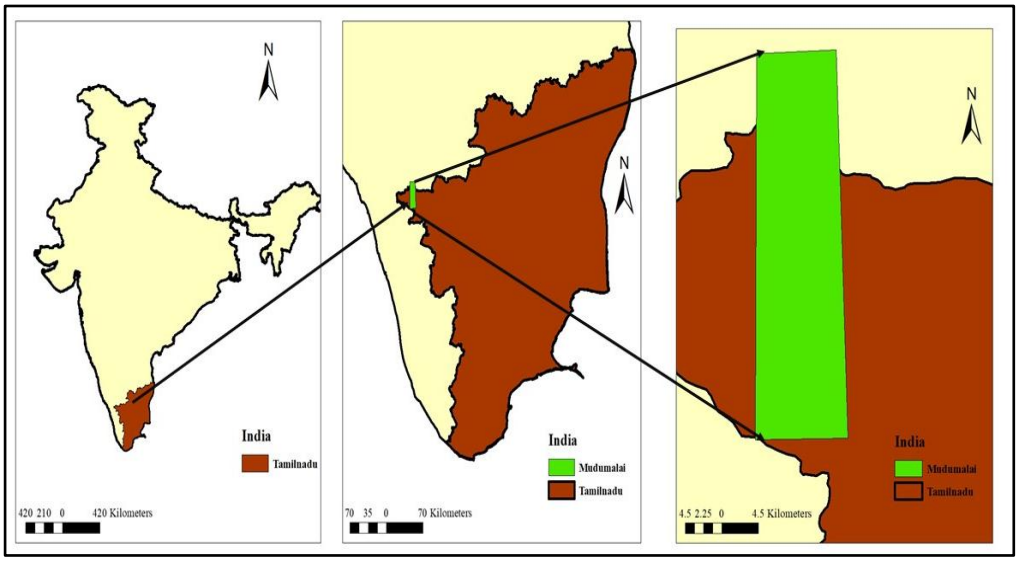

Figure 3.2: Location map of Mudumalai Reserve forest

3.1.3 Sholayar Reserve Forest

The study site, Sholayar reserved forests in Kerala state is located in between 10°30'14.97"N, 76°47'47.33"E and 10° 9'39.45"N, 76°40'51.24"E (Figure 3.3) with an area 368 square km. Sholayar forest is of tropical

deciduous and evergreen type, spreading across districts Thrissur and Ernakulam districts of Kerala with two major waterfalls - Athirapally and Vazachal. Upper Sholayar dam and lower Sholayar dam is located here which is 60 km away from Chalakkudy and 20 km from Valparai in Tamilnadu. The dominant tree species include Pallaquium ellipticum, Cullenia exarillata, Musea nagassarium, Vateria indica, etc. The climate of the region is typically warm humid with a mean annual rainfall of 3780 mm.

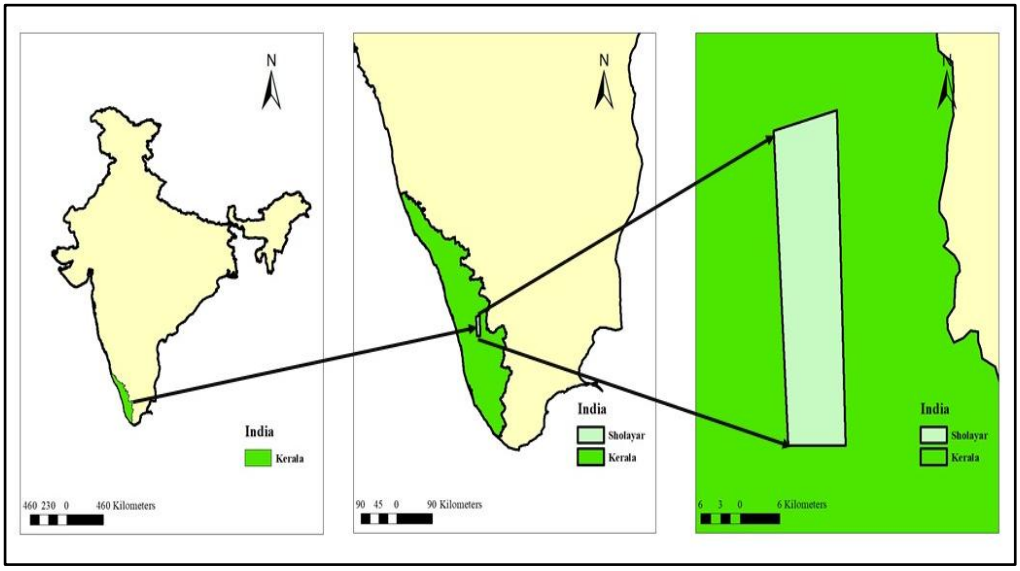

Figure 3.3: Location map of Sholayar Reserve Forest.

3.2 Data Sets

Based on the objectives and methodology of the research, optical remote sensing data and LiDAR point cloud were used for the estimation of biophysical parameters. The optical remote sensing data utilized are multispectral data and hyperspectral data. LiDAR point cloud used in the study include spaceborne LiDAR point cloud, and terrestrial laser scanned LiDAR point cloud. For the validation of the results, in situ measurements were also acquired. The data set used are described in Table 3.1.

Table 3.1: Data sets used for the study

Data Type	Name of the data	Period of acquisition	Purpose
Multispectral	Landsat ETM+	Sholayar: 8th December 2007	For the estimation of spectral parameters
		Mudumalai:17th November 2008	
	Landsat-8 OLI	Sholayar: 30th October 2016	
		Mudumalai: 31st December 2015	
	Sentinel -2	Sholayar: 5th December 2016	
		Mudumalai: 11th October 2016	
LiDAR Point Cloud	Spaceborne (ICESat GLAS 14 data)	2003-2009 for both study sites	For estimating structural parameters
	Terrestrial laser scanned data	28th March 2018	
Hyperspectral Data	AVIRIS-NG (Airborne)	January – February 2016	For estimating spectral parameters
Ground truth reference measurements	Height	2001-2006, 2006-2009 January -October 2016, March 2018	For validation
	Biomass	2001-2009 January -October 2016	
	LAI	2016 January- December, 2018 March	

3.2.1 Optical Remote Sensing Data

3.2.1.1 Multispectral Data

Multispectral data sets used in the study for obtaining the spectral characteristics of the two study area are imagery from Landsat ETM+, Landsat-8 OLI, and Sentinel-2.

3.2.1.1.1 Landsat Enhanced Thematic Mapper Plus (Landsat ETM+)

Landsat Enhanced Thematic Mapper Plus (ETM+) sensor onboard the Landsat 7 satellite has 16 days repeated cycle. The data was collected which covers both the study areas and are referenced to world reference system-2. The product consists of eight spectral bands with a spatial resolution of 30 m for bands 1 to 7. The band 8 (panchromatic band) has a resolution of 15 m. The bands of ETM+ data and the corresponding resolutions are shown in Table 3.2.

Table 3.2: Landsat ETM+ bands and their resolution

Bands	Resolution (m)
Band 1-Blue	30
Band 2- Green	30
Band 3- Red	30
Band 4- Near Infrared	30
Band 5- Short wave infrared SWIR-1	30
Band 6- Thermal	60
Band 7- Short wave infrared SWIR-2	30
Band 8- Panchromatic	15

The data sets of the two study areas were downloaded from USGS earth explorer (https://earthexplorer.usgs.gov/). For the Mudumalai forest region, the date of acquisition of Landsat ETM+ is 8th December 2007. The acquisition date for Landsat ETM+ for Sholayar is 17th November 2008.

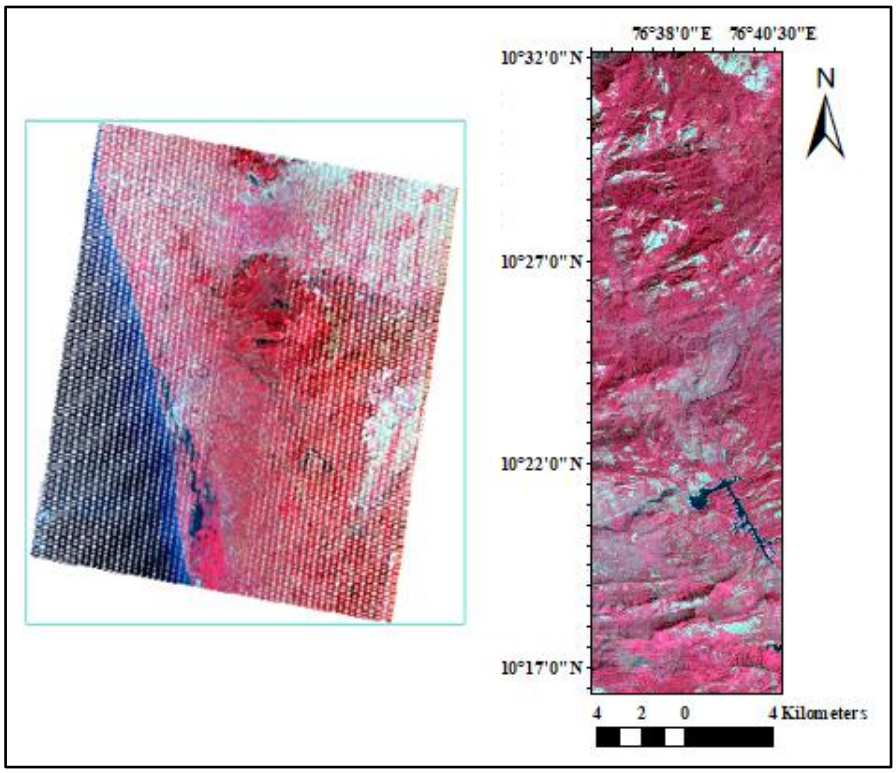

Figure 3.4: FCC of Landsat ETM+ imagery for Sholayar Reserve Forest

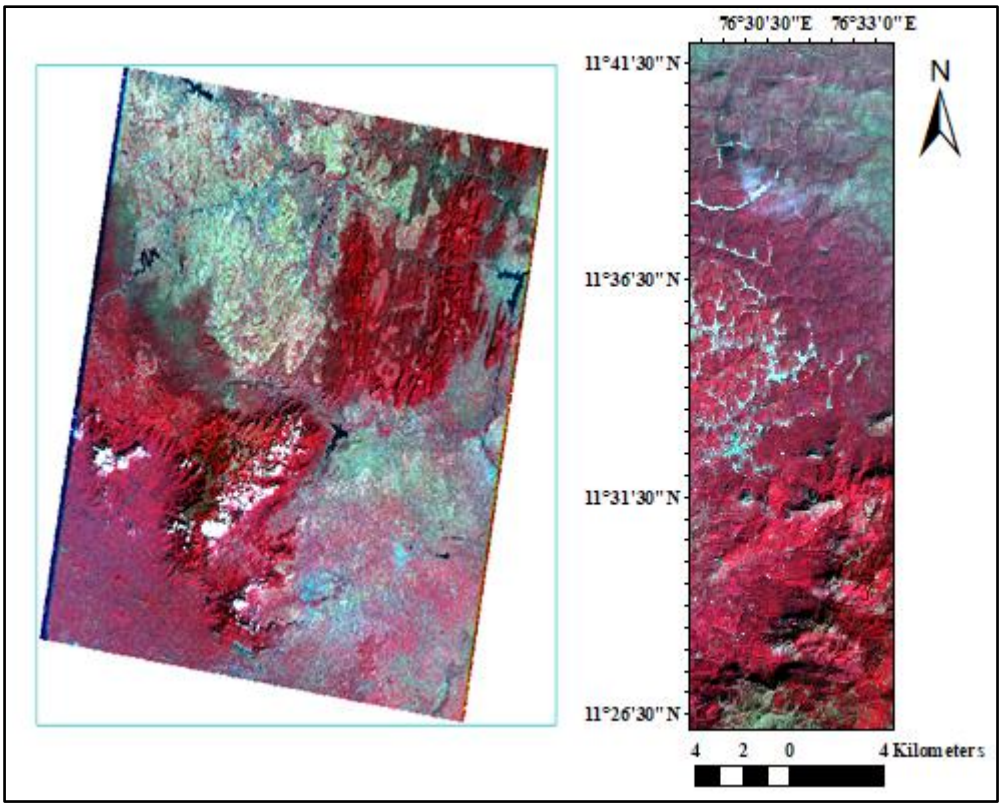

Figure 3.5: FCC of Landsat ETM+ imagery for Mudumalai Reserve Forest

Figure 3.4 and Figure 3.5 depict Landsat ETM+ data sets acquired for Sholayar forest and Mudumalai forest respectively.

3.2.1.1.2 Operational Landsat Imager (Landsat-8 OLI)

Landsat-8 OLI imagery for the two study areas are obtained from the USGS earth explorer which contains additional two new spectral bands 1 (deep blue channel for water resource and coastal zone navigation and band 9 (new infrared channel for the detection of cirrus clouds) compared to Landsat ETM+. Due to Landsat-8's near-polar orbit, the entire Earth will fall within view once every 16 days. The bands and the corresponding resolutions are shown in Table 3.3.

Table 3.3: Bands and the corresponding resolution of Landsat-8 OLI

Bands	Resolution (m)
Band 1 - Coastal / Aerosol	30m
Band 2 – Blue	30m
Band 3 – Green	30m
Band 4 – Red	30m
Band 5 - Near Infrared	30m
Band 6 - Short Wavelength Infrared (1.560 – 1.660 µm)	30m
Band 7 - Short Wavelength Infrared (2.100 – 2.300 µm)	30m
Band 8 – Panchromatic	15m
Band 9 – Cirrus	30m

The date of acquisition for Landsat-8 OLI is 31st December 2015 for Mudumalai forest, and for Sholayar forest, date of acquisition is on 30th October 2016. The False Color Composite (FCC) of Landsat-8 OLI for the two study area: Sholayar forest and Mudumalai forest, are shown in Figures 3.6 and 3.7 respectively.

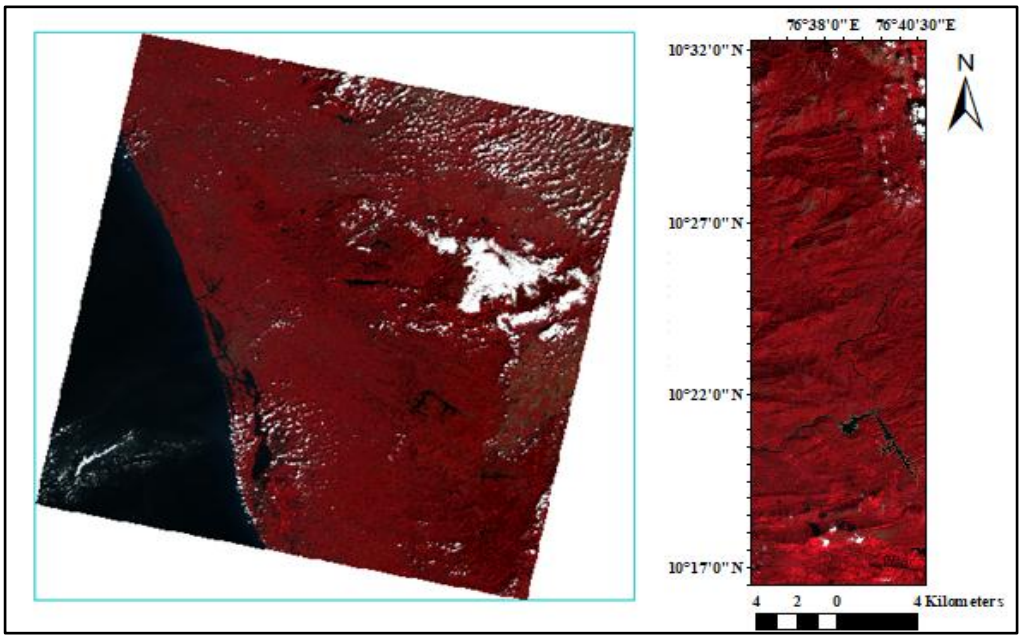

Figure 3.6: FCC of Landsat-8 OLI for Sholayar Reserve Forest

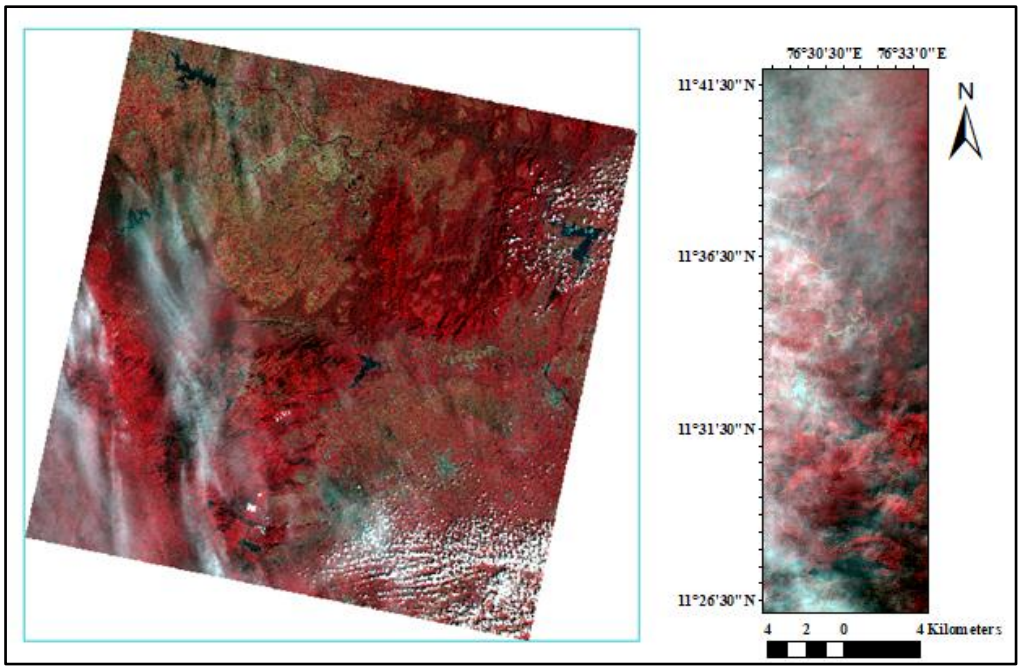

Figure 3.7: FCC of Landsat-8 OLI for Mudumalai Reserve Forest

3.2.1.1.3 Sentinel-2 Data

Sentinel-2 mission, launched by European Space Agency in 2015 is a multispectral satellite (MSI) that provides high fidelity image and have a high temporal resolution. Sentinel-2 acquires imagery which can be used primarily for forest monitoring, natural disaster management, and land cover change detection by revisiting every ten days. Sentinel-2 acquires imagery in 13 spectral bands with a spatial resolution of 10 m, 20 m, and 60 m, and is highly complementary to Landsat-8 OLI and Landsat ETM+. Sentinel-2 bands and the corresponding resolution are shown in Table 3.4.

Table 3.4: Sentinel-2 bands and the corresponding resolution

Sentinel-2 bands	Resolution (m)
Band 1- Coastal aerosol	60
Band 2- blue	10
Band 3- Green	10
Band 4- Red	10
Band 5- Vegetation Red Edge	20
Band 6- Vegetation Red Edge	20
Band 7- Vegetation Red Edge	20
Band 8- NIR	10
Band 8a- Vegetation Red Edge	20
Band 9- Water Vapour	60
Band 10- SWIR-Cirrus	60
Band 11-SWIR	20
Band 12-SWIR	20

The Sentinel-2 data was downloaded from USGS earth explorer, and the date of acquisition is October 11, 2016, for Mudumalai forest and December 5th, 2016 for Sholayar forest. The FCC of sentinel-2 imagery is shown in Figure 3.8 for Sholayar forest and Figure 3.9 for Mudumalai forest respectively.

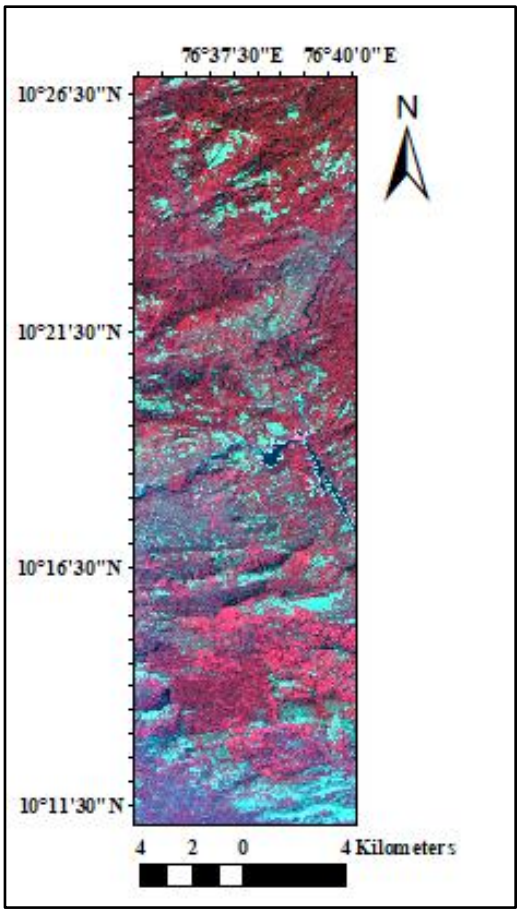

Figure 3.8: FCC of Sentinel-2 imagery for Sholayar forest

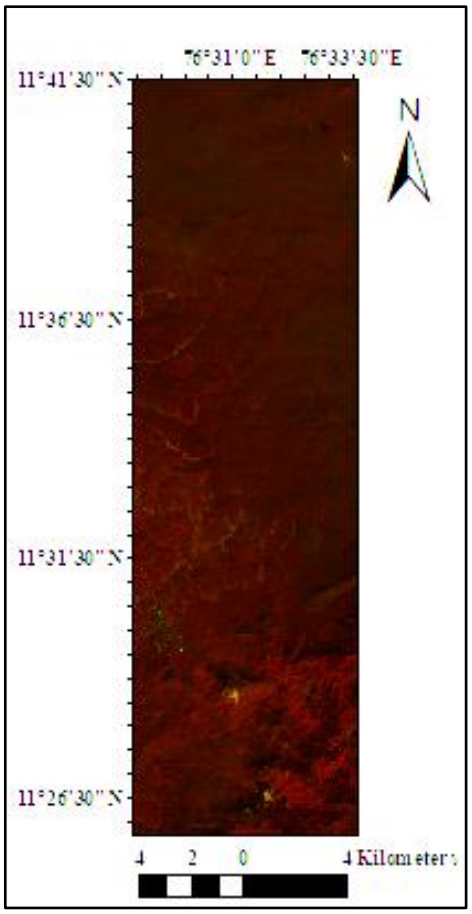

Figure 3.9: FCC of Sentinel-2 imagery for Mudumalai forest

3.2.1.2 High-Resolution Hyperspectral Data

3.2.1.2.1 AVIRIS-NG imagery

As part of ISRO-NASA cooperation in space research, Airborne Visible and Infrared Imaging Spectrometer-Next Generation (AVIRIS-NG) of JPL (Jet Propulsion Laboratory), NASA, has been acquired across several sites in India during 2016. The AVIRIS-NG has 430 narrow continuous spectral bands in VNIR and SWIR regions in the range of 380 –2510 nm at a 5nm interval with high SNR (>2000 @ 600 nm and >1000 @ 2200 nm) with an

accuracy of 95%. Ground Sampling Distance (GSD), vis-à-vis pixel resolution, varies from 4 –8 m for flight altitude of 4 –8 km for a swath of 4-6 km. The data used in this thesis were acquired at 4 m spatial resolution.

The FCC of data sets acquired over Sholayar forest and Mudumalai forest are shown in Figures 3.10 and 3.11 respectively.

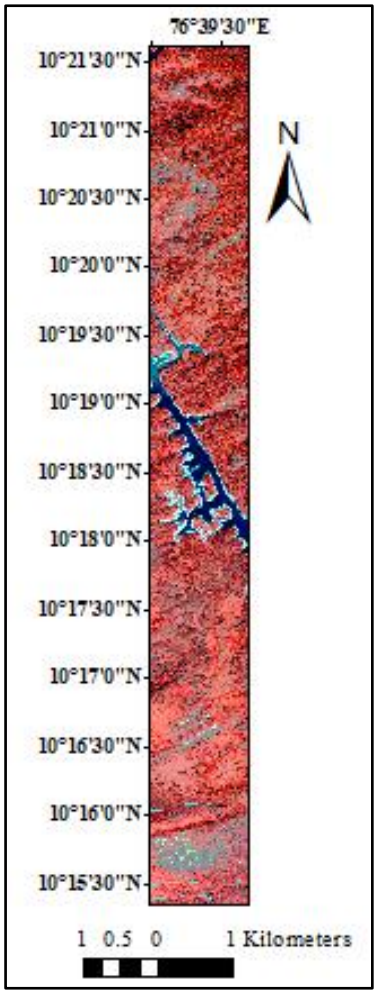

Figure 3.10: FCC of AVIRIS-NG imagery for Sholayar forest (Bands: R:83, G:65, B:55)

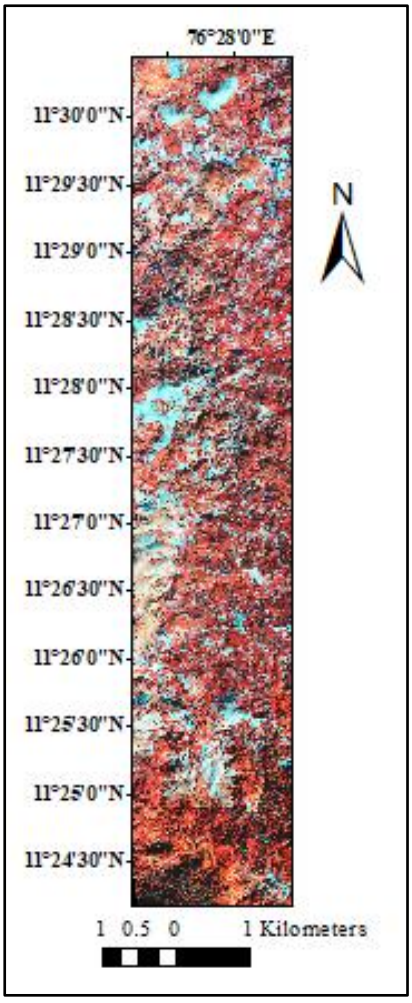

Figure 3. 11: FCC of AVIRIS-NG imagery for Mudumalai forest (Bands: R:83, G:65, B:55)

AVIRIS-NG for Sholayar forest and Mudumalai forest collected during January - 2016 was provided by Indian Institute of Space science and Technology (IIST), Thiruvananthapuram. For Sholayar region the imagery is a Level 1 (L1) product, calibrated and ortho-rectified top-of-radiance (TOA) counts. For Mudumalai forest, both Level1 and Level 2 (surface reflectance products in all the bands after atmospheric correction) are used.

3.2.2 LiDAR Point Cloud

The LiDAR point cloud used in the study includes both spaceborne and terrestrial LiDAR point cloud.

3.2.2.1 Spaceborne LiDAR Point Cloud

The spaceborne LiDAR point cloud used has been acquired by Geoscience Laser Altimeter System (GLAS) onboard ICESat. The full waveform LiDAR point cloud used were acquired from ICESat/GLAS between 2003 and 2009 in which laser footprint has a circular shape with 70 m diameter with a spacing of 170 m along the track. GLAS was originally designed for ice elevation monitoring. Its primary objective is to measure long term polar ice changes. Additional scientific objectives of GLAS were obtaining global measurements of the sea, ice, land, vegetation, oceans, forest canopy heights, land terrain changes and distribution of clouds and aerosols (Zwally et al., 2002, 2010). It can be used for vegetation analysis since it can offer global estimates of canopy height. GLAS provided 15 data products including level L1A, L1B, and L2 laser altimetry and atmospheric LiDAR measurements.

The data products range from GLA01, GLA02, GLA03 to GLA15. Level 1A altimetry data (GLA01) containing transmitted and received waveforms from the altimeter. GLA02 Level 1A atmospheric data contain the

normalized relative backscatter for the 532 nm and 1064 nm channels, and low-level instruments corrections such as laser energy, photon coincidence, and detector gain corrections. GLA04 Level 1A global laser pointing data contain 20 orbits of attitude data from the spacecraft star tracker instrument and laser reference system, and other spacecraft attitude data required to calculate precise laser pointing. GLA 05 level 1B waveform data include output parameters from the waveform characterization procedure and other parameters required to calculate surface slope and relief characteristics. GLA06 Level 1B Global elevation product contains elevation corrected for tides, atmospheric delays and surface characteristics within the footprints. GLA07 level1B global backscattering data are provided at full instrument resolution. The product includes full 532 nm and 1064 nm calibrated attenuated backscattering profiles at five times per second and from 10 to 1 km at 40 times per second for both channels. GLA 08 level 2 planetary boundary layer (PBL) heights contain ground detection heights, top and bottom heights of elevated aerosols from -1.5 km to 20.5 km and 20.5 km to 41km.

GLA09 level 2 cloud height for multilayer clouds contain cloud layer top and bottom height data at sampling rates of 4 sec, 1sec, 5 Hz, 40 Hz. GLA10 level 2 aerosol vertical structure data contains the attenuation-corrected cloud and aerosol backscatter and extinction profiles at a 4 sec sampling rate for aerosols and a 1 sec rate for clouds. Table 3.5 depicts the ICESat/GLAS standard data products.

Table 3.5: Standard data products of ICESat/GLAS distributed by NSIDC

ID	GLAS data
GLA01	Altimetry data
GLA02	Atmospheric data
GLA03	Engineering data
GLA04	LPA-LRS data
GLA05	Waveform-based elevations corrections
GLA06	Elevation
GLA07	Backscatter
GLA08	Boundary layer and Elevated Aerosol layer heights
GLA09	Cloud heights for multiple layers
GLA10	Aerosol vertical structure
GLA11	Thin cloud/Aerosol optical depth
GLA12	Elevations ice sheet
GLA13	Elevations sea ice
GLA14	Elevations land
GLA15	Elevations oceans

GLA 11 level 2 thin cloud or aerosol optical depths data contain thin cloud and aerosol optical depths. A thin cloud is one that does not completely attenuate the LiDAR signal return which generally corresponds to clouds with depths less than about 2.0. GLA06 is used in conjunction with GLA05 to create level 2 altimetry products. Level 2 altimetry data provide surface elevation for ice sheets GLA12, sea ice GLA13, land GLA14, and oceans GLA15. ICESat data are distributed by the National Snow and Ice Data Centre (NSIDC). Among the 15 products from GLA1 to GLA 15, the GLA 14 product of release 34 was used in this study which was procured through the ICESat/GLAS data subsetter. GLA 14 comprises the global land surface altimetry data. The subsetter provided GLAS footprints for both the study area. The data comprise of 39 passes for the Sholayar forest and 15 passes for the Mudumalai forest.

The GLAS data sets for the period of March 2003 to March 2009 were filtered, and these shots were used for the analysis. GLAS data passage through both the study area overlaid satellite imagery are shown in Figures 3.12 and 3.13 for Sholayar forest and Mudumalai forest respectively.

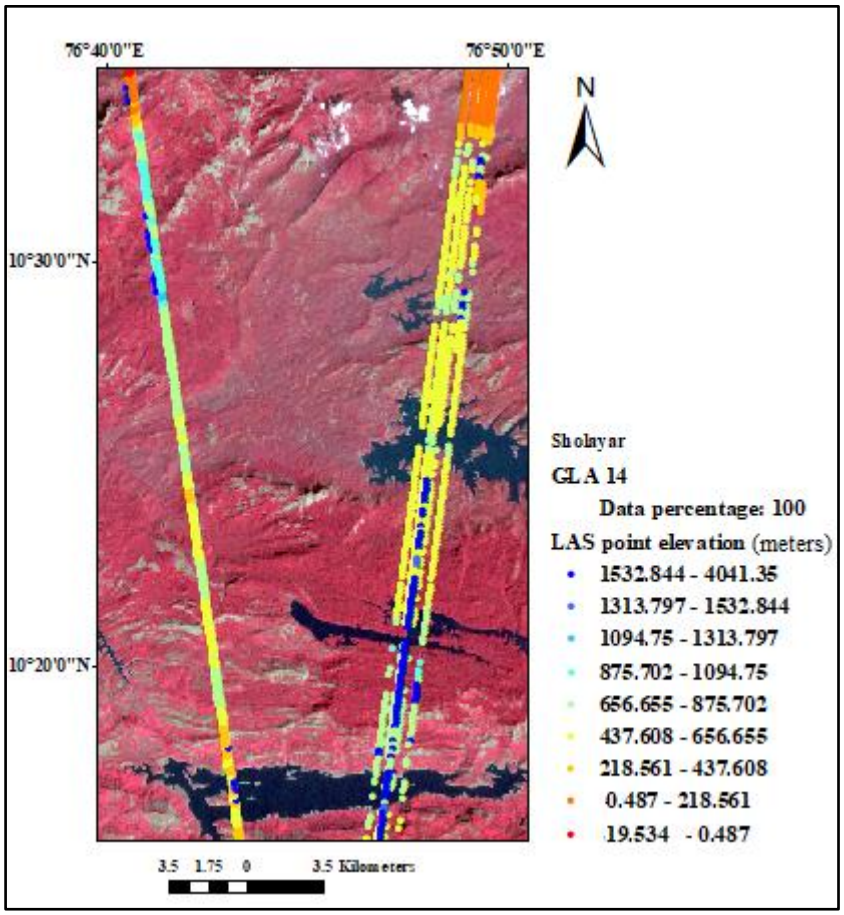

Figure 3.12: GLAS data pass through Sholayar Reserve Forest overlaid on Landsat ETM+ imagery

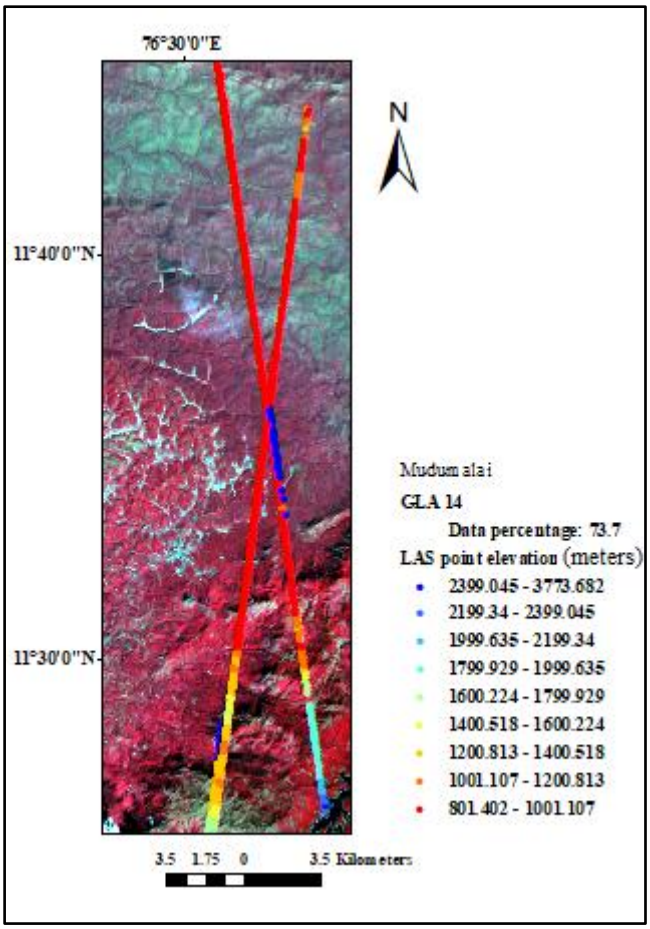

Figure 3.13: GLAS data pass through Mudumalai Reserve Forest overlaid on Landsat ETM+ imagery

3.2.2.2 Terrestrial LiDAR Point Cloud

Terrestrial Laser Scanner (TLS) point cloud used here was acquired by a terrestrial laser scanner (FARO Focus^S 350) over a small part of Mudumalai reserved forest on March 25, 2018, by IIST, Thiruvananthapuram and is thankfully shared with me for research purpose.

The terrestrial Laser scanner is a ground-based LiDAR, which rapidly acquires accurate and photo-realistic three-dimensional dense point clouds of real-world objects with millimeter-level detail. This remote sensing system

allows for extremely rapid acquisition of large amounts of three-dimensional coordinates with an unprecedented level of precision of areas that are complex or inaccessible to the traditional survey.

This instrument can acquire millions of 3D points (1 million points per second) with a very high point density with mm level accuracy (Wang et al., 2014). TLS points are often collected by fixing it on a tripod within the target area which records the x, y, z (position) and intensity which is the reflected pulses or returns from the target. The sensor continuously emits the laser beam towards the target. Sensors are designed to be easily deployed and portable. The main components of TLS include laser beam, a polygonal mirror, optical head, camera, laptop, and operating software. Distance measurement is based on two major technologies: time of flight and phase shift measurements. In the case of time of flight based scanners, the distance is calculated by measuring the travelling time of an emitted laser pulse whereas in the case of phase shift measurement, the distance is calculated by measuring the phase shift between the emitted and the received pulses (Liang et al., 2016 Lindberg et al., 2012). The measurement accuracy of phase shift based TLS is slightly higher. Point density depends on the distance from the scanner, and the angular resolution of the device. Most of the scanners usually rotate 180 degrees horizontal and 310 degrees vertical (average point density 25000 points/m^2). The data pre-processing of TLS includes preparation, scanning, registration, and filtering.

In forestry, TLS has used for detailed structural modeling of individual trees retrieval of tree attributes such as DBH, height, stem curve, branch details directly from the point cloud (Kretschmer et al., 2013; Liang & Hyyppä, 2013). TLS can provide millimeter level spatio-structural information of individual trees.

Figure 3.14 shows the picture of TLS equipment used and the raw point cloud acquired.

Figure 3.14: TLS Equipment and the Data Collected

This equipment is specially designed for outdoor applications because of its small size, extra lightweight, and extended scanning range. It can acquire point cloud in challenging environments, dusty or humid areas, and the integrated GLONASS/GPS receiver does the easy positioning. HDR imaging and HD photo resolution ensure detail scan results with high data quality.

- Range Focus^{S} 350: 0.6 – 350 m
- High Dynamic Range (HDR) photo recording 2x/3x/5x
- Measurement speed: 976000 points/second
- Ranging error: ± 1 mm
- Sealed design – Ingress Protection (IP) Rating Class 54
- On-site compensation

- On-Site registration (with FARO SCENE)
- Scan Group Feature (rescanning of distant targets in higher resolution)
- Accessory Bay
- Angular Accuracy: 19 arc sec for vertical/horizontal angles
- Integrated Colour camera: Up to 165 megapixel
- Laser class: Laser class 1
- Weight: 4.2 kg
- Multi-Sensor: GPS, Compass, Height Sensor, Dual Axis Compensator
- Size: 230 x 183 x 103 mm
- Scanner control: touch screen display and WLAN

General specification of the laser scanner along with the specific configurations is given in Table 3.6.

Table 3.6: TLS general configuration

General Scanner Configurations	
Range	0.6 m-350 m
Ranging error	±1 mm
Laser wavelength	1550 nm
Beam divergence	0.3 mrad
Beam diameter at the exit	2.12 mm, circular
Colour unit Resolution:	Up to 165 megapixels
Point spacing	6 mm

The TLS point cloud acquired for the Mudumalai forest study site is shown in Figure 3.15.

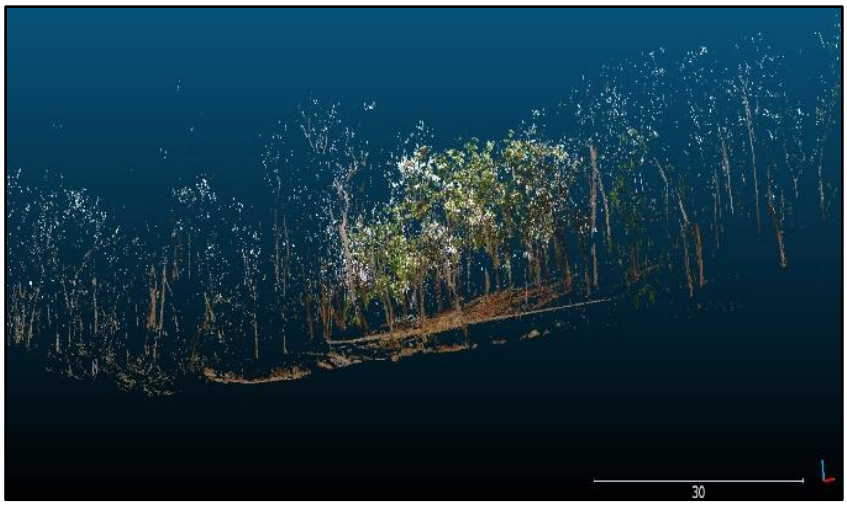

Figure 3.15: TLS point cloud for Mudumalai Reserve Forest

3.2.3 Ground Truth Measurements for Calibration and Validation of Optical Imagery and LiDAR Point Cloud Based Analysis.

Ground truth data acquired during multiple field data acquisition campaigns held as part of national level tropical biodiversity assessment at stand level programme undertaken during 2001-2006 and 2007-2009, were shared by Indian Institute of Space Science and Technology (IIST), Thiruvananthapuram. Biomass values were estimated by allometry method. Understory vegetation height and canopy heights were estimated by the actual measurement using pole and tape. Measurements of tree height, canopy cover, diameter at breast height, woody tree density, LAI, chlorophyll concentration, aerosol optical density were acquired using various instruments namely Laser Distance meter, plant canopy analyzer, chlorophyll meter, sunphotometer, and GPS. As part of the AVIRIS -NG hyperspectral imaging campaign across several sites in India, ground truth measurements were acquired by IIST for multiple sites during January 5-15, March 5-11, October 15-23, 2016. The ground truth data acquired during the acquisition of AVIRIS-NG data (January

5 – 7, 2016) were used in this study for the calibration and validation of results from AVIRIS-NG imagery. Also, tree height and LAI were measured at the same time where TLS point cloud was acquired during 5- 8 March 2018.

3.3 Software Tools used for the Analysis of Data

For the analysis of optical imagery and LiDAR point cloud, a host of software was used including both the image processing as well as visualization tools and are listed below.

a) For the processing of optical imagery, the set of software used include-

1. ENVI – pre-processing of Landsat imagery and Sentinel-2 imagery including radiometric calibration and atmospheric correction, estimation of vegetation indices and biomass, pre-processing of AVIRIS NG imagery, analysis of optical imagery including integration and linear stretching.
2. ArcMap- estimation of canopy density, vegetation indices, preparing maps
3. SNAP tools for the pre-processing of Sentinel 2 imagery
4. Landsat Gap fill tool for pre-processing of Landsat imagery.

b) For the processing of spaceborne LiDAR point cloud, the software used include-

1. NGAT tool: for converting the GLAS data to text format.
2. GLAS read: for extracting the required parameters including latitude-longitude values, elevation, etc
3. GLAS visualizer: for the visualization of GLAS 14 data.

The above tools were used for extraction of the GLAS data parameters from the ICESat GLA 14 data product.

c) For the processing LiDAR point cloud, software used include

1. GLOBAL MAPPER: for filtering point cloud, developing DEM, DSM, CHM.
2. LAStools: data conversion and filtering of the point cloud.

d) For the processing of the terrestrial LiDAR data, the tools used are-

1. PCL library: segmentation of TLS point cloud.
2. Visual Studio C++: segmentation, filtering of TLS point cloud.
3. C Make: for the installation of PCL.
4. 3D Forest: for the estimation of structural parameters and tree reconstruction by processing TLS data.
5. Cloud Compare: for the visualization, clipping, filtering of TLS point cloud.
6. Fugro viewer: for visualization of TLS point cloud.

3.4 Chapter Conclusion

This chapter described in detail the study site, data tools and experimental set up of this research. The relevance of each of the data set for the overall area of the study was also presented.

******

Chapter 4

METHODOLOGY

Contents

This chapter presents the overall workflow of the research. There are three main tasks in this research work:

- estimation of forest biophysical parameters with fused data generated by integrating GLAS point cloud and multispectral imagery,
- estimating height, DBH, and LAI using terrestrial LiDAR point cloud, and the development of a new algorithm for direct estimation of LAI.
- further, the possibility of the synergic integration of AVIRIS-NG airborne hyperspectral imagery and GLAS point cloud has also been explored for estimating LAI and biomass.

Overall workflow

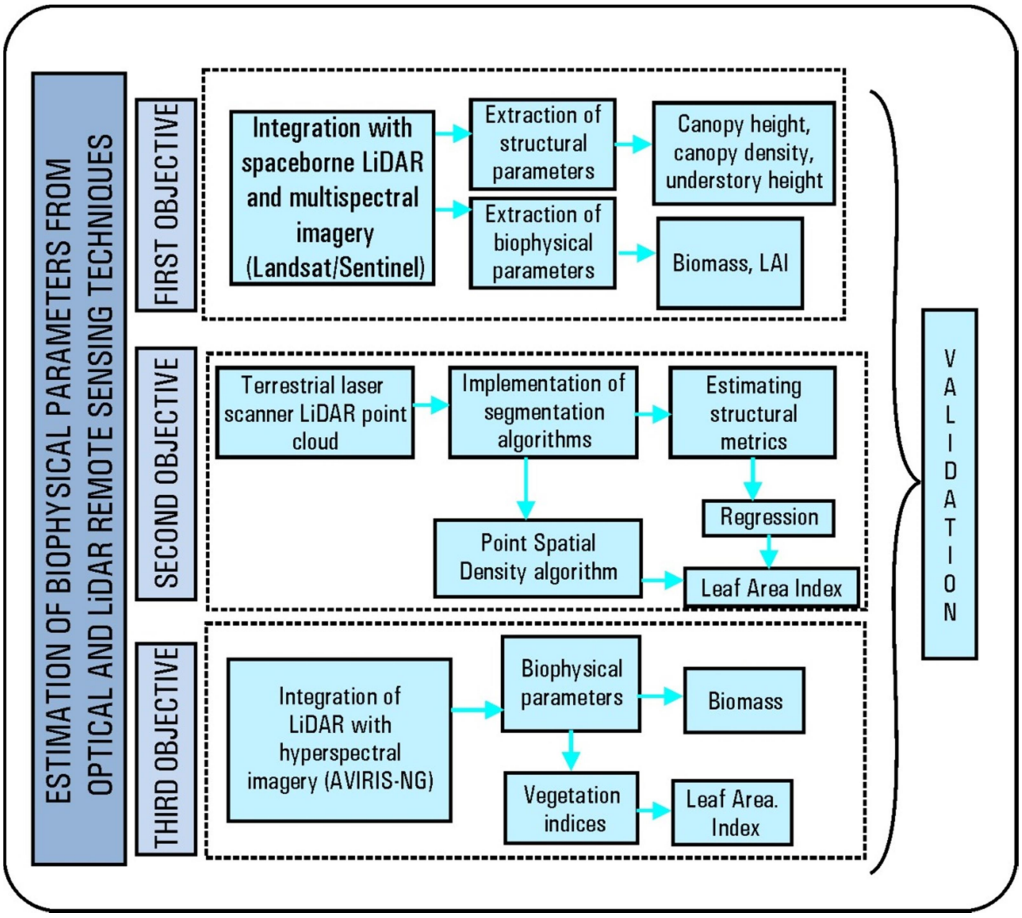

Figure 4.1: Overall Workflow

Overall workflow is depicted in Figure 4.1. Details of algorithms and sequence of steps followed in the methodology are described in the following sections.

4.1 Estimation of Biophysical Parameters by the Integration of Spaceborne LiDAR Data and Multispectral Imagery

4.1.1 Methodology

The methodology followed in the study is shown in Figure 4.2. GLAS point cloud data after the pre-processing to readable form were analyzed, and the useful parameters were separated from the filtered data.

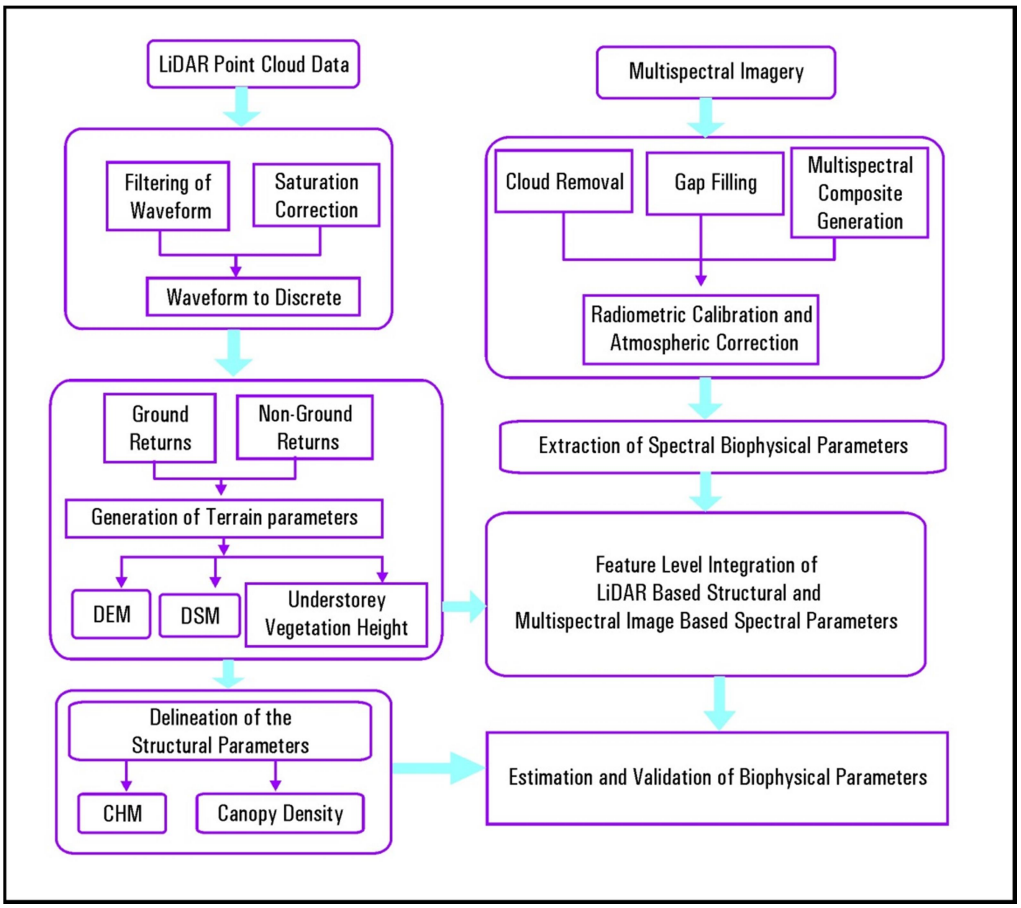

Figure 4.2: Process flow diagram depicting the typical steps in the methodology

4.1.2 Pre-Processing of LiDAR Point Cloud

The GLAS point cloud was converted from binary to text format using NGAT tools and was further processed to extract the required parameters. The NGAT lets a user extract information from an ICESat/GLAS binary altimetry file. The output obtained included: -

Record Number - 1 record (40 samples)

Date - MM/DD/YYYY

Time - HH:MM: SS.sss

Latitude - ‘ i_lat' converted to degrees

Longitude - 'i_lon' converted to degrees

Elevation - the 'i_elev' field for the chosen product number, converted to meters

Geoid - the 'i_gdHt' values, interpolated for each shot also converted to meters.

The information is presented in an easy to use column output format. The output data of one of the passes is shown in Table 4.1.

Table 4.1: Sample GLAS data after conversion from binary to text

Date	Latitude	Longitude	Elevation(m)
02/20/2008	10.463544	76.692438	741.849
02/20/2008	10.465098	76.692216	738.031
02/20/2008	10.466651	76.691984	718.504
02/20/2008	10.468203	76.691762	723.117
02/20/2008	10.469757	76.691544	742.707
02/20/2008	10.471311	76.691324	754.184
02/20/2008	10.472867	76.691081	733.408
02/20/2008	10.474423	76.690862	757.661
02/20/2008	10.475981	76.690654	803.711
02/20/2008	10.477541	76.690445	846.108
02/20/2008	10.479102	76.690225	861.898
02/20/2008	10.480662	76.690004	872.511
02/20/2008	10.482217	76.689811	941.268
02/20/2008	10.483769	76.689639	1051.352
02/20/2008	10.485321	76.689452	1127.907
02/20/2008	10.486875	76.689244	1152.883
02/20/2008	10.488433	76.688984	1063.683
02/20/2008	10.489993	76.688726	974.745
02/20/2008	10.491552	76.688493	938.762
02/20/2008	10.493112	76.688281	944.487
02/20/2008	10.494675	76.688062	933.268
02/20/2008	10.496239	76.687858	949.723
02/20/2008	10.497804	76.687634	920.112
02/20/2008	10.499368	76.687412	890.899
02/20/2008	10.500929	76.687199	876.742
02/20/2008	10.502488	76.686985	860.106
02/20/2008	10.504045	76.686796	895.352
02/20/2008	10.505602	76.686588	891.534

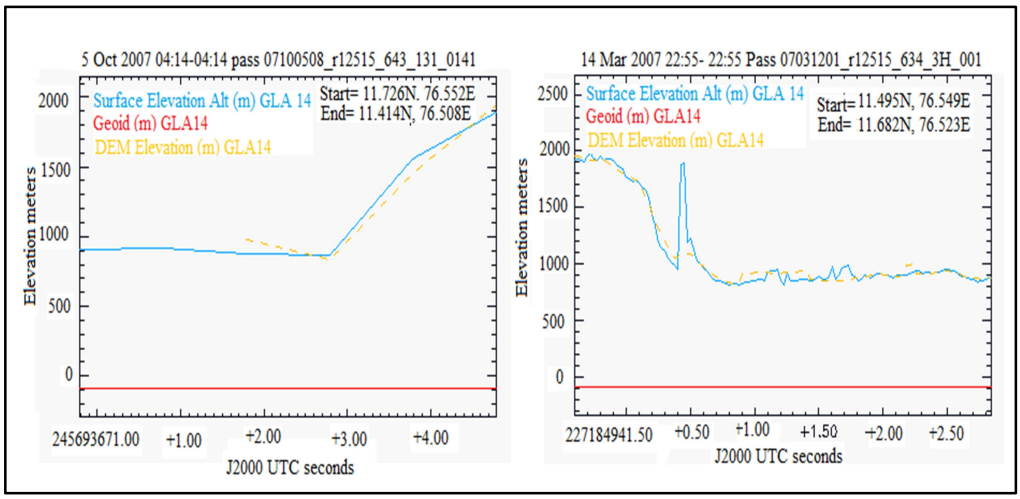

Figure 4.3: Visualization of GLAS 14 data

Visualization of the multiple returns of target was done using the IDL visualizer (ICESat visualizer) tool provided by NSIDC. An example of full waveform data visualized is shown in Figure 4.3.

The noise or invalid point cloud was filtered out using the quality flags provided in the GLA 14. The point clouds were verified for saturation, the presence of cloud and validity of elevation. GLAS data sets which correspond to the year 2003-2009, were filtered for integration. The spatial distribution of GLAS point cloud and the corresponding altitude of the terrain of the study area are shown in Figure 4.4.

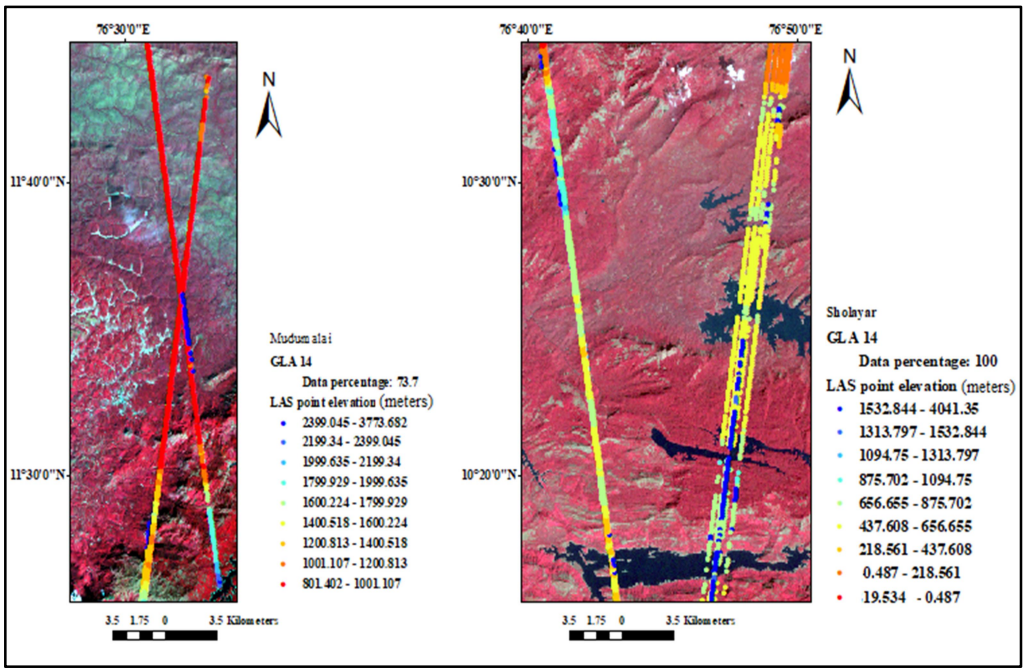

Figure 4.4: Spatial distribution of GLAS LiDAR point cloud over Mudumalai forest and Sholayar forest

4.1.3 Pre-Processing of Multispectral Imagery

Multispectral satellite imagery from Landsat ETM+, Landsat-8 OLI, and Sentinel-2 were used for the spectral information extraction of the corresponding study site. All the multispectral imagery were calibrated for atmospheric correction resulting in surface reflectance.

4.1.3.1 Landsat ETM +

The Landsat ETM+ imagery acquired for the study area has systematic data gaps. Based on the gap flags available, data gaps were filled using multiple linear transformations (Landsat gap fill tool). The discrete integer counts were calibrated to surface reflectance using radiative transfer modeling based Fast Line-of-sight Atmospheric Analysis of Spectral Hypercubes (FLAASH)

atmospheric correction modules. FCC of the Landsat ETM + imagery for Sholayar and Mudumalai forests after pre-processing is shown in Figure 4.5.

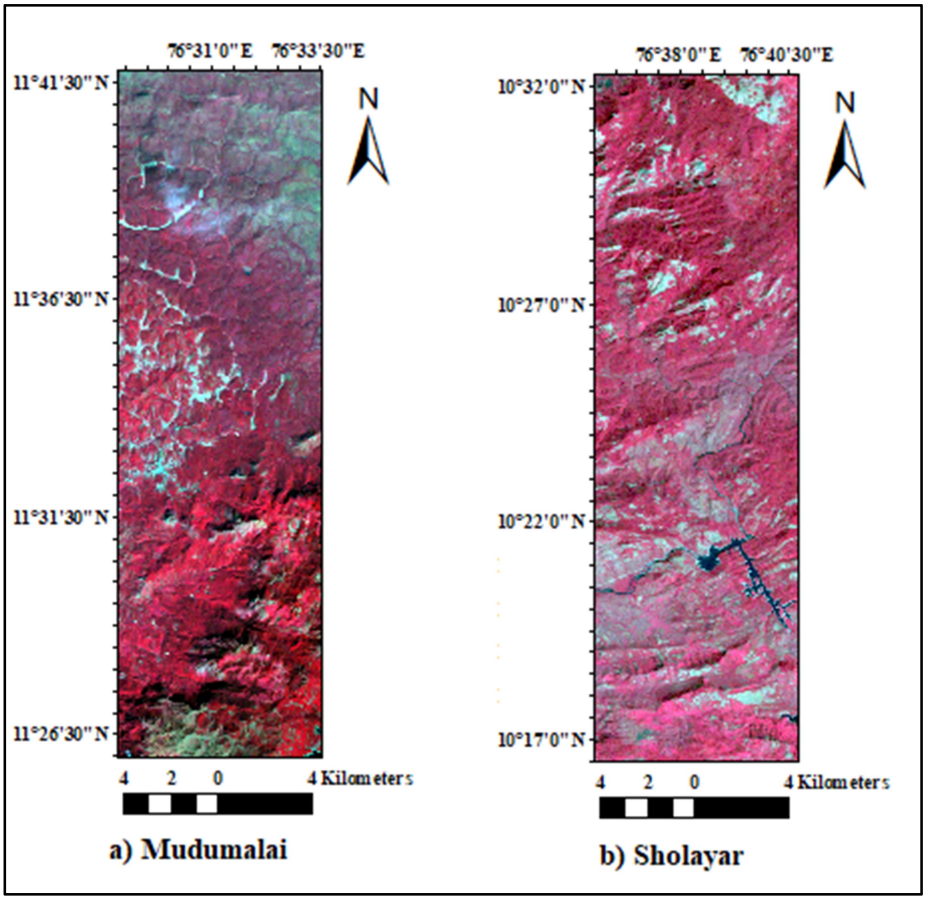

Figure 4.5: FCC of Landsat ETM+ imagery data after pre-processing for (a) Mudumalai Reserve Forest and (b) Sholayar Reserve Forest

4.1.3.2 Landsat-8 OLI

Atmospheric corrections including dark subtraction and radiometric calibration were done as part of pre-processing. FCC of the data sets after pre-processing for both the study sites are shown in Figure 4.6.

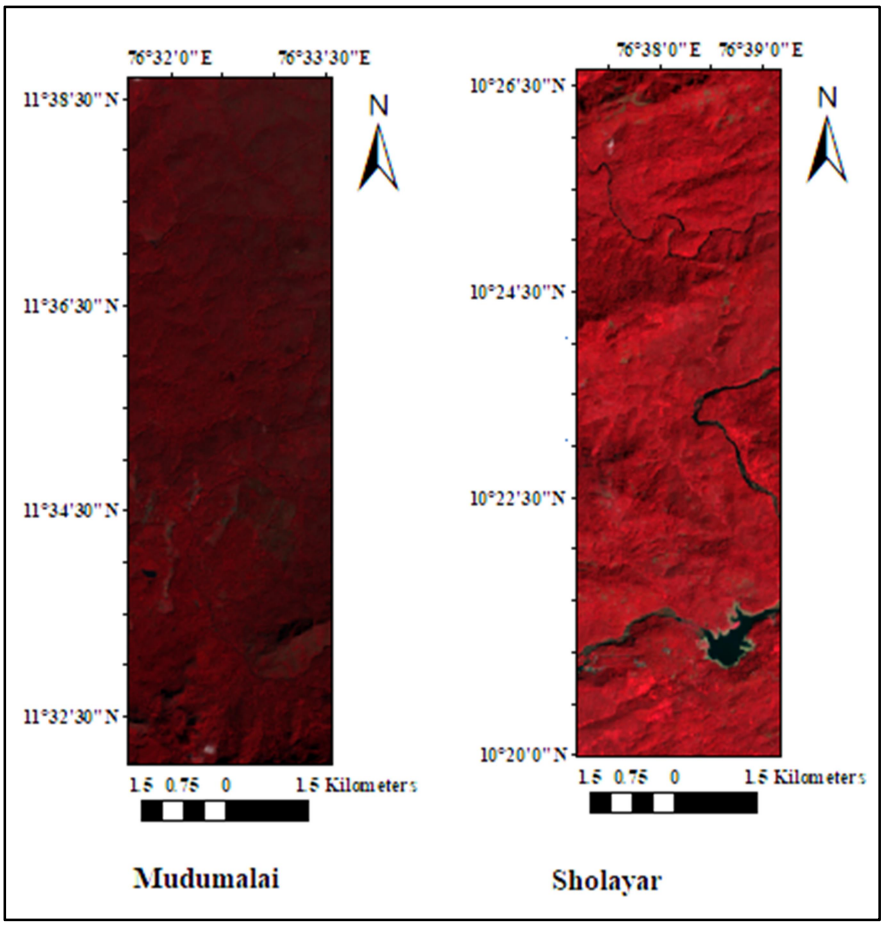

Figure 4.6: FCC of Landsat-8 OLI imagery after pre-processing for Mudumalai and Sholayar forest regions

4.1.3.3 Sentinel-2

The data were pre-processed using the SNAP toolbox which is a common platform for processing of Sentinel-2 data sets developed by the European Space Agency. The Sentinel-2 imageries were resampled and spatially subset. Cloud removal was also done by SNAP. Atmospheric corrections and radiometric calibrations were done for both the data sets. FCC of Sentinel-2 imagery for Mudumalai and Sholayar forests after the pre-processing are shown in Figure 4.7.

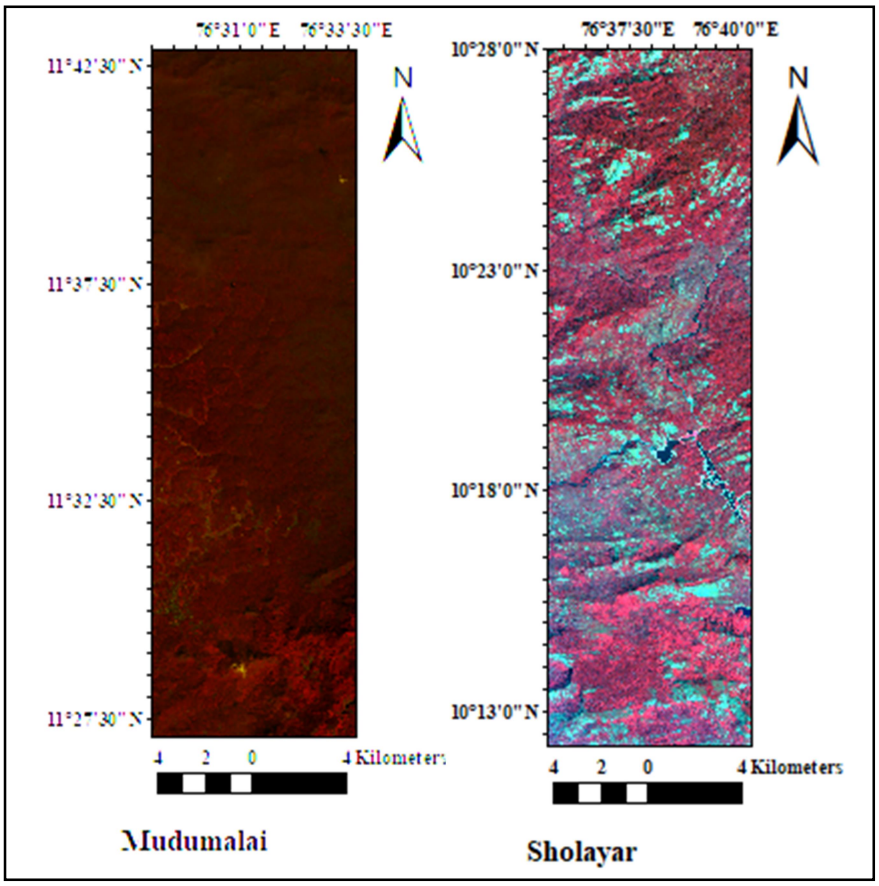

Figure 4.7: Sentinel-2 imagery (a) Mudumalai forest and (b) Sholayar forest after pre-processing

4.1.4 Canopy Height Model (CHM)

The GLAS parameters extracted from the data include i_lat (latitude), i_lon (longitude), i_elev (waveform reference ellipsoid), i gdHt (geoid Height interpolated for each shot), i_DEM _elev (DEM elevation), i sigBegOff (signal begin range increment), i_ldRangeOff (land range offset), i_sigEndOff (signal and end range offset), i_gpCntRangeOff (centroid range up to six peaks), i_maxSmAmplitude (peak amplitude of the smoothed received echo), i_numPk (number of peaks found in the return), i_Gamp (amplitude of up to six Gaussian peaks), i_satElevCorr (saturation elevation correction), and

i_SatCorrFlg (saturation correction flag). Other waveform metrics obtained is i_deltaEllipsoid, whose value is the surface elevation (T/P ellipsoid) minus the surface elevation (WGS ellipsoid), i_SatElev_Corr (saturation gain corrections) and i_GmC whose value is the difference in transmit pulse Gaussian fit and the centroid of the transmit pulse. The waveform parameters included the leading edge and trailing edge which is the range between the ground return and the signal extent were taken for the height derived models.

The signal beginning (represents the highest intercepted surface of forest canopy) and signal end were extracted, and the differences were taken. The invalid LiDAR points were removed by selecting cloud-free and saturation free waveform parameters. The waveform data were then converted into the discrete format and filtered into the ground and non-ground returns (Meng et al., 2009; Mongus et al., 2012). From the LiDAR returns, DSM and DEM were developed by creating an elevation grid. Canopy heights are obtained using the following equation.

CHM (Canopy Height Model) = Digital Surface Model (non-ground returns) - Digital Elevation Model (ground returns). (1)

CHM of Sholayar forest and Mudumalai forest are obtained by comparing the elevation grids. CHMs' are found to be useful in estimating biophysical attributes of single tree and at stand level (Popescu et al., 2004; Erfanifard et al., 2018) in forestry. Canopy heights were obtained for the forest regions where GLAS shots were procured.

4.1.5 Estimation of Canopy Density and Understory Vegetation Height

Canopy density is one of the useful parameters in forest management for the ecologists. The LiDAR points from the normalized GLAS waveform were filtered out for certain heights-cut off (for height >3 m). The canopy density was estimated from the ratio of the points with cut off heights with respect to the total returns. The height of the understory vegetation was estimated based on the canopy height model and the spatial variation of discrete returns from the trees, which generally have heights above a threshold.

4.1.6 Integration of Point Cloud and Multispectral Imagery

The LiDAR point cloud derived elevation and canopy models were linearly stretched in order to avoid the inconsistencies in the geometrical arrangement of data from different sensors. This point cloud-based models were further integrated with multispectral imagery as pixel level fusion strategy incorporating for each pixel canopy height, surface height, spectral vegetation index and spectral reflectance values of all the visible and near-infrared bands of Landsat ETM+ and Landsat-8 OLI multispectral imagery. In addition, spectral reflectance values, several different vegetation indices - Difference Vegetation Index (DVI), Enhanced Vegetation Index (EVI), Ratio Vegetation Index (RVI), Green Difference Vegetation Index(GDVI), Green Normalized Vegetation Index (GNDVI), Green Ratio Vegetation Index (GRVI), Soil Adjusted Vegetation Index (SAVI), Normalized Difference Vegetation Index (NDVI), Moisture Stress Index (MSI), Normalized Difference Water Index (NDWI) were computed and appended to the feature vector formed by the integration of point cloud based structural attributes and

imagery based spectral attributes of forest canopies. Similarly, Sentinel-2 imagery for both the regions was integrated with the LiDAR point cloud.

The following vegetation indices were extracted from the integrated data set.

4.1.6.1 Normalized Difference Vegetation Index (NDVI)

Normalized Difference Vegetation Index (NDVI) (Rouse et al., 1974) was calculated as

$$NDVI = \frac{NIR - RED}{NIR + RED}. \quad (2)$$

The values of NDVI range from 0 to 1 and sensitive even for low vegetation and NDVI is related to canopy structure and canopy photosynthesis but is sensitive to the effects of soil brightness, soil color, canopy shadow. NDVI is calculated for the integrated data sets.

4.1.6.2 Difference Vegetation Index (DVI)

Difference Vegetation Index (DVI), has been applied to vegetation ecological monitoring (Tucker, 1979). The DVI is calculated using

$$DVI = NIR - RED. \quad (3)$$

Using both the Landsat imagery, DVI was obtained. The DVI accounts for the background difference between soil and vegetation.

4.1.6.3 Enhanced Vegetation Index (EVI)

Enhanced Vegetation Index (EVI) corrects the soil and atmospheric effects and is useful in high leaf area where NDVI may saturate (Huete et al., 2002). Blue reflectance region is used in order to correct for soil background

regions and reducing atmospheric influences. The EVI for the study site was calculated using

$$EVI = 2.5 \frac{NIR - RED}{NIR + 6 * RED - 7.5 * BLUE + 1}. \quad (4)$$

4.1.6.4 Green Difference Vegetation Index (GDVI)

Green Difference Vegetation Index (GDVI) was calculated for the study areas, and it is related to nitrogen content (Sripada, 2005). The GDVI for the given study was computed using

$$GDVI = NIR - GREEN. \quad (5)$$

4.1.6.5 Green Ratio Vegetation Index (GRVI)

Green Ratio Vegetation Index (GRVI) is simple to interpret and less sensitive to variations with high vegetation cover areas (Sripada et al., 2006). It is very sensitive to photosynthetic rates in forest canopies. The GRVI for the study area was calculated using

$$GRVI = \frac{NIR}{GREEN}. \quad (6)$$

4.1.6.6 Leaf Area Index (LAI)

Leaf Area Index (LAI) is defined as the total one-sided green leaf per area. It is considered as a climate variable as well as an essential canopy characteristic. All vegetation indices have different levels of correlation with LAI (Boegh et al., 2002). LAI is used to calculate the foliage cover and is an indication of vegetation dynamics, water, and carbon cycling. For the results given, the LAI was calculated using an empirical relationship described as

$$LAI = 3.618 \times EVI - 0.118. \quad (7)$$

4.1.6.7 Green Normalized Difference Vegetation Index (GNDVI)

Green Normalized Difference Vegetation Index (GNDVI), is sensitive to chlorophyll concentration measuring green spectrum from 540 m to 570 m (Gitelson et al., 1998). GNDVI is calculated using

$$GNDVI = \frac{NIR - GREEN}{NIR + GREEN} . \quad (8)$$

4.1.6.8 Moisture Stress Index (MSI)

Moisture stress is found to be very sensitive to increasing canopy water content and can be used in canopy stress analysis, productivity prediction and modeling ecosystem physiology (Ceccato et al., 2001). The higher MSI values indicate great water stress and less water content. MSI was calculated using

$$MSI = \frac{SWIR}{NIR} . \quad (9)$$

4.1.6.9 Normalized Difference Water Index (NDWI)

Normalized Difference Water Index can distinguish water and vegetation, and is a ratio combining NIR and green which can enhance water spectral signals. It has wide applications in forest canopy stress analysis, leaf area studies, fire hazard studies, and plant productivity analysis (Gao, 1995). This can be calculated using

$$NDWI = \frac{NIR - SWIR}{NIR + SWIR} \quad (10)$$

4.1.6.10 Ratio Vegetation (RVI)

Ratio Vegetation (RVI) is used for green biomass estimation and monitoring at high-density vegetation cover because it has a high correlation with biomass (Jackson et al., 1991). RVI is given by

$$RVI = \frac{NIR}{RED}. \quad (11)$$

4.1.6.11 Soil Adjusted Vegetation (SAVI)

Soil Adjusted Vegetation (SAVI) suppresses the effect of soil background pixels, and contain a canopy background adjustment factor which is a function of vegetation density and can be used in areas with relatively sparse vegetation (Huete, 1988). SAVI is given by

$$SAVI = \frac{1.5 \times (NIR - RED)}{NIR + RED + 0.5}. \quad (12)$$

Vegetation Indices extracted from Sentinel-2 data (Adan, 2017) are given below.

4.1.6.12 NDVI for Sentinel Data

NDVI for Sentinel-2 was calculated using Equation 2 in which NIR is the 8th spectral band and RED is the 4th spectral band.

4.1.6.13 EVI for Sentinel Data

For Sentinel-2 imagery data, EVI was calculated using

$$EVI = 2.5 \frac{NIR - RED}{NIR + 2.4 * RED + 1}. \quad (13)$$

4.1.6.14 Red Edge Ratio Vegetation Index (RERVI)

It is a ratio between NIR and red edge spectral band as given below (Cao et al., 2016). Red edge spectral band is the 6th band, and NIR is the 8th band of Sentinel-2 imagery.

$$RERVI = \frac{NIR}{RED}. \quad (14)$$

4.1.6.15 Red Edge Normalized Difference Vegetation Index (RENDVI)

A modification of NDVI (Chen et al., 2007) and uses red edge spectral band the (6^{th} band 740 nm) instead of Red.

4.1.6.16 Red Edge Enhanced Vegetation Index (RE EVI)

A modification of EVI (Abdel-Rahman et al., 2017) in which instead of red, red edge spectral band is used.

4.1.6.17 Normalized Difference Infrared Index (NDII)

It is used for studying water content in the canopy, and its value increases with an increase in the water content (Wang et al., 2013). NDII is calculated using

$$NDII = \frac{NIR - SWIR}{NIR + SWIR} \quad . \tag{15}$$

NIR is the 8^{th} spectral band, and SWIR (2190 nm) is the 13th spectral band of Sentinel-2 imagery.

4.1.7 Estimation of Biomass

As described in section 4.1.4, from the waveform analysis, digital surface and elevation models were developed, followed by the generation of forest canopy height model (CHM). However, forest biomass is a predictive parameter and is not estimated from the LiDAR point cloud or multispectral data directly per se. In general, forest biomass has been retrieved from remote sensing data by employing various statistical regression models between samples of field measurements of biomass and various spectral vegetation indices. However, the inherent non-linearity existing in the spectral reflectance values, number of spectral bands, and their weak relation to the spatial diversity of forest tree canopies and biomass make the statistical regression

analysis a very site-specific and tedious when the relationships are non-linear. Non-parametric and learning based algorithms have been gaining wider usage and acceptability as the standard methods for remote sensing data based classification and regression. The support vector machine (SVM) algorithm, a robust statistical supervised learning (Cortes & Vapnik, 1995) has promising application in the estimation of biophysical parameters. In this work, the SVM algorithm was used as a predictive algorithm deploying it as a classification and regression method for estimation of biomass from the integrated LiDAR point cloud and multispectral data. For handling the non-linearity amongst the input features, we used the Radial Basis Function (RBF) as the kernel function and Laplacian function as the loss function for handling the maximum allowed deviation of the predicted biomass from the measured values. In the thesis, input parameters extracted for SVM regression included LAI and CHM for the estimation of biomass. The predicted biomass values were validated with reference measurements of biomass.

4.2 Biophysical Parameter Estimation in Mudumalai Region using Terrestrial Laser Scanner (TLS)

Two methods were used here for estimating the selected biophysical parameters using TLS point cloud which are described in sections 4.2.1 and 4.2.2. The data sets acquired for the study area (Mudumalai forest) are shown below in Figures 4.8 and 4.9 respectively.

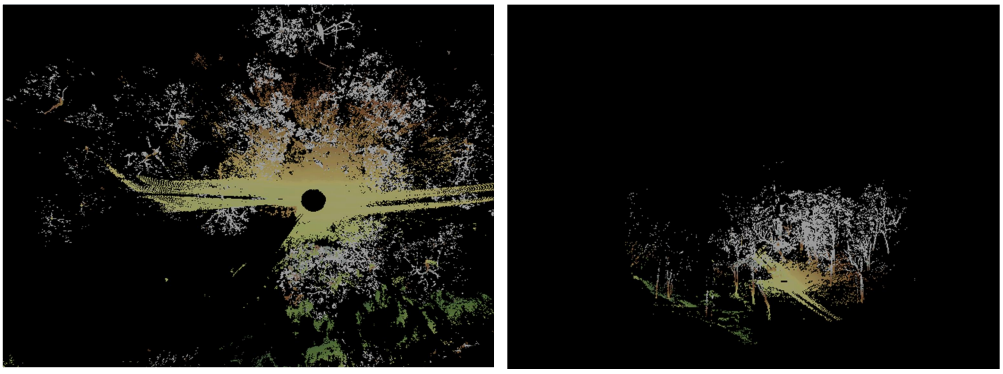

Figure 4.8: TLS point cloud visualized in Fugro viewer

Figure 4.9: TLS point cloud visualized in cloud compare

4.2.1 Three-Dimensional Reconstruction of Trees and the Estimation of Leaf Area Index from Structural Metrics using Terrestrial Laser Scanner

Three-dimensional point clouds were collected by FARO Focus^S 350 terrestrial laser scanner which performs a leveling of each scan with an accuracy of 19 arcsec valid within ±2° for a small part of Mudumalai reserve forest. The point cloud covering the study site is shown in Figure 4.10.

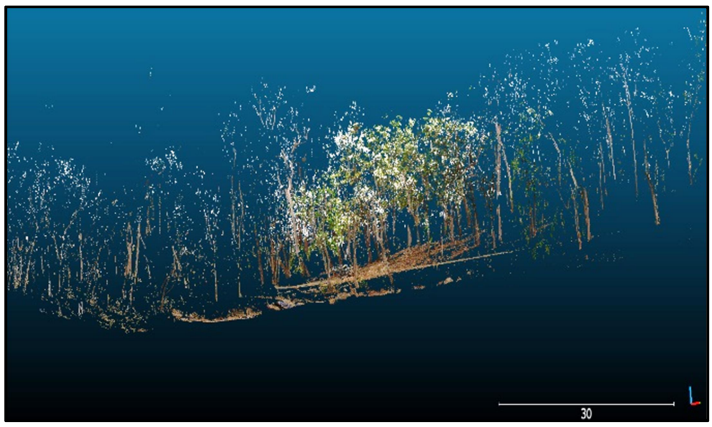

Figure 4.10: TLS point cloud for the Mudumalai forest

As part of pre-processing, the point cloud representing the forest was filtered into a terrain point cloud and vegetation point cloud. The proposed technical workflow for the processing of the TLS point cloud is depicted in Figure 4.11. It contains the main steps such as 1) pre-processing, the filtering of the point cloud, 2) segmentation: hierarchical min cut segmentation and super voxel segmentation, 3) extraction of structural metrics including height, DBH and 4) estimation of LAI by multivariate regression.

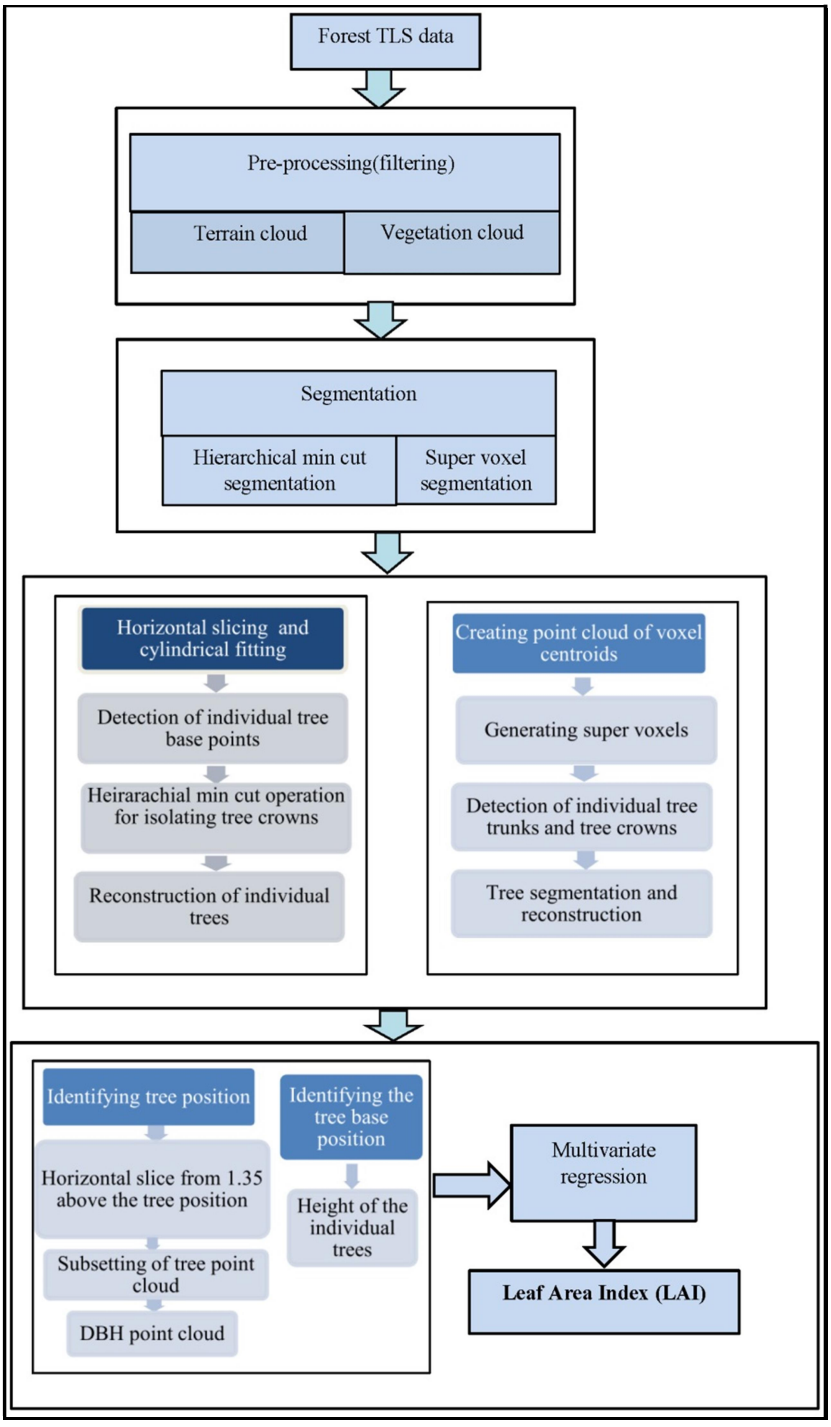

Figure 4.11: Flowchart depicting the methodology of TLS point cloud processing

4.2.1.1 Pre-Processing

As a general pre-processing step, the raw TLS point cloud was filtered to separate ground points and vegetation points. Then an octree search (Bassier et al., 2017; Trotcha et al., 2017) dividing the 3D space of the point cloud into cubes was built to remove outliers. The point cloud was thus divided into terrain cloud and vegetation cloud. Figures 4.12 and 4.13 depicts the terrain point cloud and vegetation point cloud after filtering. Vegetation point cloud in 3D form after filtering when visualized through cloud compare software is depicted in Figure 4.14.

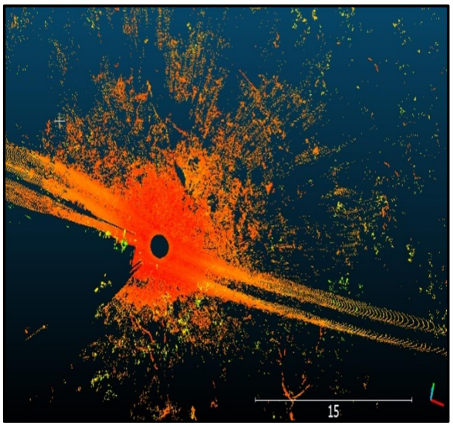

Figure 4.12: TLS terrain point cloud

Figure 4.13: TLS vegetation point cloud

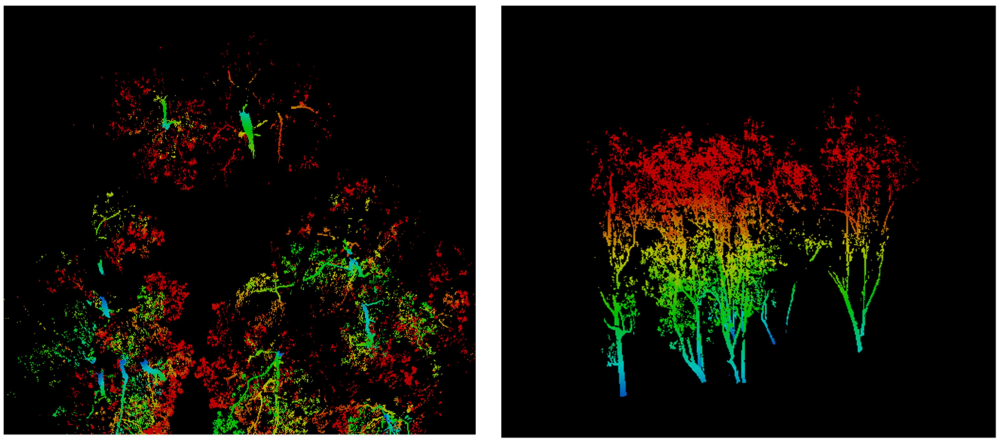

Figure 4.14: Vegetation point cloud in 3D form

4.2.1.2 Segmentation

Two different segmentation methods were implemented for individual tree detection in the TLS point cloud.

4.2.1.2.1 Hierarchical min cut segmentation

Min-cut based segmentation algorithm was implemented from the point cloud library which makes a binary segmentation of the TLS point cloud. Considering the object radius and the center, the min-cut algorithm enabled to divide the point cloud into two groups namely foreground and background. The main steps are depicted in Figure 4.15.

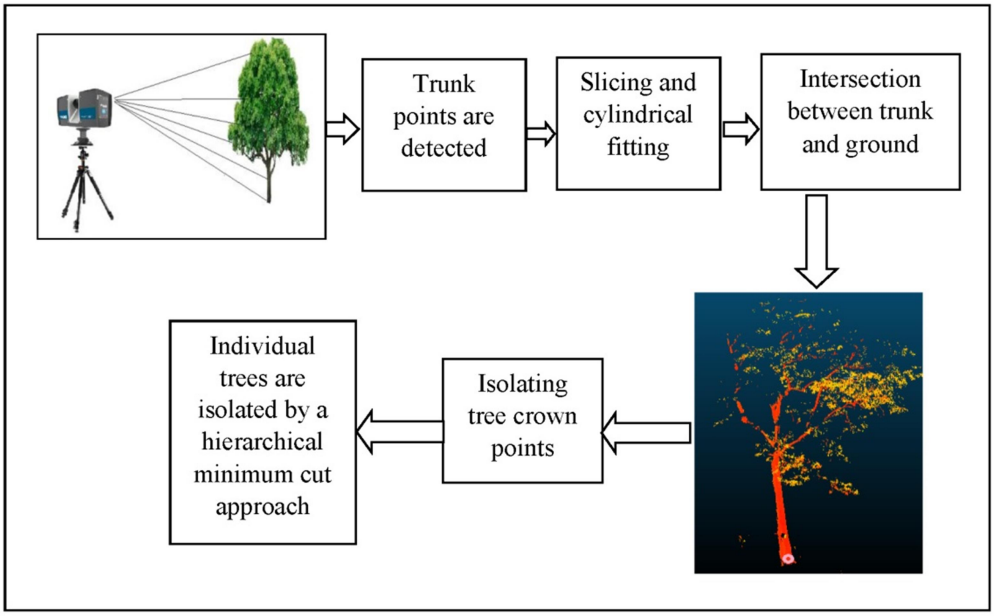

Figure 4.15: Hierarchical min-cut segmentation

For implementing the min-cut algorithm, the point cloud needs to be divided into two major groups, foreground points and background points (Golovinskiy & Funkhouser,2009; Yang et al.,2016; http://pointclouds.org/ documentation/tutorials/ min-cut-segmentation). From the vegetation point cloud comprising the tree trunk points, crown points, and the base, the location of each tree was identified where the trunk meets with its base. Euclidean cluster segmentation was implemented on the point cloud. The points were segmented based on the geometrical characteristics in which the tree trunk points are having a pole like characteristics were fitted with a cylinder and the remaining points as the tree crown points. The TLS point cloud corresponding vegetation comprises of tree trunks, crown points, and base points. Based on the geometric shape characteristics tree trunks were detected. Tree locations were identified as the intersection between the tree trunks and the base. The point cloud was divided into horizontal slices, and clusters with a user-defined

number of points and maximum distance between the nearest neighbors were computed using Euclidean cluster extraction (www.pointclouds.org). The base of the tree was located and merged into segments. Hierarchical min-cut algorithm was implemented for isolating the tree crown points which are often overlapped and connected. The minimum cut operator extracted the tree crown points corresponding to each tree trunk under minimum cost function thereby achieving globally optimal segmentation results. The points which are neighbors to each tree trunk were identified by a cylindrical buffering zone. These points were used to calculate the cost function and were segmented as tree crown points. The hierarchical min-cut approach was implemented by taking the individual tree trunk points as foreground points and the remaining other trunk points as background points.

4.2.1.2.2 Super Voxel Segmentation

Vegetation point cloud was segmented into super voxels based on the Voxel Cloud Connectivity Segmentation (VCCS) super pixel method (Aijazi et al., 2013; Xu et al., 2017; http://pointclouds.org/documentation/tutorials). For this task, the super voxel segmentation algorithm was applied on 3D TLS point cloud. The algorithm group pixels in images into perceptually meaningful regions which correspond to tree trunks and crowns. The pixels were grouped as superpixels as the base level for nodes. Voxel Cloud Connectivity Segmentation (VCCS) super pixel method was used which generates volumetric over-segmentation of 3D point cloud data, known as super voxels. VCCS uses a region growing variant of k-means clustering for generating its labeling of points directly within a voxel octree structure. Super voxels have two important properties; they are evenly distributed across the 3D space, and they cannot cross boundaries unless the underlying voxels are spatial connected. Segmentation is shown in Figure 4.16.

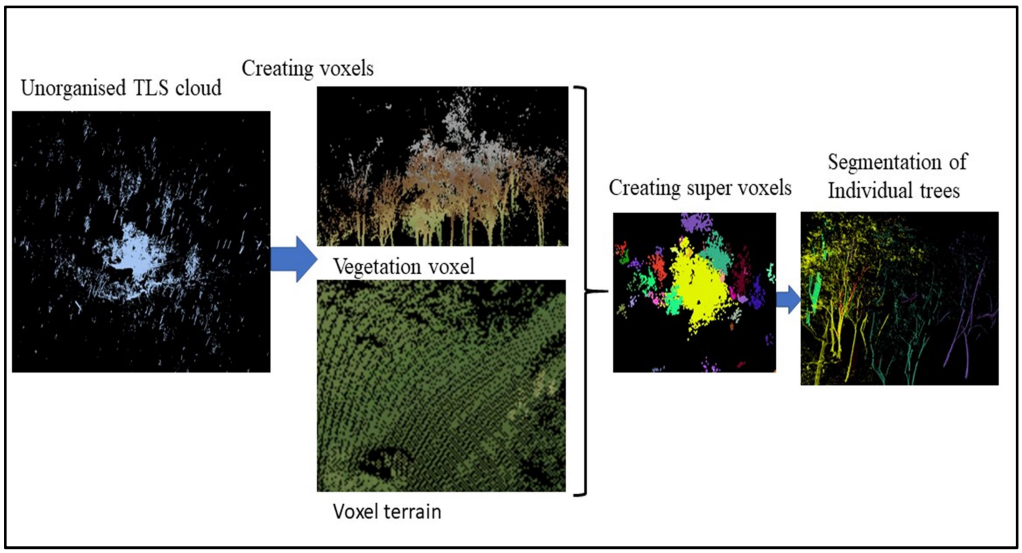

Figure 4.16: Super voxel method based segmentation of TLS point cloud

The vegetation point cloud was segmented into super voxels based on the voxel cloud connectivity. Treetop locations and the trunk points were extracted based on the classification of super voxels. If the number of points in the trunk is less than a user-defined value or the height is less than a user-defined value, the trunk points were not considered. The points near the trunk were also filtered out. Then the individual trees were reconstructed. The reconstructed tree point clouds by voxel segmentation are depicted in Chapter 5.

After the segmentation process, tree reconstruction was done by using the automatic segmentation of the results obtained.

4.2.1.3. Estimation of Tree Parameters from the Segmented Point Clouds

The reconstructed trees, resulting from the point cloud library segmentation algorithms offers the potential to compute several structural metrics. Tree height and DBH are the structural metrics estimated from the potential tree candidates. In order to calculate both the metrics, tree position or

base of the tree is to be identified. The height and DBH of each tree were calculated by selecting each tree as the computing unit.

4.2.1.3.1 Estimation of the Height of Individual Trees

Tree height is estimated as the difference in Z coordinates between the highest point of the tree cloud to the tree location at ground level using

$$\text{Tree height} = Z_{\text{highest point}} - Z_{\text{tree base.}} \quad (16)$$

$Z_{\text{highest point}}$ is the highest elevation of the tree point, and $Z_{\text{tree base}}$ is the location of the base of the tree.

4.2.1.3.2 Estimation of DBH of Individual Trees

To calculate DBH, least square regression method was used, which uses a subset of tree point cloud including horizontal slice from 1.25 m to 1.4 m above the located tree position. Figure 4.17 depicts the height calculation and DBH of the individual trees.

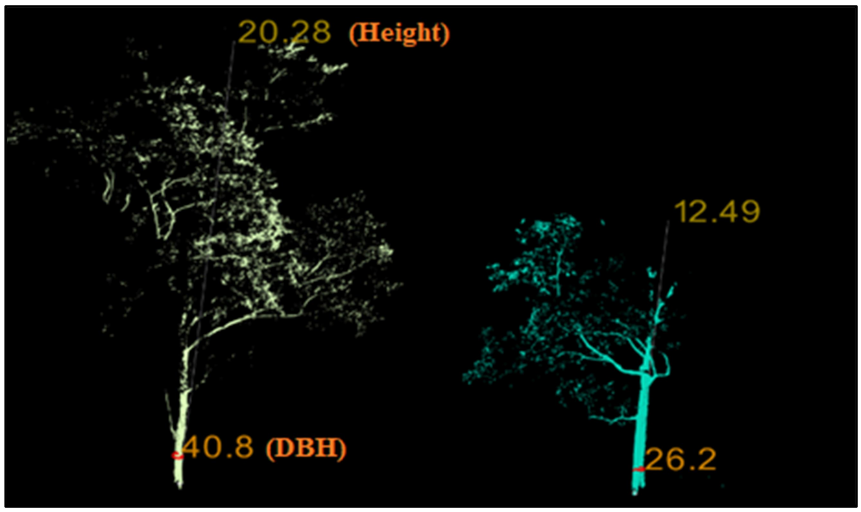

Figure 4.17: Height and DBH estimation of individual trees

4.2.1.3.3 Estimation of LAI from DBH and Height of the Individual Tree

For estimating LAI for individual trees, multivariate regression approach was applied to predict the value based on two dependent metrics, DBH, and height. After extracting the heights and DBH of all the reconstructed trees, multivariate regression analysis was done to estimate LAI. The results obtained were validated with the ground measurements and are detailed in the next chapter.

4.2.2 Direct Estimation of Leaf Area Index of Tropical Forests using Terrestrial Laser Scanner LiDAR Point Cloud

4.2.2.1 Methodology

The proposed methodology involves two significant steps for direct estimation of LAI. The first part consists of individual tree reconstruction by implementation of hierarchical minimum cut segmentation and super voxel clustering segmentation algorithm as described in the previous sections. The second part implements the proposed Point Spatial Density algorithm from the estimation of LAI to the reconstructed trees. The overall workflow of the study is depicted in Figure 4.18.

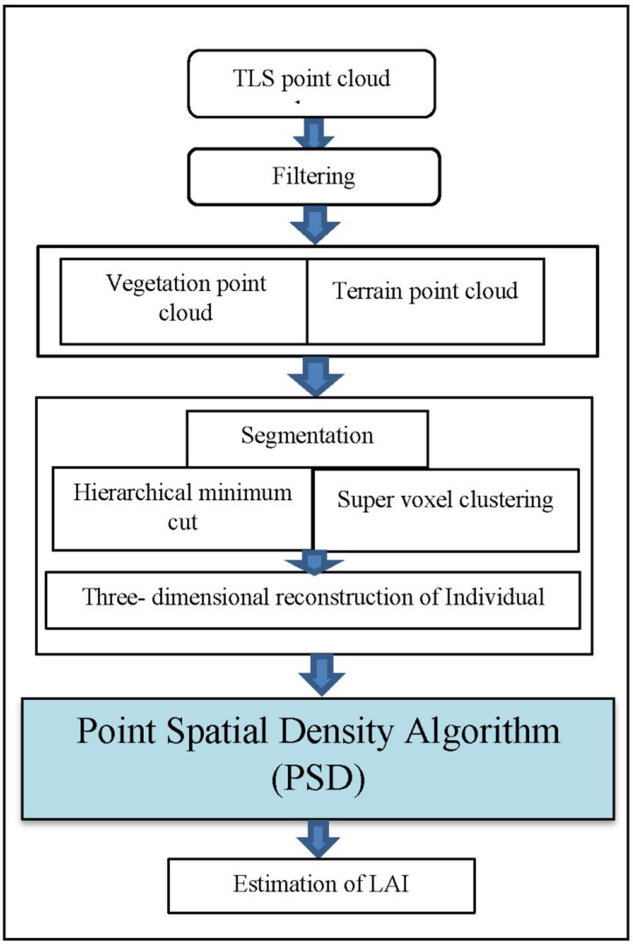

Figure 4.18: Flowchart depicting the overall workflow of LAI estimation

4.2.2.2 Pre-Processing of the TLS Point Cloud: Filtering

Before the implementation of the segmentation algorithm, the raw point cloud must be pre-processed. The point cloud was filtered into vegetation point cloud and terrain point cloud (Figures 4.12 and 4.13) using a thresholding based filtering algorithm (Zhang et al., 2003; Zhang et al., 2016).

4.2.2.3 Three-Dimensional Reconstruction by Segmentation Methods

The TLS point cloud was segmented by using a hierarchical minimum cut segmentation and super voxel clustering segmentation. The segmented tree crown points and the tree trunk points which result in individual tree reconstruction were extracted as described in Section 4.2.1.2.1. The tree crown points and trunk points were extracted, and the individual trees along with the segmented super voxels were obtained as explained in Section 4.2.1.2.2.

4.2.2.4 Estimation of LAI by Point Spatial Density Algorithm

The reconstructed trees from both the segmentation methods were further processed to estimate LAI by developing a new algorithmic approach named as Point Spatial Density (PSD) algorithm. The number of points inside a box can be noted accurately. The following section describes the proposed PSD algorithm

4.2.2.4.1 Point Spatial Density Algorithm (PSD)

The algorithm is based on establishing a relationship between the number of points within a given area (n_p), point spacing (d). The proposed PSD estimates LAI as

$$\textbf{Leaf Area Index, LAI} = \frac{\boldsymbol{n_p\, d(x_t + y_t)}}{\boldsymbol{x_t y_t}} \left(\frac{\mathbf{1}}{\boldsymbol{z_t}}\right) \qquad (17)$$

where n_p is the number of points within a box dimension of height z_t, length x_t, and breadth y_t, d is the point spacing of the TLS point cloud. For the present study, the individual trees within a box dimension were segmented, and the PSD algorithm was implemented based on the point density of trees. The point spacing of the TLS point cloud is 6 mm. The LAI was calculated for

all the reconstructed trees in the study area. The performance of the PSD algorithm was validated by comparing the estimated LAI values with in-situ LAI measurements.

4.3 Estimation of Biophysical Parameters from AVIRIS-NG Hyperspectral Data by Integration with LiDAR Point Cloud

4.3.1 Methodology

The workflow of the methodology used in the study is depicted in Figure 4.19

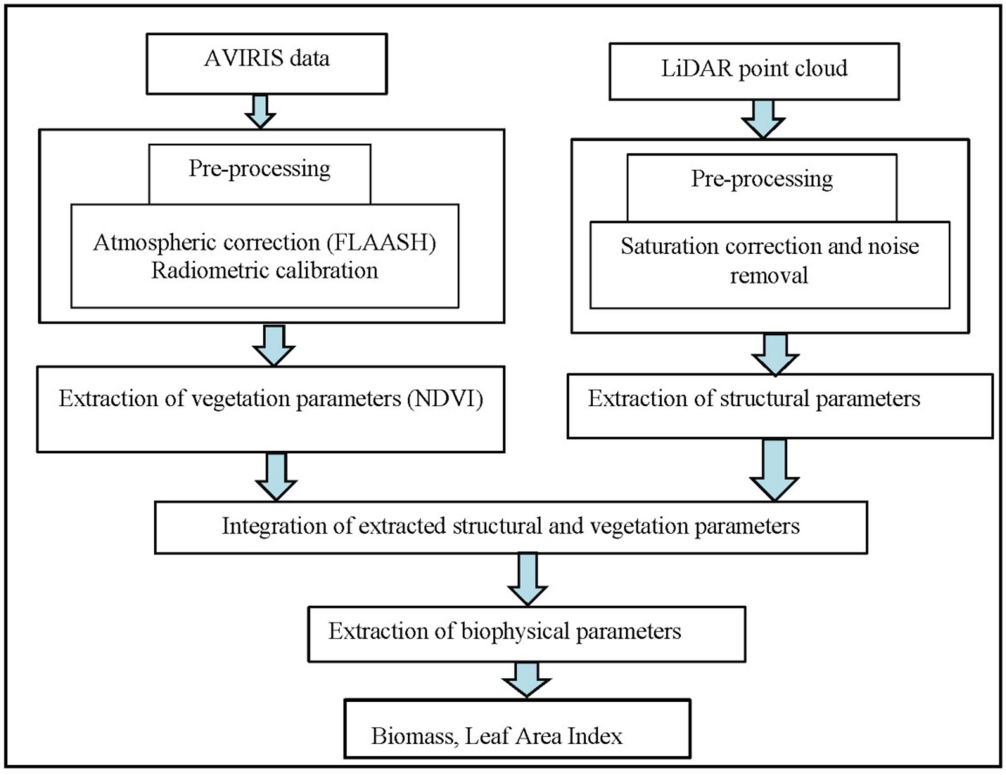

Figure 4.19: Flowchart depicting the methodology

4.3.2 Pre-Processing of AVIRIS - NG imagery

The AVIRIS-NG hyperspectral imagery was converted for radiometric and atmospheric distortion using FLAASH atmospheric correction (Adler-Golden et al.,1998; Matthew et al., 2000). The FCC of AVIRIS-NG after the correction is shown in Figure 4.20.

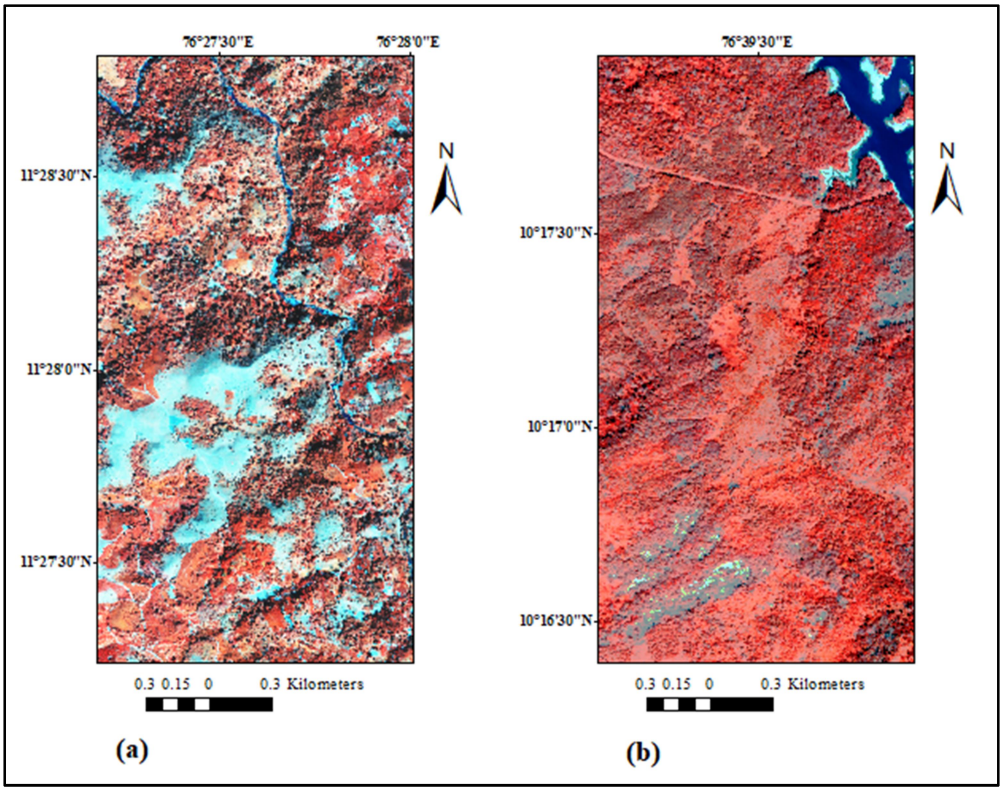

Figure 4.20: FCC of AVIRIS imagery after pre-processing for (a) Mudumalai forest and (b) Sholayar forest (Bands: R:83, G:65, B:55)

4.3.3 Integration of LiDAR Point Cloud and Hyperspectral Imagery

The point cloud-based raster canopy height models were integrated with hyperspectral imagery based spectral index on a pixel level fusion

strategy after linearly stretching the imagery and forming a new imagery with pixel vectors formed by applying spectral and canopy height values.

4.3.4 Estimation of Biophysical Parameters

4.3.4.1 Canopy Height Models

Canopy height was directly estimated from the LiDAR point cloud by the analysis of the waveform LiDAR point cloud. Canopy height models of both Sholayar forest and Mudumalai forests were linearly stretched to 5% and were then co-registered with the corresponding AVIRIS-NG imagery.

4.3.4.2 Estimation of Leaf Area Index

Leaf Area Index is obtained for both the study areas using

$$LAI = 0.57*\exp(2.33\ NDVI) \quad (18)$$

4.3.4.3 Estimation of Biomass

Forest biomass was estimated by support vector machine regression with radial basis function as the kernel function and Laplacian function as the loss function for handling the non-linearity among the input features. The biomass was obtained based on the non-parametric regression relationship between LAI and canopy height for both the study areas.

4.4 Chapter Conclusion

This chapter presented detailed methodologies used for the implementation of the objectives of the work. Results of the work are presented in the next Chapter.

******

Chapter 5

RESULTS AND DISCUSSION

Contents

This chapter presents the comprehensive results obtained from various cases of experiments. A comparative statistical analysis was made for all the methods with the corresponding reference field measurements. This chapter further elaborates the analysis of estimated biophysical parameters retrieved from the integration of multispectral imagery, hyperspectral imagery with spaceborne LiDAR point cloud. The results of LAI, height, and DBH of the trees sampling in Mudumalai forest from the terrestrial laser scanner point cloud are also described. The results are analyzed specifying the significance of each result and the relevance of the findings. The results are presented in the same order followed in the Chapter 4 methodology and experiments.

5.1 Estimation of Biophysical Parameters by the Integration of Spaceborne LiDAR Point Cloud and Multispectral Imagery

5.1.1 Estimation of Canopy Height

The Digital Elevation Model (DEM), Digital Surface Model (DSM) and the Canopy Height Model (CHM) generated from the GLAS point cloud

captured over Mudumalai forest are depicted in the Figures 5.1, 5.2 and 5.5. The DEM, DSM, and CHM for the Sholayar forest are shown in Figures 5.3, 5.4 and 5.6. The CHM of Sholayar forest indicates the tree heights ranging from 1m to 66 m. Most of the trees are within the height of 20.52 m, the mean height of the area. For the Mudumalai forest, the range of the tree height is 1m to 60 m.

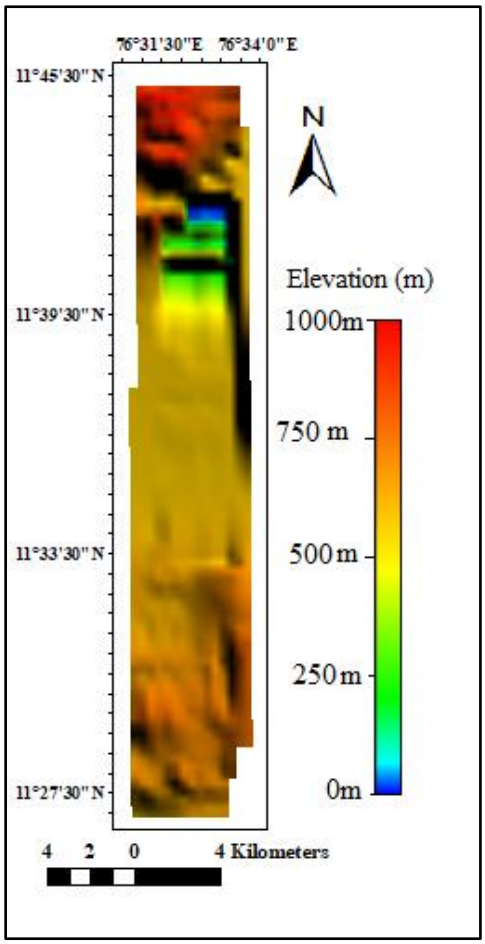

Figure 5.1 DEM of Mudumalai forest

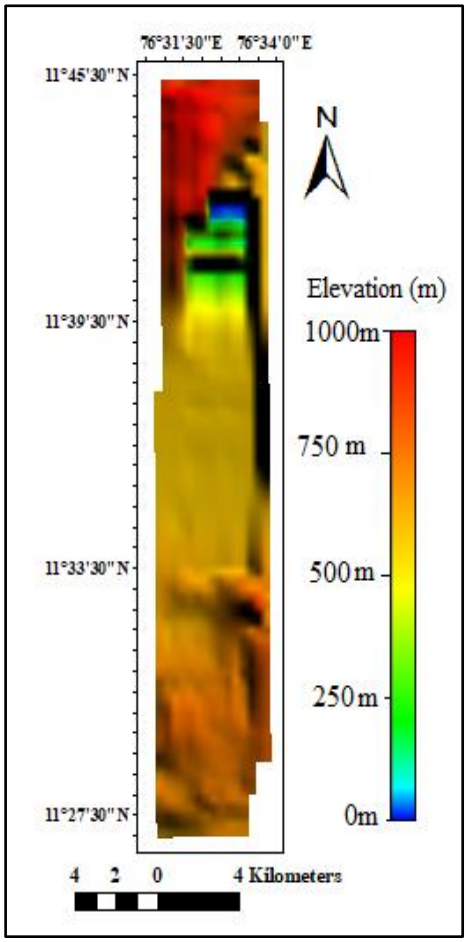

Figure 5.2 DSM of Mudumalai forest

The elevation values of the Mudumalai forest vary between 1 m to 1000 m (Figure 5.1). From the DEM and DSM, canopy height models were obtained by normalizing DEM and DSM. The elevation values of Sholayar

forest are also varying up to 1000 m as given in DEM and DSM. From Figures 5.1 and 5.2, there are regions with lower elevation values (0 to 250 m) and higher elevation values (750 m- 1000 m).

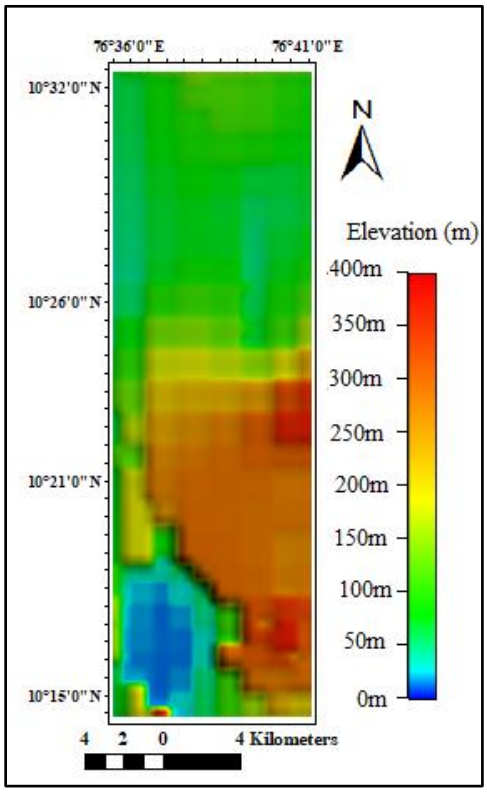

Figure 5.3 DEM of Sholayar forest

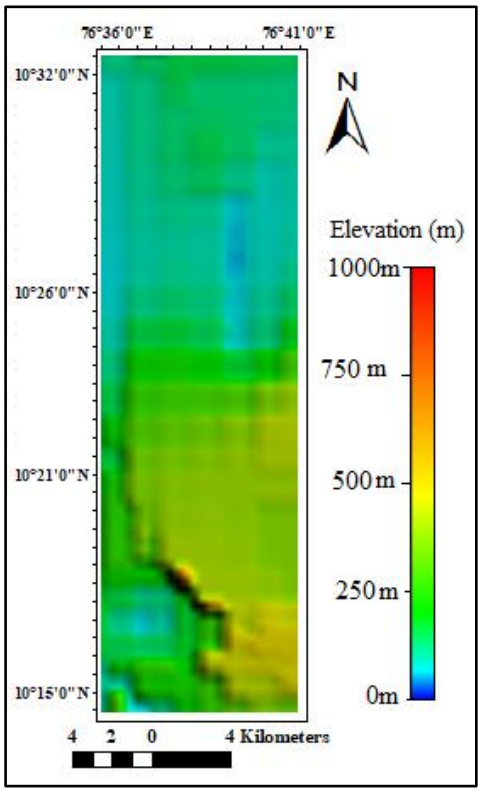

Figure 5.4 DSM of Sholayar forest

The DEM of Sholayar forest shows the highest elevation of 400 m at the middle left portion of the image (Figure 5.3). Lower elevation regions are also there of range 1 m to 40 m. DSM of Sholayar forest indicates a maximum elevation value of 1000 m as in Figure 5.4.

As evident from Figure 5.6 most of the trees are in the height of range 1 to 66 m in the Sholayar forest. The canopy height model indicates the possibility to model the canopy height of the dense forest of Mudumalai and Sholayar forest from the GLAS full waveform datasets. The CHM of Sholayar

region indicted the canopy height values of forest area. From the CHM model (Figure 5.6), the bottom portion and the middle portion of the image in the Sholayar forest indicate lower canopy height in the range 1 m to 15 m

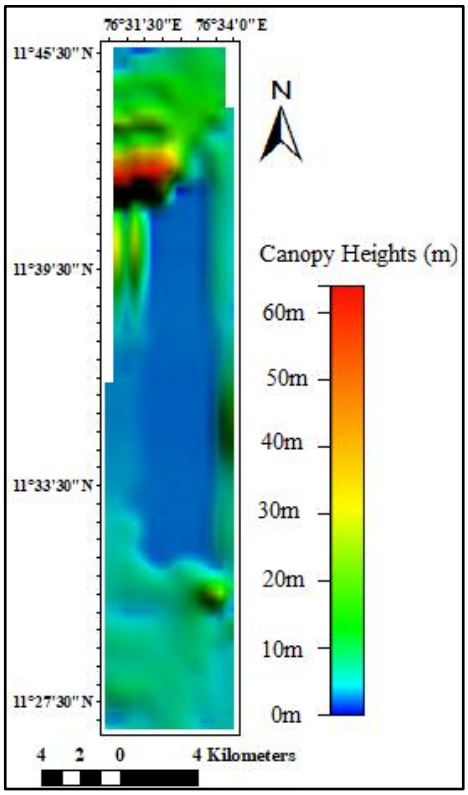

Figure 5.5 CHM for Mudumalai Forest

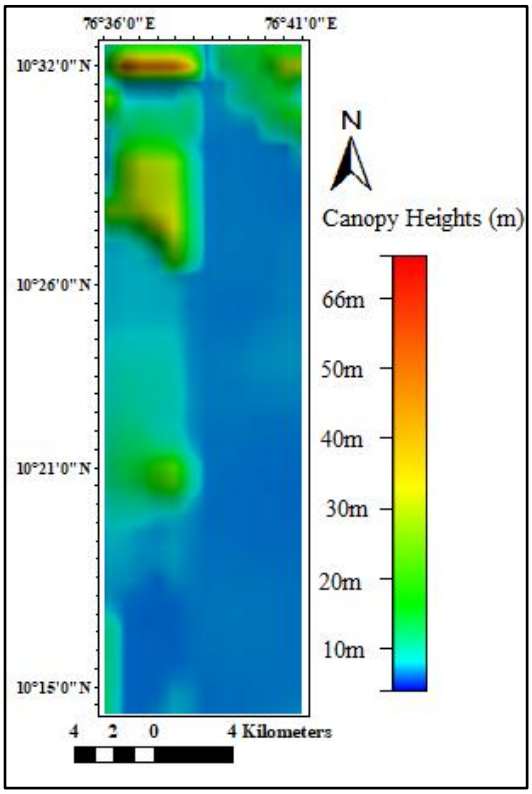

Figure 5.6 CHM for Sholayar Forest

In the region with height values 1 to 5 m, the presence of undergrowth is predominant. In some regions of Sholayar forest, the height of the canopy is in the range 20 m to 30 m which indicates taller tree species. From the CHM model, it is also evident that there are regions with taller tree species with height in the range 40 m to 66 m.

From the CHM of Mudumalai forest, trees of height 1m to 5 m indicates the predominance of undergrowth and most of the trees are of height values between 1 m to 15 m. In some regions of Mudumalai forest, the tree

height varies from 15 m to 30 m as in Figure 5.6. There are also regions with taller trees of height 40 m – 60 m range indicating the presence of old preserve woody forest species, specific to the Western Ghats.

5.1.1.1 Validation of Canopy Height of Mudumalai Forest and Sholayar Forest

The canopy height obtained from CHM of both the forest region is compared with field measurements in the corresponding sites. Figure 5.7(a) shows the comparison of estimated canopy height and the measured canopy height. A strong correlation of about R^2 =0.98 exists between the estimated canopy height and the measured canopy height for Mudumalai forest.

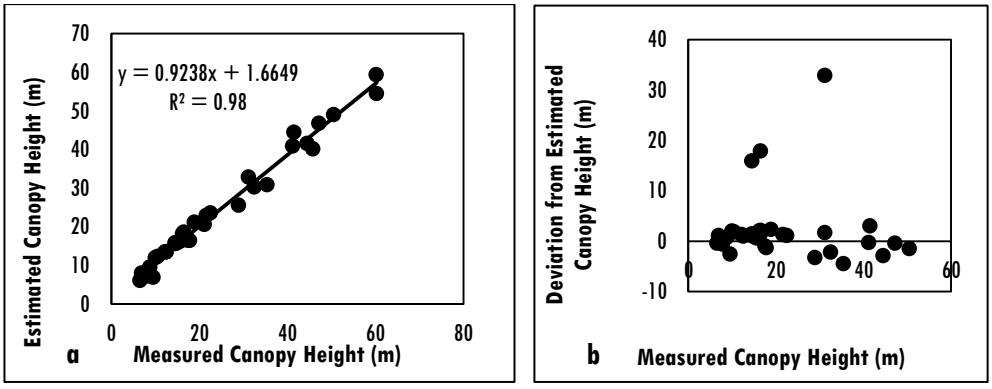

Figure 5.7: a) Variation of estimated tree height with respect to the measured tree height of Mudumalai region, and b) Deviation of the estimated tree height with respect to the measured height for Mudumalai forest

Deviation of the estimated height from the CHM with respect to the measured canopy height is shown in Figure 5.7(b). The deviation of the estimated canopy height is about $\pm$ 15% of the measured tree height. Contrary to some of the studies, which have used airborne LiDAR point cloud and indicate a consistent underestimation of the canopy height, the results indicate both the possibilities of underestimation and overestimation of the canopy height. The

presence of substantial understory and the generally rugged nature of the terrain of the study site may be responsible for the change of sign of the deviation of estimated canopy height in comparison with the measured canopy height. From Figure 5.7(a) it is clear that most of the study area is covered with trees of lower and medium height, indicating vertical degradation of the forest, the loss of tall and woody tree species for which this study site (Mudumalai forest) is known generally.

The scatter diagram plotted for comparing the image estimated height and the measured tree height of Sholayar region indicated a strong correlation of about R^2 =0.97, and as shown in Figure 5.8.

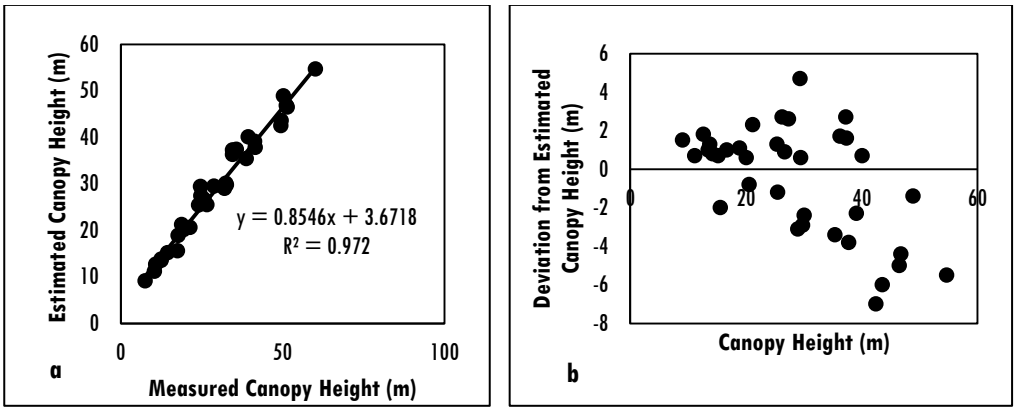

Figure 5.8: a) Estimated canopy height versus measured tree height and b) Deviation of the estimated canopy height from the measured height for Sholayar forest

Figure 5.8(a) shows the comparison of estimated canopy height and the corresponding measured canopy height. A strong correlation of about R^2=0.97 exists between the estimated and the measured canopy heights for Sholayar forest. Deviation of the estimated height with respect to the measured canopy height is shown in Figure 5.8(b). The deviation of the estimated canopy height is about $\pm$ 15% of the measured tree height.

Similar to the observed deviation for canopy heights of Mudumalai, the deviation indicates both the possibilities of underestimation and overestimation

of the canopy height. As the tree height increases, the LiDAR point cloud based canopy height is substantially underestimated. From Figure 5.8(a), most of the study area is covered with trees of lower and medium height, indicating vertical degradation of the forest, as also observed in Mudumalai forest region.

5.1.2 Estimation of Canopy Density and Understory Vegetation Height

The canopy density for both the Mudumalai forest and Sholayar forest was obtained and are presented in Figures 5.9 and 5.10 respectively.

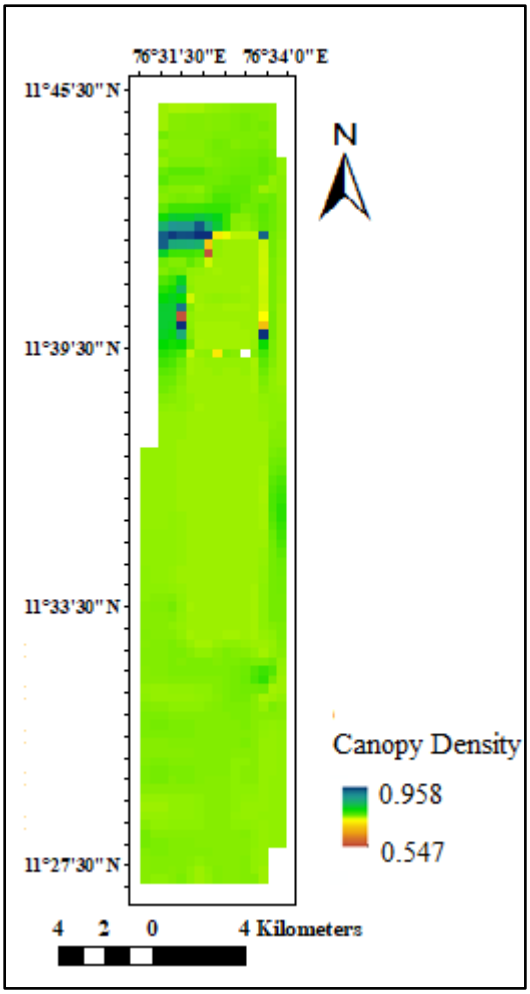

Figure 5.9 Canopy density of Mudumalai forest

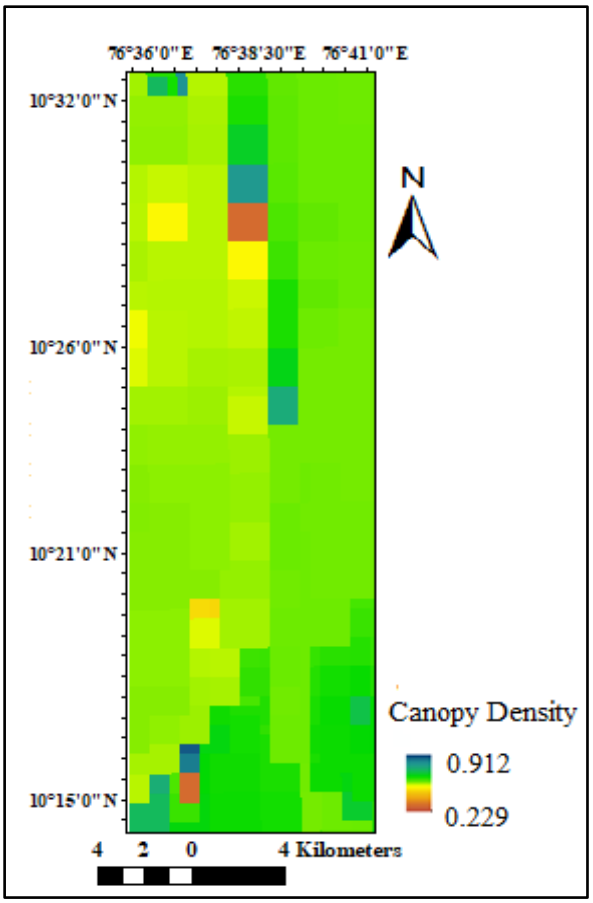

Figure 5.10: Canopy density of Sholayar forest

The canopy density of Mudumalai forest shows great variation from 0.547 to 0.958. The regions with higher canopy density are correlated with the location of thick forest coverage with some extent of understory vegetation. A variety of tree species with clumped branches are seen with some thick understory vegetation of different shrub species. Similar to Mudumalai forest, the canopy density of Sholayar region exhibits a great variation in the density ranging from 0.22 to 0.912. Dense forests can be seen at forest regions where the canopy density is higher. The spatial variation indicates the degradation of forest patterns.

The estimated undergrowth vegetation with height up to 5 m is represented in Figure 5.11 for Mudumalai forest. The height of undergrowth of Sholayar forest (Figure 5.12) is found to be slightly lower (up to 4 m).

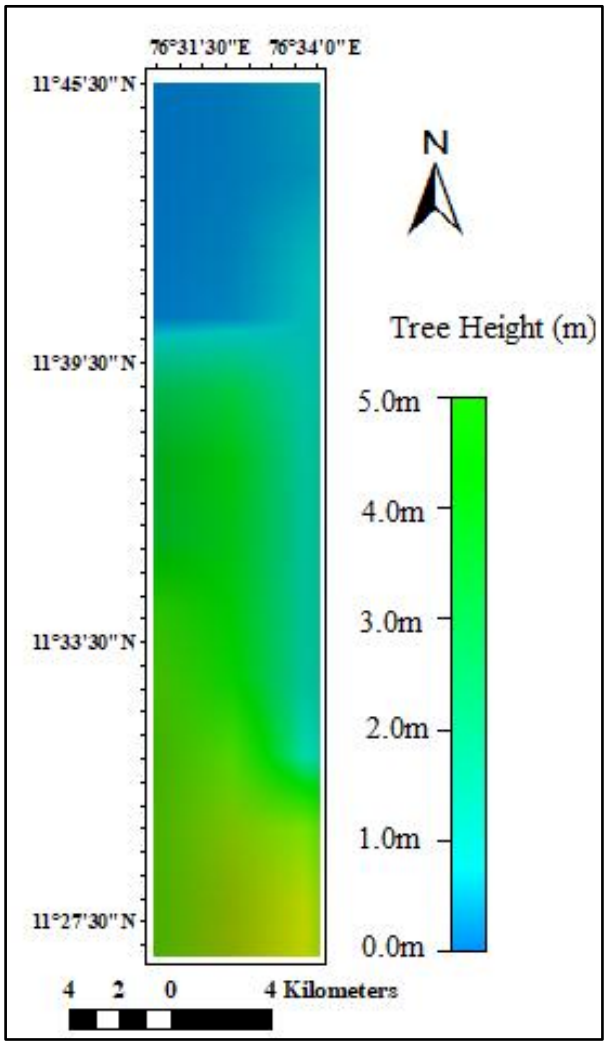

Figure 5.11: Understory vegetation height of Mudumalai forest

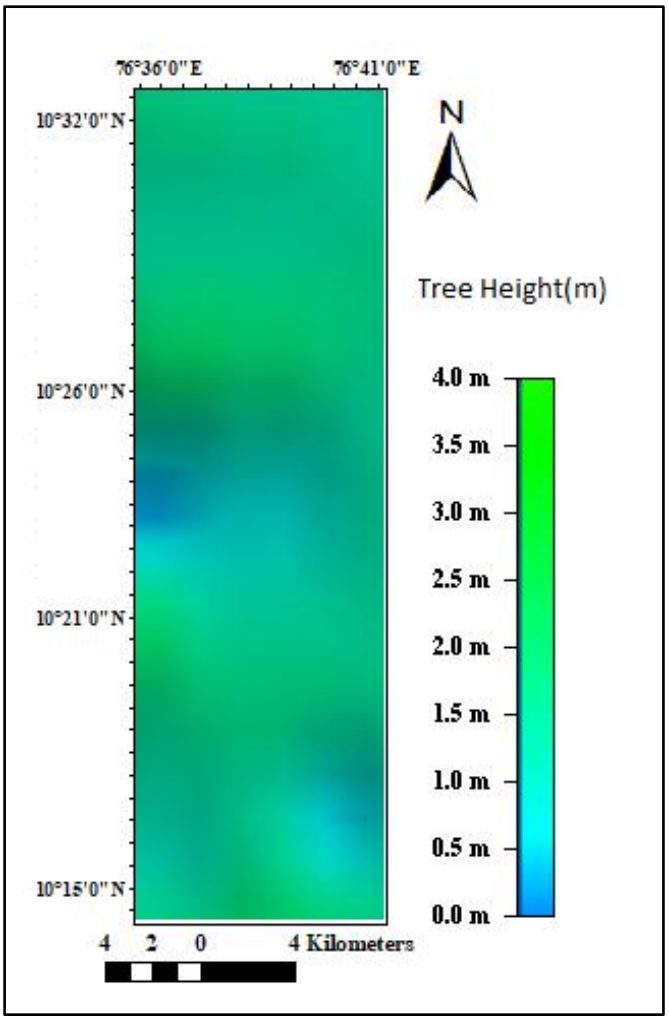

Figure 5.12: Understory vegetation height of Sholayar forest.

The spatial variation of understory vegetation height of the Mudumalai forest indicates the presence of thick undergrowth, mainly perennial weed/shrub species height cut off up to 5 m. Various studies have reported the presence of a range of invasive species such as Lantana Camera in these forests. A large number of shrubs, moss cover, grassy species and also a variety of species with medicinal significance are estimated to be covering most of the undergrowth of these forest regions. Similarly, for Sholayar

forest, the understory indicates the presence of a variety of shrubs, moss covers with medicinal properties as undergrowth. For regions with taller trees, thick understory vegetation is found.

From the canopy density estimates, for the regions having higher canopy density, the understory vegetation growth is found to be less. Canopy density for Mudumalai forest has an average value of 95% and the region having lower canopy density indicates the presence of thick undergrowth vegetation. For the Sholayar forest, the canopy density has an average value of 91%. Thick understory vegetation growth is seen in the region with lower canopy density.

5.1.2.1 Statistical Validation of Understory Vegetation Height of Mudumalai and Sholayar Forests

The height of understory vegetation of Mudumalai forest and Sholayar forest were compared with the measured height. As the trend of over-story vegetation, there is a strong correlation (R^2=0.91) between the estimated and measured understory vegetation heights. The minimum and maximum deviation from the measured tree height is also indicated as a scatter diagram. Figure 5.13 (a) shows the scatter plot of estimated understory vegetation height versus measured understory vegetation heights in the case of Mudumalai forest.

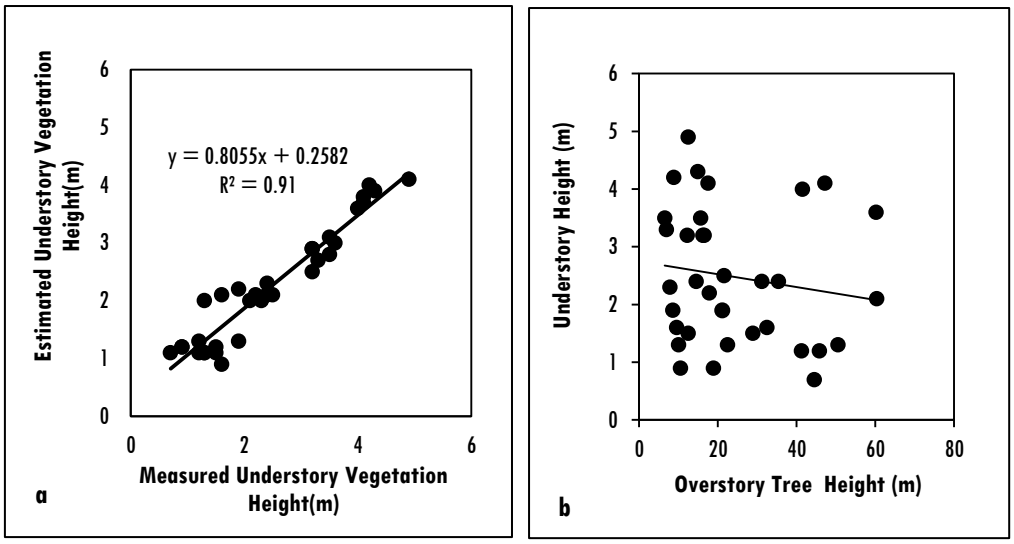

Figure 5.13: a) The variation of estimated understory height from measured values and b) Relationship of understory vegetation height with the canopy height for Mudumalai forest

Comparison of the understory vegetation height of Mudumalai forest with respect to canopy height indicates that for the canopy height of lower to medium height, there is substantial understory vegetation with height varying between 1 and 5 m. However, in the case of taller trees, relatively less proportion of understory growth is evident with height less than 2 m. Scatter plot showing the variation of understory vegetation height with respect to the canopy height of Mudumalai forest is also shown in Figure 5.13 (b). As evident from the results of canopy height modeling, most of the areas with lower to medium level canopy heights have thick understory. Based on the literature available, the dominant vegetation species which form part of the understory vegetation are invasive species which include Lantana Camera, Crotalaria Laevigata, Nilgirianthus Barbatus, Mimosa Pudica etc (Muthuramkumar et al., 2006; Latifi et al., 2017) and shrubs with medicinal values like Mimosa pudica, Leucas indica, Tectonia grandis etc. As the trees become much taller, the presence of undergrowth is low. The undergrowth

species typically found when trees are taller are grass species and other small herbs which are less than 1m tall which indicates the healthy status of vegetation in these regions.

Similarly, the height of understory vegetation was compared with the measured height for Sholayar forest. As the trend of overstory vegetation, there is a correlation (R^2 =0.73) between the estimated and measured understory vegetation heights. The minimum and maximum deviation from the measured tree height is plotted as a scatter diagram. Figure 5.14(a) shows the scatter plot comparing estimated understory vegetation height with measured understory vegetation height of Sholayar forest.

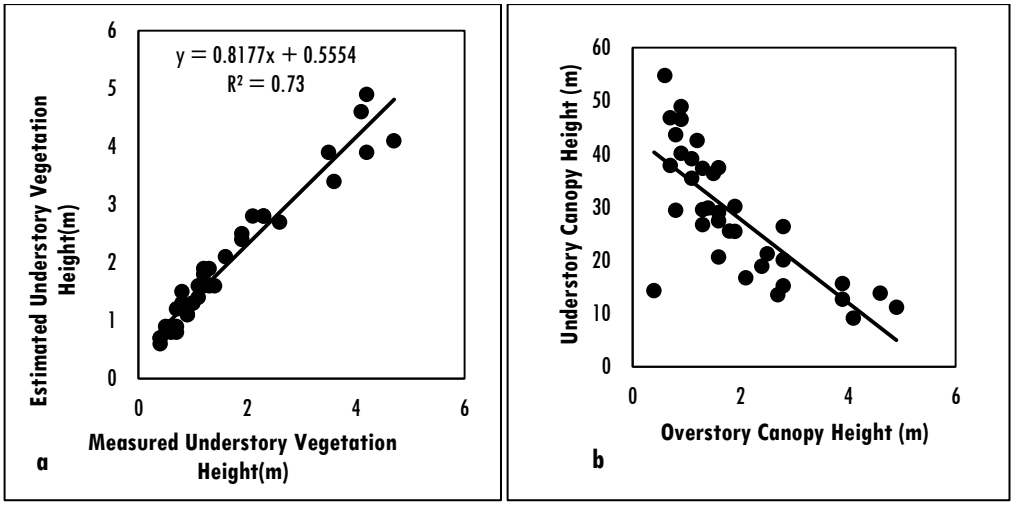

Figure 5.14: a) Scatter plot showing the variation of understory vegetation height with the measured understory height and b) the variation of estimated understory vegetation height and the canopy height estimated for Sholayar forest

Scatter plot showing the variation of understory vegetation height with respect to the canopy height for the Sholayar forest is also shown in Figure 5.14(b). Comparison of the understory vegetation height with respect to canopy height indicates that for the canopy height of lower to medium height,

there is a substantial understory vegetation growth with height varying between 1 and 4 m. However, in the case of taller trees, relatively less proportion of understory growth is evident with height less than 2.5 m.

As evident from the results of canopy height modeling, most of the area with lower to medium level canopy height have thick understory, as also observed for Mudumalai forest. The vegetation species which form part of the understory vegetation are invasive species which include Lantana Camera, Hydrocotyle javanica and moss covers (Muthuramkumar et al., 2006). There are several shrubs which have medicinal values like Anona squamosa, Dioscoeia bulbifera, Momordica dioica, Ficus racemosa, etc. are found to be abundant in these regions. The medicinal values of these shrubs include treatment of tumors, cancer, diabetes, etc. As the tree heights become much taller, the presence of undergrowth is low. In the case of the taller trees, the common undergrowth species are grass or herbs with a height of approximately 1 m to 2 m. The undergrowth species typically found when trees are taller are grass species, and other small herbs which are less than 1 m tall indicates the healthy status of vegetation in these regions.

The estimated canopy height and understory vegetation height values indicate consistent correlation with the measured values. A strong correlation is obtained between canopy density and understory vegetation height. The variation in canopy density is due to several factors like fire, landslides or ecological successions, etc. which severely disturb forest (Vandermeer, 1995). Also, anthropogenic activities like population pressure, fuel and fodder collection, fire, grazing, timber extraction affect the forest canopy and reduce the canopy density considerably (Hussin and Sha,1996; Geist & Lambin,2001). The variation in canopy density is also due to the microenvironmental factors like light availability, nutrients, and soil moisture.

The observed lower canopy density indicates the human intervention as well as forest microenvironmental conditions. LiDAR point cloud is found to be leading overestimation at lower level tree canopy height and understory invasive species of minimum height 1 m can also be estimated by LiDAR point cloud. Underestimation is less compared to overestimation. In the case of taller trees, the deviation is less when comparing the canopy height estimated with the in-situ measurements. Similar kind of observations of overestimations and moderate underestimation are reported in the literature (Lim et al.,2003; Wulder et al., 2007).

The canopy height is an important significant source of information for biomass prediction and carbon accounting. Also, estimation of the height of the undergrowth provides potential information about soil condition, canopy gaps and the possible existence of invasive species in the understory.

5.1.3 Estimation of Vegetation Indices by Integrating Landsat Imagery and LiDAR Point Cloud

Vegetation indices were extracted for Mudumalai and Sholayar forest regions. NDVI, DVI is shown in Figure 5.15 and EVI, GDVI for Mudumalai are represented in Figure 5.16. GRVI and LAI are shown in Figure 5.17, MSI and NDWI for Mudumalai are shown in Figure 5.18. GNDVI and RVI of Mudumalai are given in Figure 5.19, and SAVI for Mudumalai is given in Figure 5.20.

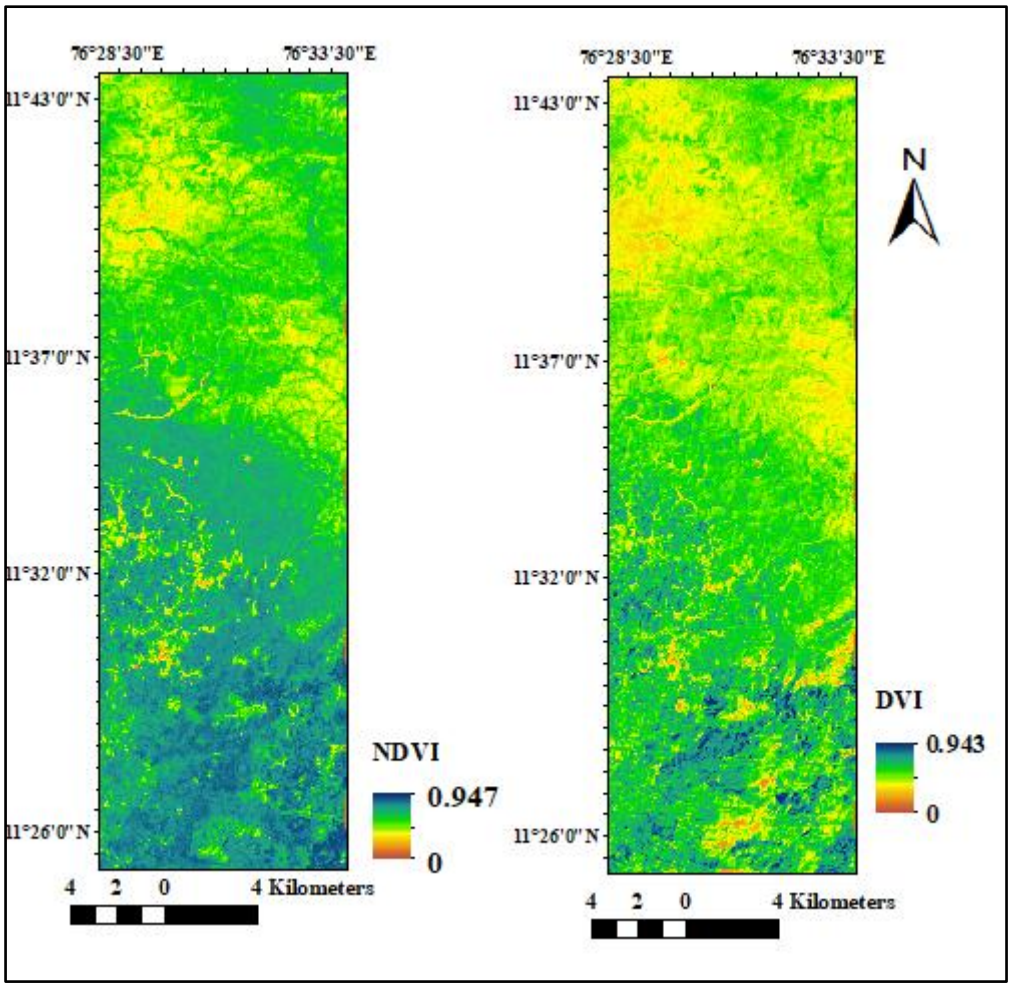

Figure 5.15: NDVI and DVI of Mudumalai Forest

NDVI values indicates a maximum of 0.947 and the values predict the structure of the canopies in the forest. The lower portion of Figure 5.15 indicates a higher value of NDVI which shows the predominance of woody and nonwoody tree species and less level of disturbance of forests. Here the trees with height range 10-30 m are predominant as evident from the CHM model. The presence of understory species is also dominant in these regions with height ranging from 0.5 m to 4 m. In the upper portion and middle portion, there are some regions with lower value of NDVI which indicates the

disturbed forest area, settlement area, and waterbody. DVI of Mudumalai forest varies with a maximum value of 0.943. The DVI is found to be higher for the bottom portion of the study area which indicates the presence of diverse forests with woody and nonwoody tree species with a height range 10 - 35 m with marginal disturbance. In the top portion of the image (Figure 5.15), the lower DVI indicates the degradation of forest and the presence of the built-up area.

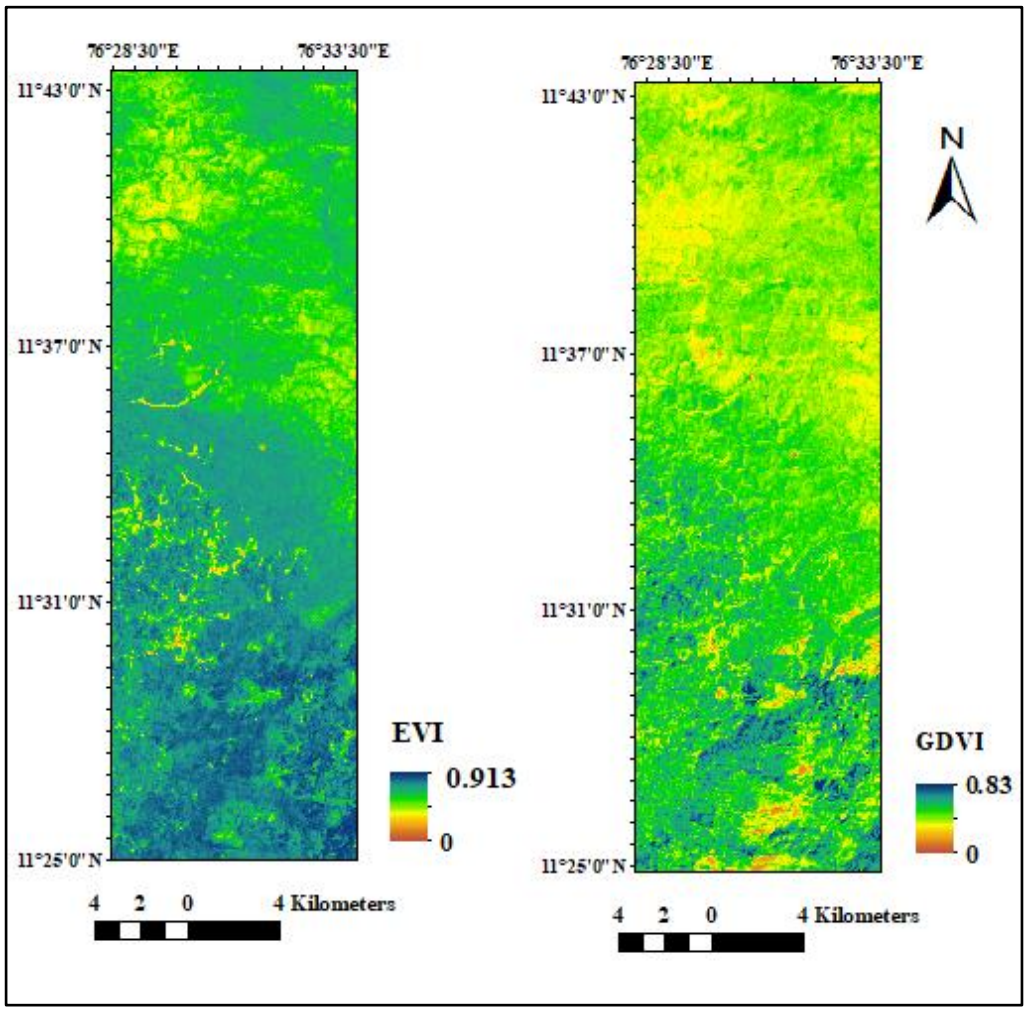

Figure 5.16: EVI and GDVI of Mudumalai Forest

EVI of Mudumalai forest varies with a maximum value of 0.913 indicates the regions with higher LAI values. Only a few portions of the image (Figure 5.16) indicate lower values of EVI, at the bottom portions higher value of EVI indicates the presence of thick canopy and understory vegetation as clear from the CHM model. GDVI indicates a maximum value of 0.83, showing the presence of moderate to higher nitrogen in the trees. In the bottom left portion of the image (Figure 5.16), the higher value of GDVI can be observed. In the upper portion of the image, the lower value of GDVI is dominant.

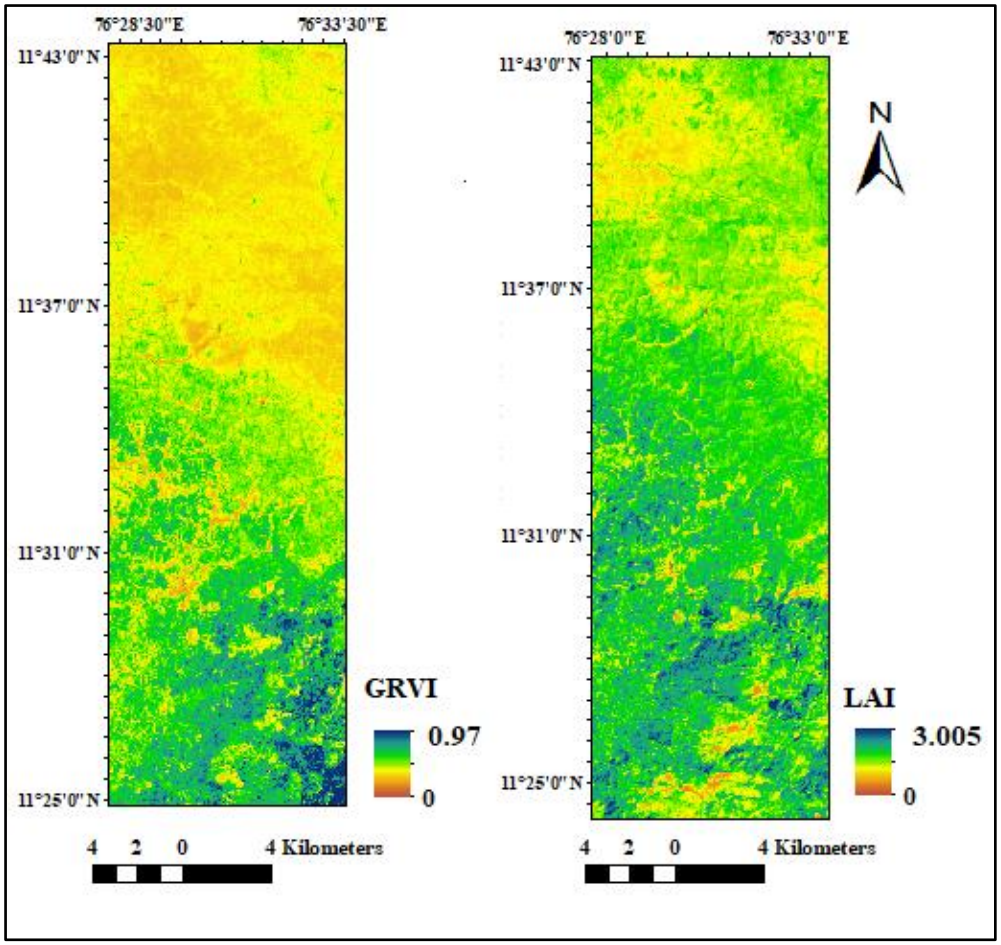

Figure 5.17: GRVI and LAI of Mudumalai

GRVI of Mudumalai forest indicates a maximum value of 0.97. The regions of the bottom portion of the image (Figure 5.17) indicates higher values of GRVI in which the canopy height of the region range from 15- 30 m as per CHM model. This shows the diversity of the forest in these portions, with a large number of tree species and a thick understory. The LAI value of Mudumalai forests has a maximum value of 3.005.

LAI is found to be higher at the bottom portion of the image (Figure 5.17). In these regions, a large number of tree species along with thick understory are seen, and height of the trees in these regions varies from 10 m - 30 m with thick understory vegetation with 1m to 5 m height as shown in the CHM model. The region with lower value of LAI indicates the degradation of forests, or the presence of built up lands, shrubs or water body.

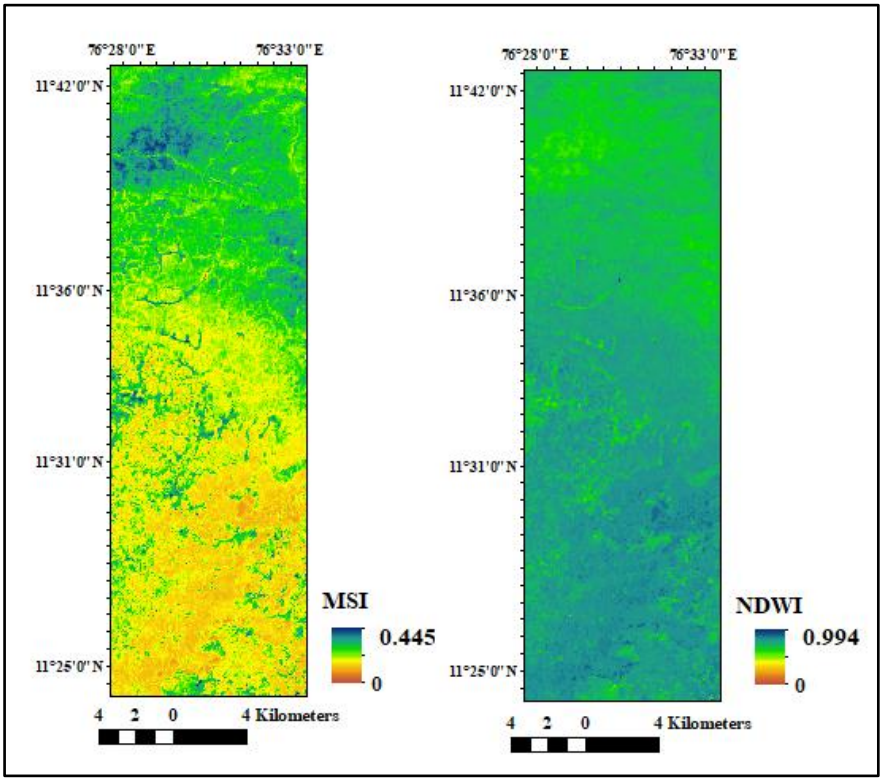

Figure 5.18: MSI and NDVI of Mudumalai Forest

Moisture stress index of Mudumalai forest indicates a maximum value of 0.445 and the regions with the high values indicated a water stress region with less water content. The bottom portion of the image (Figure 5.18) indicates lower values of MSI. The top right portion has a higher value of MSI which indicates water content is high in this region. The NDWI of Mudumalai forest indicates a maximum value of 0.994, which indicates higher forest water content and forest cover. NDWI can indicate the moisture content and is a drought indicator which gives quicker response to drought. GNDVI is found to be higher at the bottom portion of the image (Figure 5.19) in which the tree species having height 10 m-30 m are found to be dominant as per the CHM model. In the image, yellowish portions indicate lower GNDVI values.

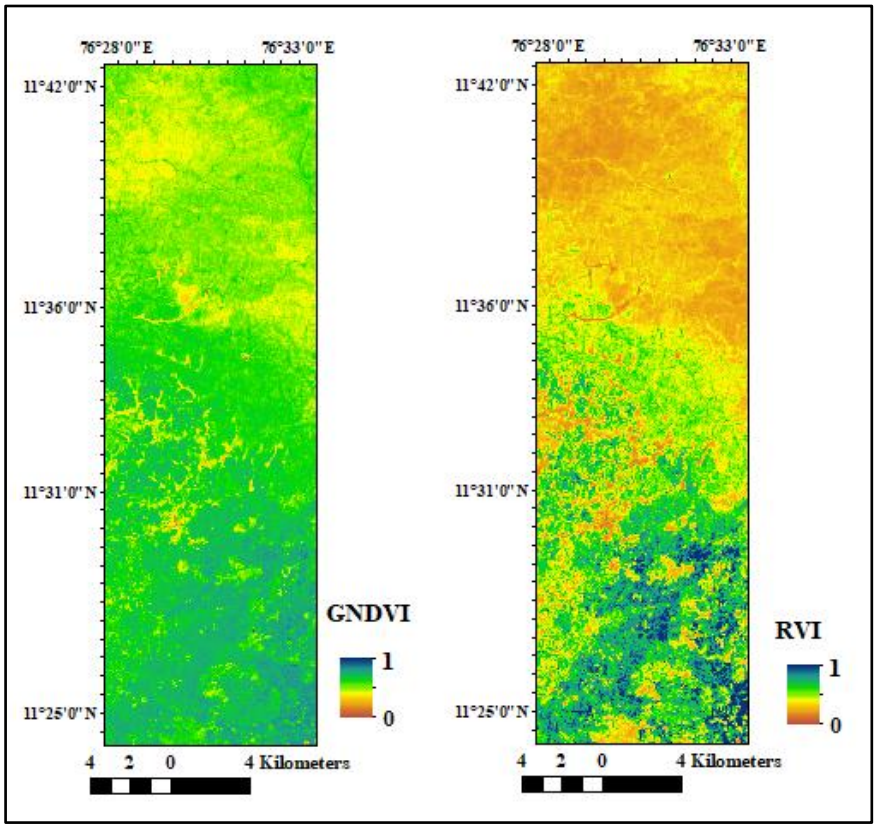

Figure 5.19: GNDVI and RVI of Mudumalai forest

GNDVI value of Mudumalai forest calculated has a maximum value of 1. The maximum value of RVI is 1 and can be used to infer about forest biomass condition. RVI is found to be less at the upper right portion of the image (Figure 5.19) wherein these regions tree species are found to be less, and the degradation of the forests is high. At the bottom portion of the image, RVI is high which shows the presence of thick canopy and understory tree species.

SAVI of Mudumalai forest indicates a maximum value of 1.32 which is also related to forest biomass. At the bottom portion of the image (Figure 5.20), SAVI value is higher which indicates the presence of thick canopy. The height of the tree species is in the range 10 m- 30 m as in the CHM model. In some upper left regions of the image, SAVI is found to be lower, and in these regions, the degradation of forests can be high or there is less proportion of forest.

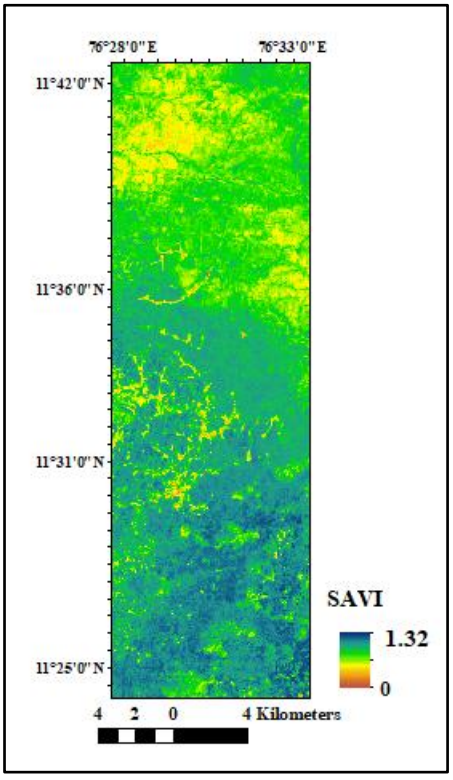

Figure 5.20: SAVI of Mudumalai Forest

For the Sholayar forest, the vegetation indices extracted for the Landsat imagery are shown in the following figures. Figure 5.21 indicates the DVI and EVI of Sholayar forest

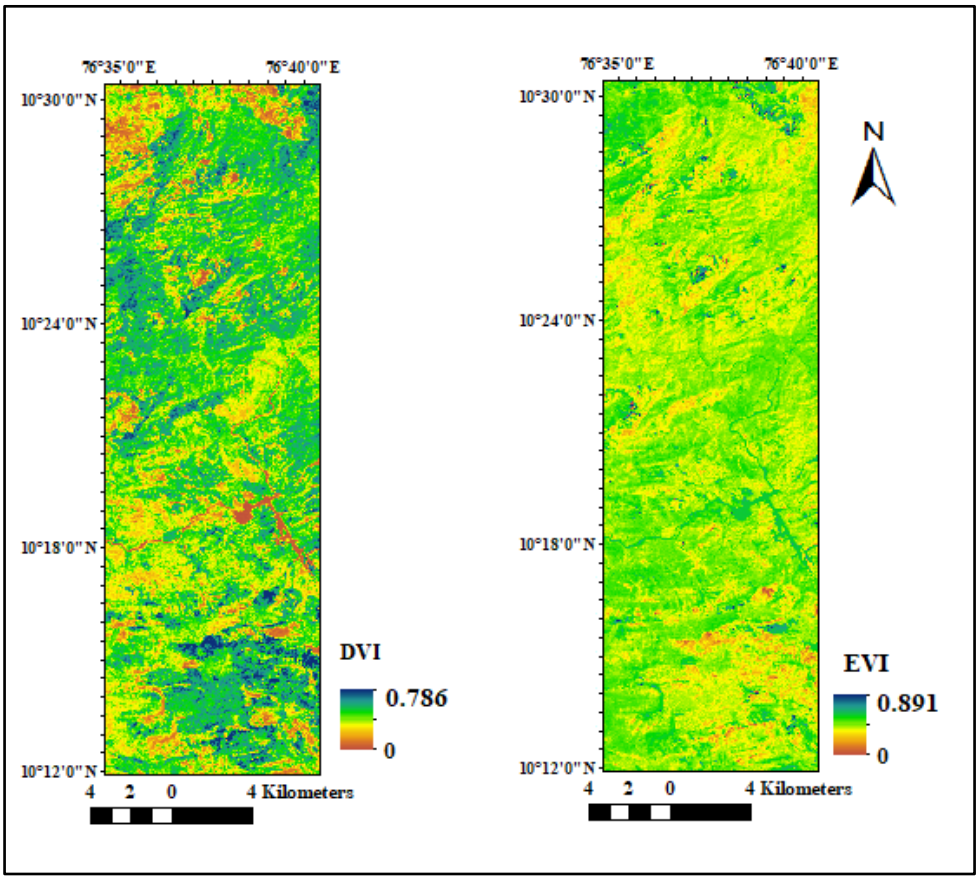

Figure 5.21: DVI and EVI of Sholayar forest

DVI of Sholayar forest varies with a maximum value of 0.786. The red portions of the image (Figure 5.21) indicates lower values of the DVI, which shows the absence of vegetation. EVI of Sholayar varies up to a maximum value of 0.891 and indicates the regions with higher LAI values. Some of the bottom right portions of the image (Figure 5.21) indicates lower values of EVI, mainly in the regions without vegetation area or the waterbody.

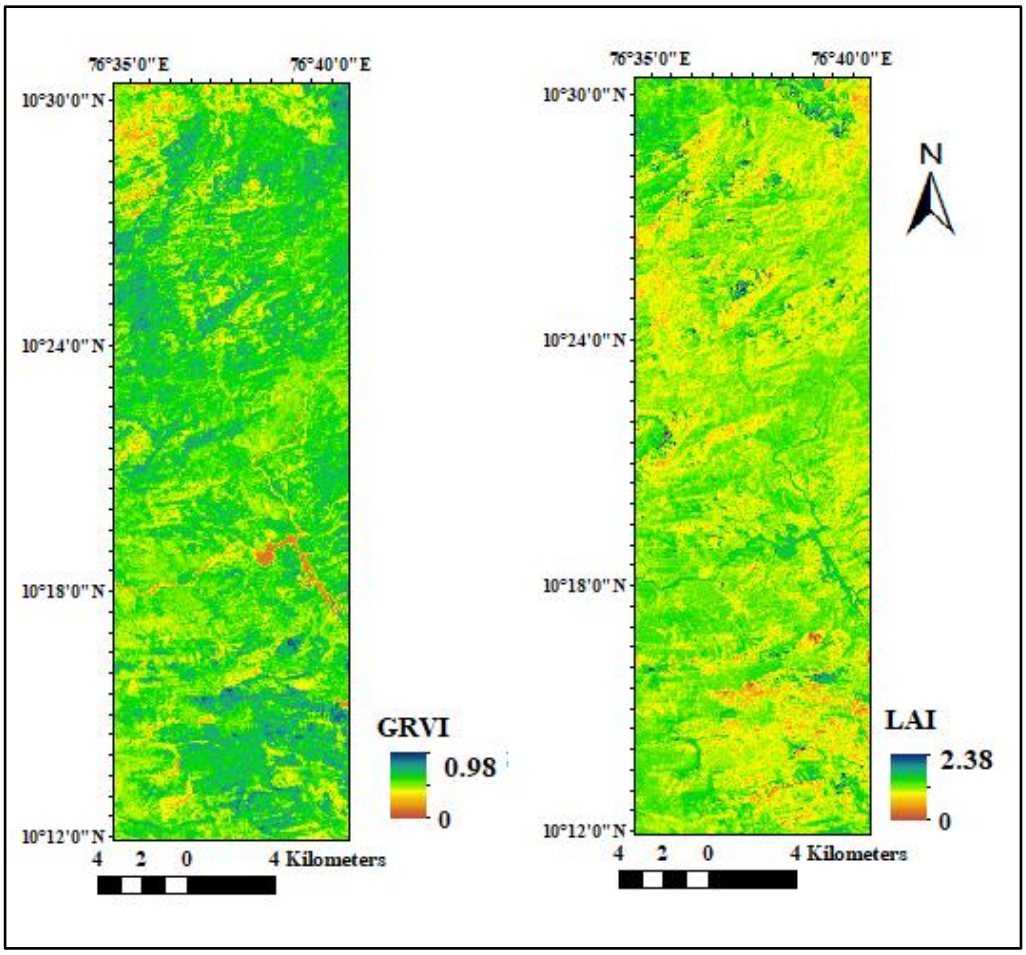

Figure 5.22: GRVI and LAI of Sholayar forest

Figure 5.22 depicts the GRVI and LAI of Sholayar forest. GRVI indicated a maximum value of 0.98 and is less sensitive to regions with high vegetation cover. The regions with red color in the image (Figure 5.22) indicate a lower value of GRVI in which forest is degraded or absent. LAI value of Sholayar forest has a maximum value of 2.38. The bottom left portion of the image (Figure 5.22) indicates lower LAI values indicating severe degradation of forest. The portions with a higher value of LAI is found because of the thick canopy with height ranging from 5 m-25 m as also evident in the CHM with a large number of tree species with a thick understory.

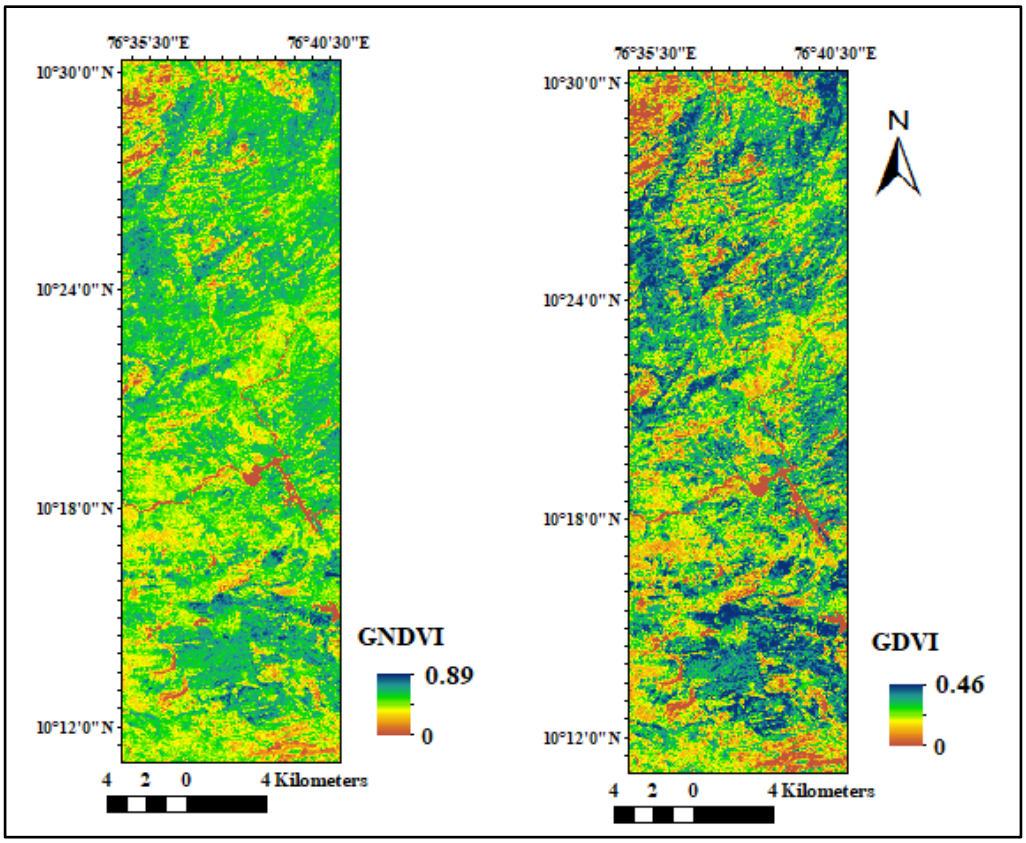

Figure 5.23: GNDVI and GDVI of Sholayar forest

The GDVI and GNDVI of Sholayar forest area are shown in Figure 5.23. The upper portions and some regions of the middle and lower portion of the image (Figure 5.23) with lower values of GNDVI are indications of degradation of the forest. GDVI indicates a maximum value of 0.46, indicating the substantial portion of the Sholayar forest degraded. The portions with a higher value of GDVI have a thick canopy with height ranging from 5 m to 25 m, as shown in the CHM model of Sholayar forest. The Moisture Stress Index and NDWI of Sholayar forest are shown in Figure 5.24. Moisture stress index of Sholayar forest indicates a maximum value of 2.07 and the regions with the high value indicates water stress. The NDWI of Sholayar forest indicated a

maximum value of 1 which indicates higher forest water content and forest cover. NDWI can indicate the moisture content and is a drought indicator which gives quicker response to drought. The upper portion of the image (Figure 5.24) and in some parts of the lower portion indicates lower values of NDWI, which shows the degradation of the forest.

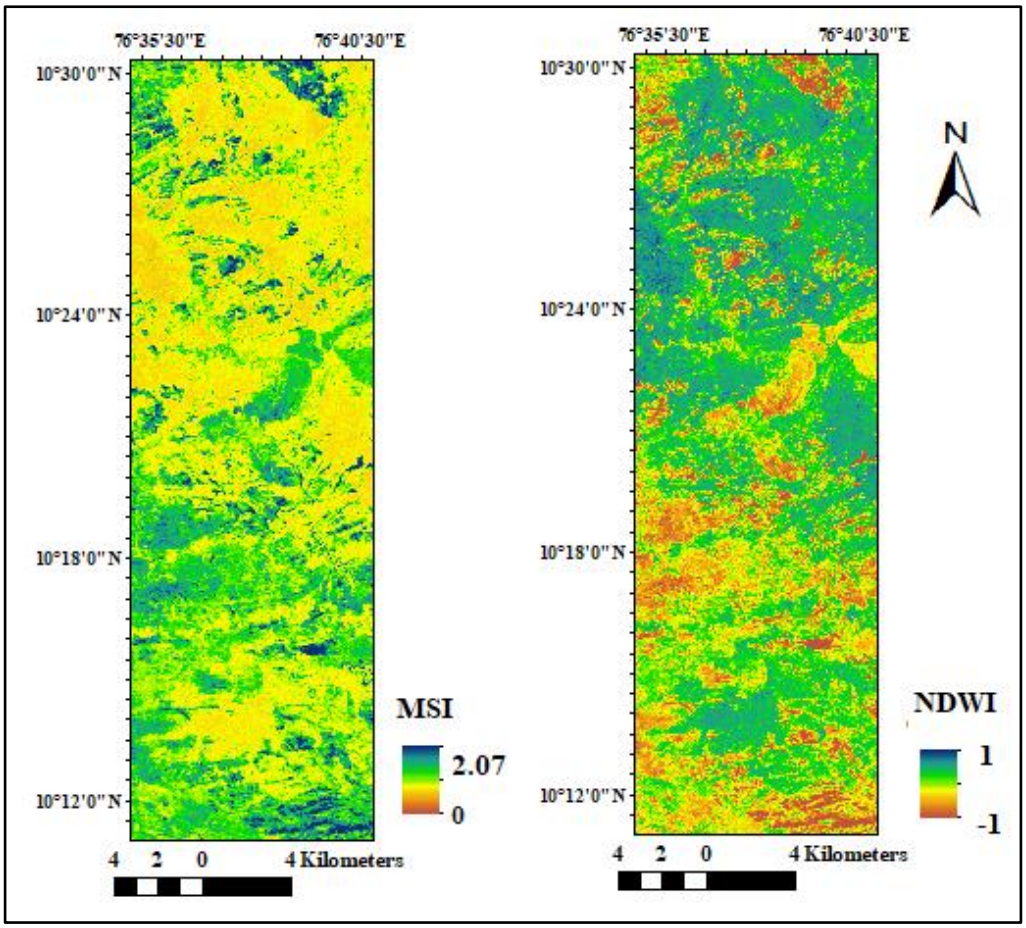

Figure 5.24: Moisture Stress Index (MSI) and NDWI of Sholayar

The RVI, SAVI, and NDVI of Sholayar forest are presented in Figures 5.25 and 5.26 respectively.

SAVI of Sholayar forest indicated a maximum value of 0.794. The portion of the image (Figure 5.25) with lower RVI are indicated by yellow and orange colors. In the upper portion of the image (Figure 5.25) and some middle portion of the image SAVI is found to be less.

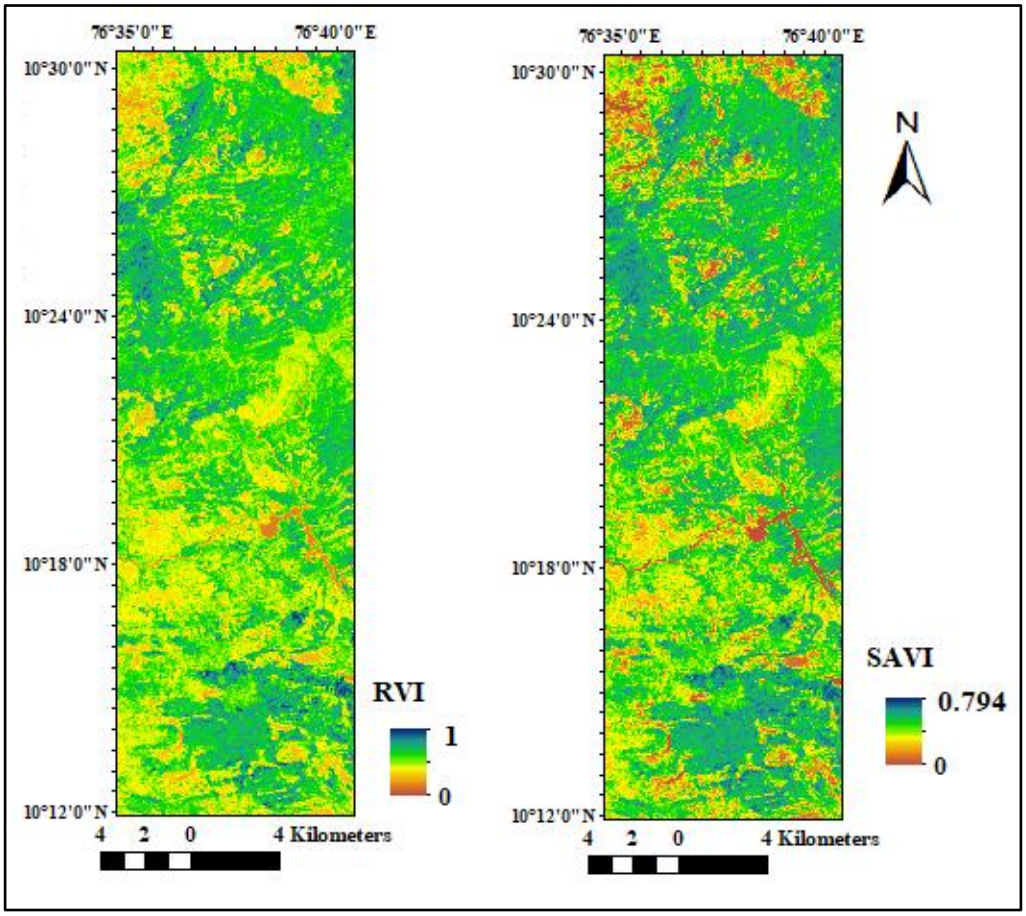

Figure 5.25: RVI and SAVI of Sholayar forest

NDVI values indicate a maximum of 0.849 indicating the presence of healthy and dense woody trees in some regions.

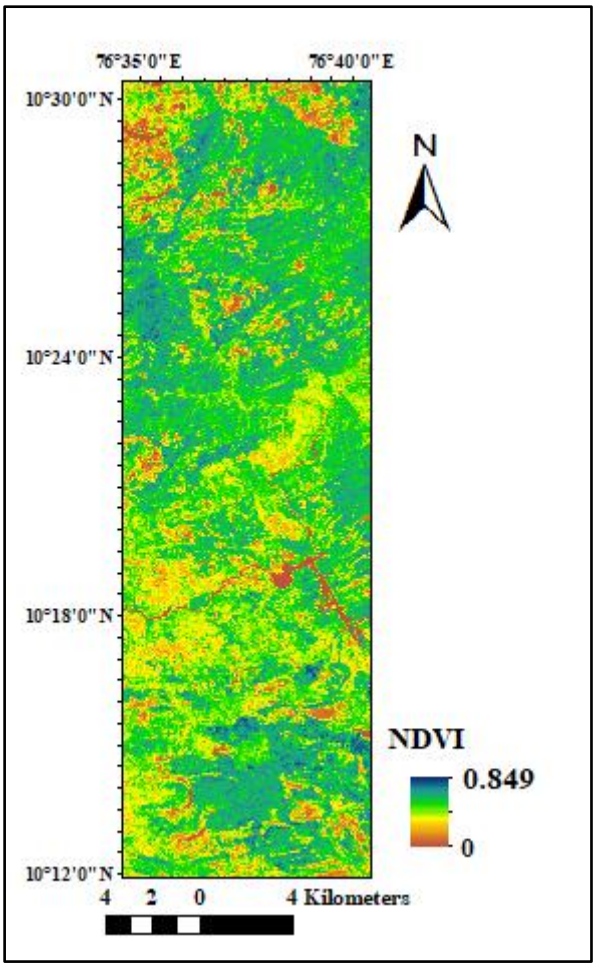

Figure 5.26 NDVI of Sholayar forest

NDVI value is found to be higher in the regions with a thick canopy and understory vegetation. The height of tree species in these regions varies from 5 m- 45 m which is evident from the CHM of Sholayar forest. The portion of the image (Figure 5.26) in red color shows the lower values of NDVI, indicating the absence of thick vegetation due to the human intervention, or due to the degradation of forest.

5.1.4 Estimation of Biomass

The predicted biomass from the integrated multispectral Landsat imagery and GLAS point cloud of the Mudumalai forest have values range from 130.5 Ton/Ha to 385.4 Ton/Ha as in Figure 5.27 and for the Sholayar forest, estimated values range from 65.7 Ton/Ha to 389.5 Ton /Ha as shown in Figure 5.28.

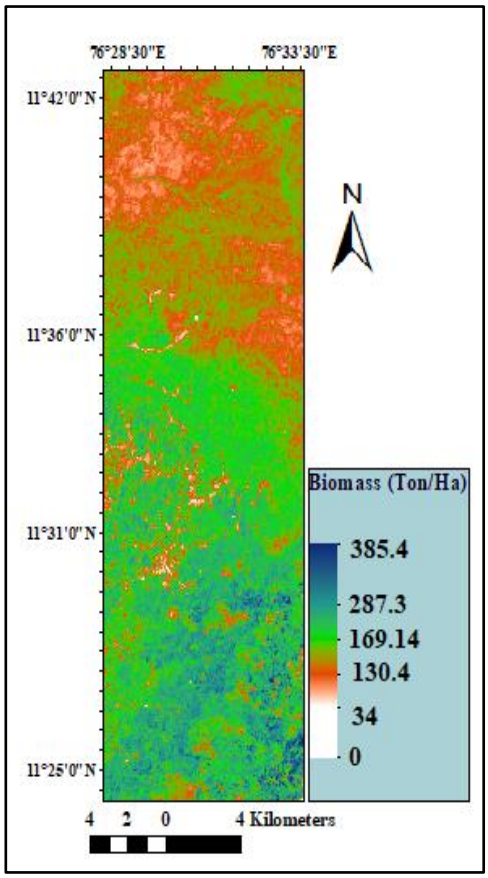

Figure 5.27: Estimated biomass of Mudumalai forest

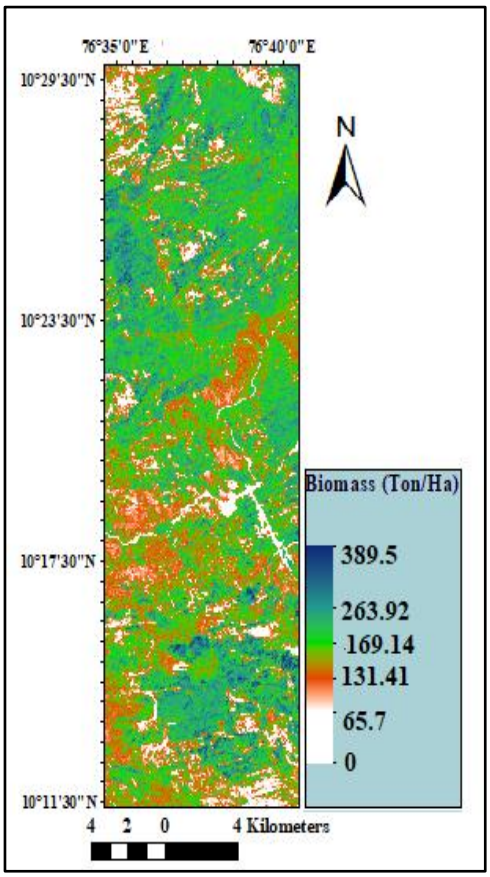

Figure 5.28: Estimated biomass for Sholayar forest

The upper portion of the image (Figure 5.27) in orange shows lower biomass values. These regions indicate degradation of forest due to shifting cultivation, forest fire or logging. The other regions indicate good amounts of

biomass which indicates the healthy status of those regions in the forest. These regions consist of a large variety of woody and nonwoody tree species with height range 5 m to 50 m as shown in CHM of Mudumalai forest. Thick understory vegetation is also identified with height range 1 m to 4 m from the estimates of CHM.

In Figure 5.28, the region which appears as white indicates very low biomass are areas of non-forest lands, intensely populated or water bodies. Degradation of forests is also indicated. Variety of tree species having a height varying from 5 m to 55 m is found as also indicated by the CHM of Sholayar forest.

5.1.4.1 Statistical Analysis of Biomass of Mudumalai and Sholayar Forests

Results of comparison of estimated biomass of Mudumalai forest and the reference biomass values are shown in Figure 5.29(a) Results shows a strong correlation (R^2 =0.97) between the reference biomass values and the estimated biomass.

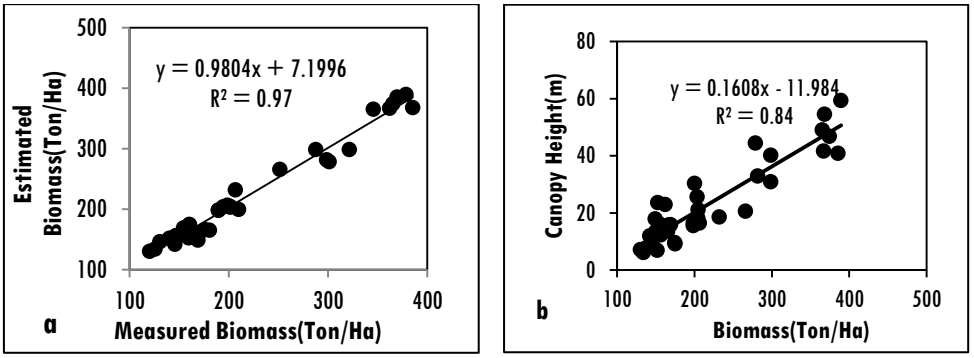

Figure 5.29: a) Variation of estimated biomass values with reference biomass and b) the variation of estimated biomass with canopy height of Mudumalai forest

The deviation of biomass is noted by plotting biomass as a function of tree height for Mudumalai forest as shown in Figure 5.29(b). It is noted that biomass values are higher for taller trees species for the study area.

Further, the estimated biomass compared with the NDVI generated, indicate a strong correlation for the Mudumalai forest. Biomass is higher for regions with higher NDVI values. For the NDVI values varying between 0.784 to 0.947, the biomass values are found to be higher with values from 250 Ton/Ha to 385.4 Ton/Ha.

Results of the comparison of estimated biomass and the reference biomass values of Sholayar forest are shown in Figure 5.30(a) There is a moderate correlation between estimated and measured biomass (R^2=0.96), as against the observed strong correlation for the same for Mudumalai forest.

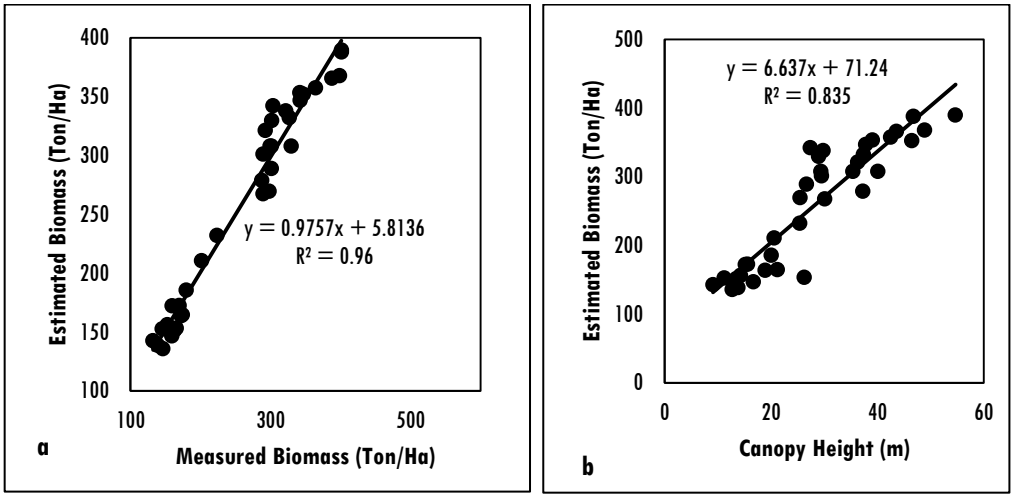

Figure 5.30: a) Scatter plot showing a comparison of estimated biomass of Sholayar region with reference biomass and b) the scatter plot showing biomass as a function of canopy height

The variation of biomass as a function of canopy height as shown in Figure 5.30(b) indicates a consistent correlation. The direction of the difference between estimated and reference biomass is almost independent of the magnitude of canopy height.

Further, the estimated biomass compared with the NDVI indicate a strong correlation for the Sholayar forest. It is clear that biomass is higher for regions with higher NDVI values. For the NDVI values varying between 0.484 to 0.849, the biomass values are found to be higher with values from 280 Ton/Ha to 389 Ton/Ha.

5.1.5 Estimation of Vegetation Indices and Biomass by the Integration of LiDAR with Sentinel-2 Imagery

5.1.5.1 Estimation of Vegetation Indices

Vegetation indices estimated by integrating Sentinel-2 data imagery with GLAS point cloud shown in Figures 5.31 and 5.32. EVI indicates a maximum value of 2.49 for Mudumalai forest. NDWI has the maximum value 0.606 indicating the forest stress due to less moisture content.

The bottom portion of Figure 5.31, in yellow, indicates a lower value of EVI. The region with higher values of EVI correlate with regions with a wide variety of tree species, thick canopy and understory vegetation reported.

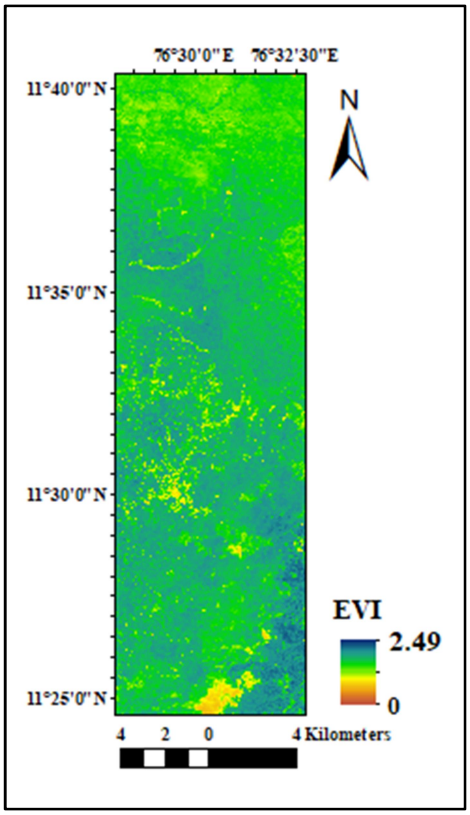

Figure 5.31: EVI of Mudumalai forest

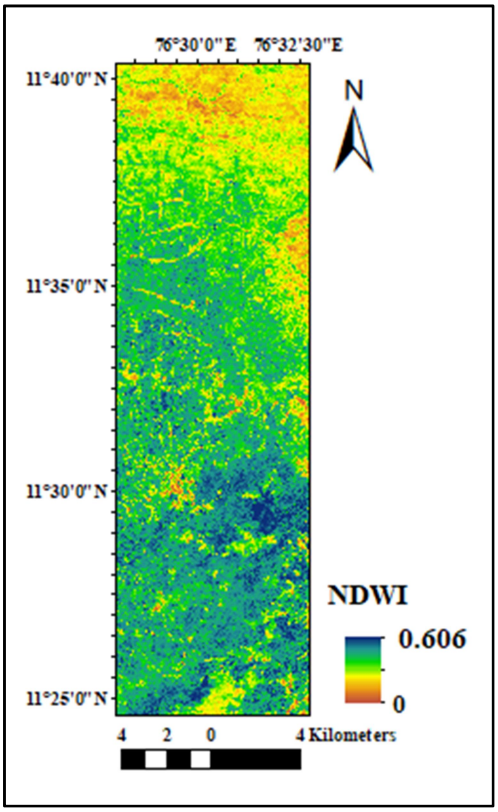

Figure 5.32: NDWI of Mudumalai forest

The Normalized Difference Infrared Index (NDII) and LAI values of Mudumalai forest are depicted in Figures 5.33 and 5.34 respectively. The maximum value calculated for NDII is 1, and it indicates the presence of lesser water content. LAI calculated for Mudumalai forest has a maximum value of 5.67. In most of the region in the image (Figure 5.34) the canopy water content is high, but in a few portions, which shows in yellow, the canopy water content is less. LAI value is found to be higher in the topmost portion of the image (Figure 5.34).

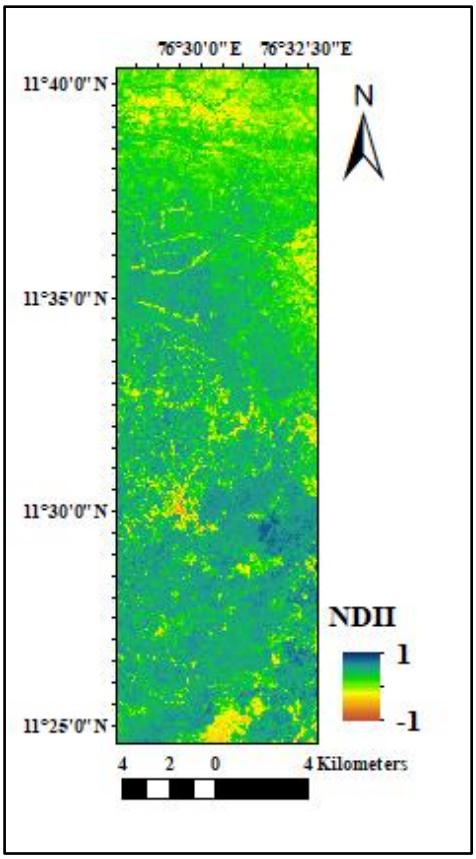

Figure 5.33: NDII of Mudumalai forest

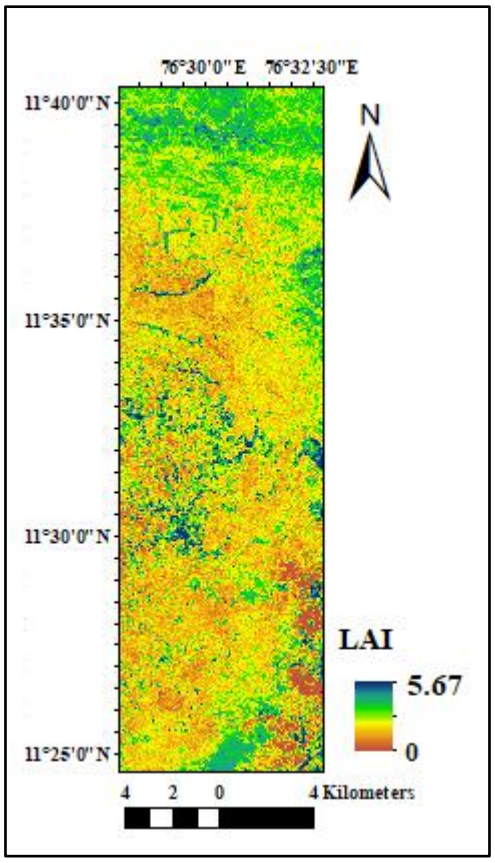

Figure 5.34: LAI of Mudumalai forest

For the Sholayar forest, NDII, LAI, and EVI were calculated and are shown in Figure 5.35. It is shown that NDII showed higher values at regions having higher water content. EVI indicates a maximum value of 2.47 in the Sholayar forest. Estimated LAI has a maximum value of 5.34.

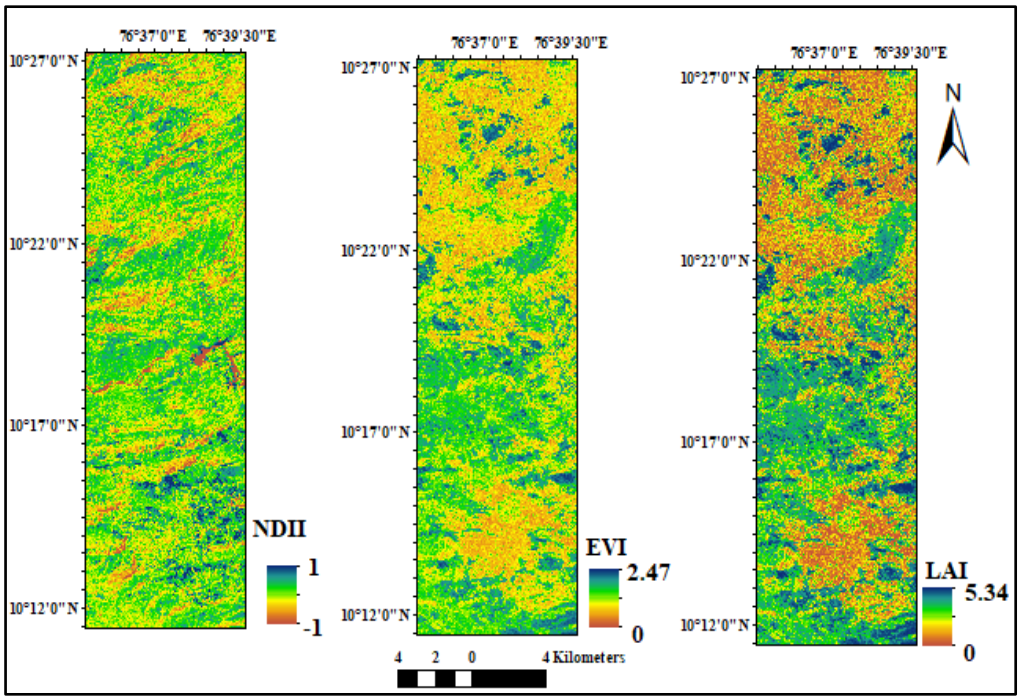

Figure 5.35: NDII, EVI, and LAI of Sholayar forest

The value of NDII is found to be higher in most part of the image (Figure 5.35) though some regions which are red in color indicates a very low value of NDII. From the image, the upper portion indicates a lower value of LAI. Other portions have a higher value of LAI, which shows the presence of a wide variety of tree species.

5.1.5.2 Estimation of Biomass

The estimated LAI from the Sentinel-2 imagery for both the study regions and the canopy height obtained from GLAS point cloud were regressed using support vector regression, for the estimation of biomass. The estimated biomass for Mudumalai forest and Sholayar forest are shown in Figures 5.36 and 5.37 respectively.

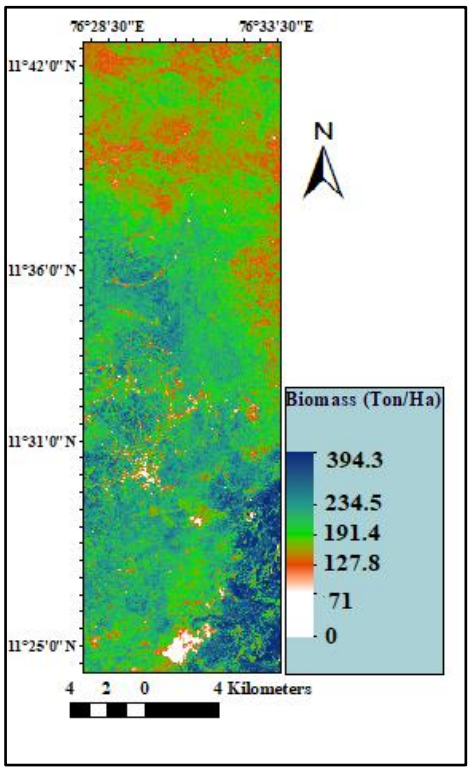

Figure 5.36: Estimated biomass of Mudumalai forest

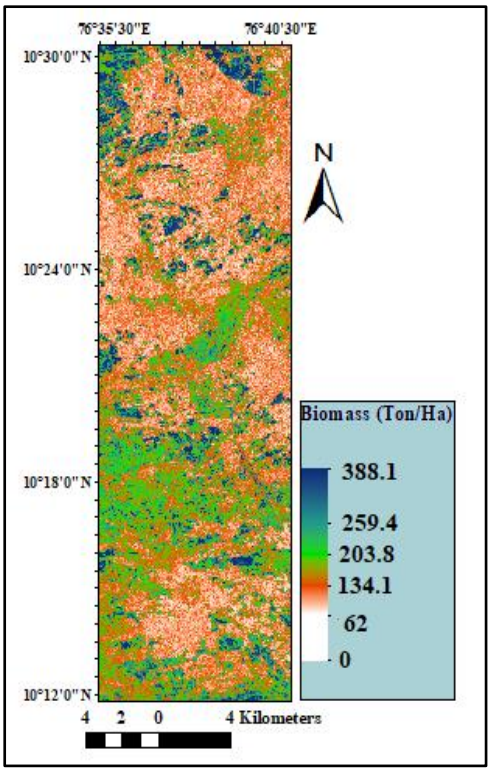

Figure 5.37: Estimated biomass of Sholayar forest

For Mudumalai forest, the estimated biomass has a maximum value of 394.3 Ton/Ha, and for Sholayar forest, the estimated biomass has a maximum value of 388.1 Ton/Ha. The image shows a significant gradient in biomass. These regions show a wide variety of tree species woody and nonwoody species with height attributes of 5 m-55 m from the CHM of the Mudumalai forest. For the image (Figure 5.37) the middle left portions which appear in green shows higher biomass values indicating the presence of thick forest and understory vegetation. These regions show the spatial variation with substantial biomass values.

5.1.5.3 Statistical Analysis of the Results on Integration with Sentinel Data

The estimated biomass using Sentinel-2 imagery integrated with GLAS point cloud were compared with the reference biomass values. LAI values were also compared with the field measurements of LAI, and the scatter plot showing the variation of the estimated LAI with the measured values of LAI is shown in Figure 5.38.

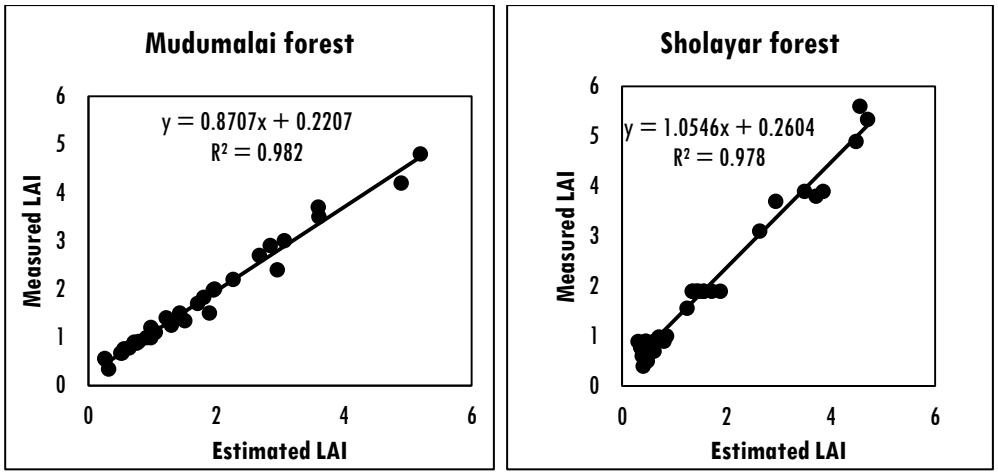

Figure 5.38: Scatter plot showing the variation of LAI with field measured LAI for Mudumalai forest and Sholayar forest

A strong correlation of about $R^2 = 0.98$ is obtained when LAI estimated is compared with the field measured LAI values for Mudumalai forest. For Sholayar forest similar correlation is existing ($R^2 = 0.978$). The scatter plot showing the variation of the estimated biomass with the measured biomass of both the forest regions are shown in Figure 5.39.

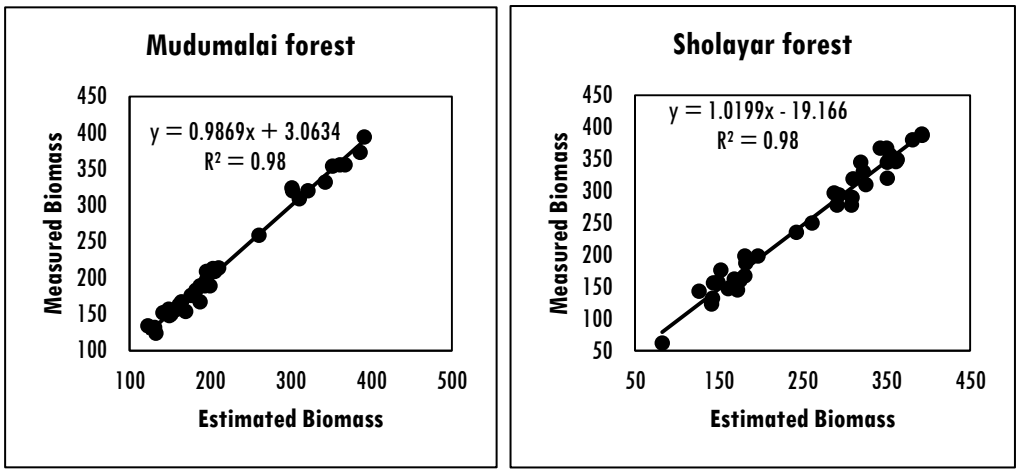

Figure 5.39: Scatter plot comparing the estimated biomass and reference biomass for both the study sites.

Results indicate that the integrated analysis of Sentinel-2 imagery and LiDAR point cloud effectively estimated biomass of Mudumalai and Sholayar forest.

5.1.6 Discussion

Biophysical Parameters' Estimation by the Integration of Multispectral Imagery with the Spaceborne LiDAR Point Cloud.

The comparison of the image estimated height values and the measured height values for the two study areas indicate a strong correlation (R^2= 0.98, R^2 = 0.97). For the understory vegetation heights also, a strong correlation is evident for Mudumalai forest, R^2=0.91 and Sholayar forest, R^2 =0.73. Trees of height 5-10 m including Anogenessius Latifolia, Bambusa Arundunacea, Butea monosperma, Ficus Benghalensis, etc are found to be dominant in the Mudumalai forest (Reddy et al., 2008). The deviation of estimated canopy height in comparison with the measured canopy height indicates the presence of aggressive invasive undergrowth species such as Eupatorium odoratum,

Lantana Camera and grass species like Cyrtococcum patens, Apluda mutica and Imperata cylindrica (Sukumar et al., 1991) in Mudumalai forest. For the Sholayar forest, the results indicate tree species of the average height of 24 m and typical tree species are Palaquium ellipticum, Cullenia exarillata, etc (Nair and Sasidharan, 1985). The highest biomass value of Sholayar forest is 389.5 Ton/Ha and of Mudumalai forest is 385.4 Ton/Ha.

The thesis focusses on the application of spaceborne full waveform LiDAR point cloud for the estimation of the forest structural variables and undergrowth. The work also validated the application of large footprint spaceborne LiDAR to accurately determine the canopy topography, forest structure, and canopy density in dense vegetation conditions and varied topography of complex forest environment of the Western Ghats. Disparity arises in the estimated canopy height in specific regions because of the missing of the GLAS point cloud in these regions. For the effective modeling of the forest structural variables, it is required that the LiDAR footprints should be continuous. Hence, a continuous coverage of data is needed since the discrete nature and fewer number of footprints of GLAS point cloud limit the extension of the study for large aerial extent of Western Ghats.

The study has estimated the forest structural variables in the selected regions of the Western Ghats region of India by utilizing the spaceborne LiDAR (ICESat/GLAS) point cloud. The structural variables estimated are canopy height, canopy density and the height of the undergrowth canopy. A strong correlation (R^2=0.98) is obtained when estimated canopy heights are compared with the ground measurements for both regions. The canopy height model developed enables the estimation of the height of invasive undergrowth species in the Western Ghats region with consistent correlation. From the results, large footprint spaceborne LiDAR point cloud can be used to develop

forest canopy height models as well as to perform forest structural analysis. The present study can as well as be applied to a large area which can lead to the national forest monitoring with the spaceborne laser altimetry. The study underscores the possibility of the GLAS ICESat point cloud for the extraction of forest variables and models which can form a significant factor for sustainable forest management. The study indicates that spaceborne full waveform LiDAR point cloud when utilized judiciously and appropriately has the potential to open the enormous application in the case of sustainable forest management practices which will significantly contribute to enhancing the knowledge and measurement practices of the forest management community.

The study has attempted the direct estimation of canopy height and biomass for Mudumalai forest and Sholayar forest of Western Ghats of India including the height of the understory vegetation. Both the spectral and LiDAR point cloud is integrated at the pixel level and supervised learning predictive algorithm; namely support vector machine has been used for the estimation of biomass across the two study areas. The estimated biomass, as well as the canopy height from the integrated LiDAR point cloud, has been validated with reference measurements. The results indicate that there is a strong correlation between estimated and measured canopy height from the GLAS point cloud and biomass for both the study areas. However, the deviation between the measured and estimated parameters is found varying consistently by the overall tree heights of the region. It is found that when tree height is less, LiDAR point cloud based estimates are found to be overestimated. Deviation of the estimated canopy height from the measured tree height is found to be more in the case of shorter trees, and similar observation of overestimation is also reported in some literature (Hopkinson et al., 2005; Lim et al., 2003; Clark et al., 2004). LiDAR point cloud is found to

overestimate at lower level tree canopy height. Lower deviation of the estimated canopy heights from the measured canopy heights is observed in the case of taller trees. A level of underestimation of tree height for taller tree species also endorses the observation made by some other earlier studies (Andersen et al., 2006; Wudler et al., 2007). Underestimation is less severe compared to overestimation. The estimation of the height of understory vegetation is possible from the LiDAR point cloud. In the case of estimation of the height of understory vegetation, invasive species having minimum 1 m height can also be estimated by LiDAR point cloud where the canopy is relatively less dense and shorter. In the case when the trees are very tall, which is likely to be of the thick canopy, there is no understory indicated by the LiDAR point cloud.

5.2 3D Reconstruction of Trees and the Estimation of LAI using Terrestrial Laser Scanner

5.2.1 3D Point Cloud Segmentation using Hierarchical Min Cut Method

The 3D segmentation and extraction of the individual trees from the perspectives of top view and side view are shown in Figure 5.40. Tree trunks are unambiguously segmented and identified, which suggests us the applicability of 3D mapping of trees using the min-cut algorithm. The hierarchical min-cut segmentation plays a potential role in individual tree reconstruction and further extraction of crown points. The algorithm successfully extracts individual tree crown points corresponding to each trunk and successfully separates individual trees in the point cloud. Trees which are very close to each other are also detected accurately thereby providing an optimized segmentation result.

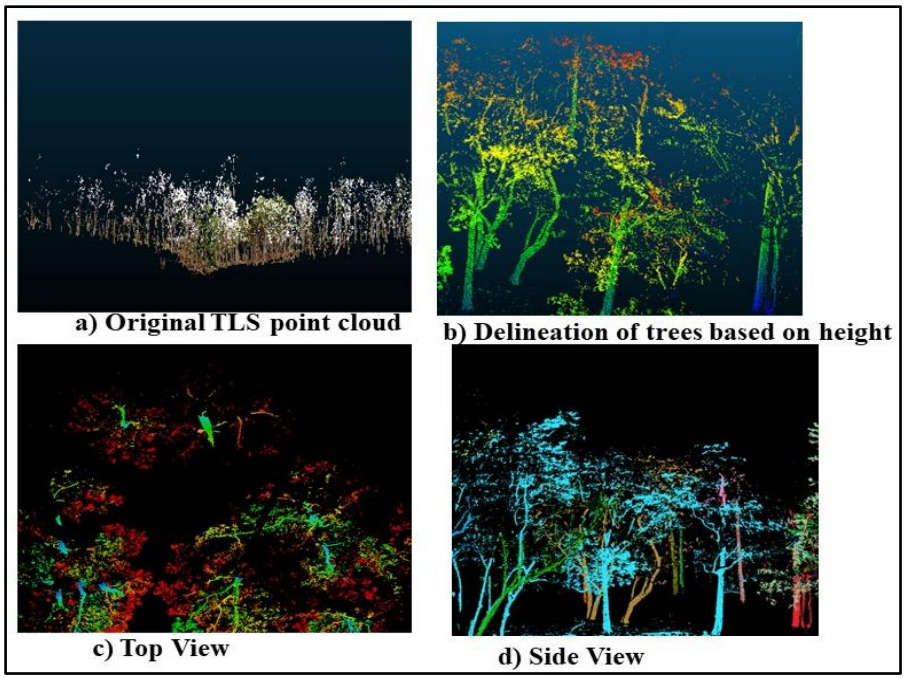

Figure 5.40: a) Original TLS point cloud; b) delineation of trees based on height; c) top view of the TLS after segmentation; d) side view of individual trees after segmentation

3D reconstruction of the trees is also possible after the 3D segmentation of the individual trees as implemented in this work.

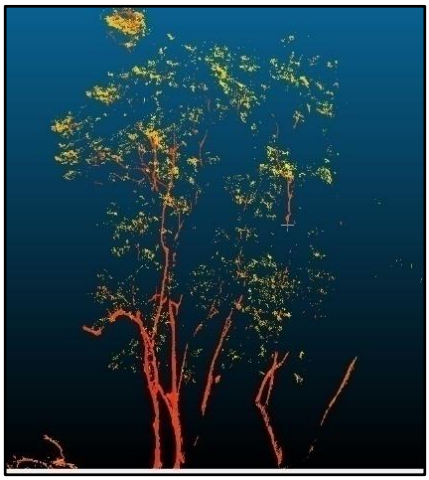

Figure 5.41: Failure in the case of tree crown detection and trunks

But the mini-cut method fails to detect trees where the tree trunks are curved and have irregular double trunks, and there is a further possibility of detecting the crowns of the neighboring trees in the case of trees with missed trunk points (Figure 5.41). There is a chance of splitting trees into two independent trees in cases when the trees are branched from the bases (Figure 5.41). But, this can be mitigated by changing the scanning positions of the equipment and by co-registering the corresponding point clouds.

5.2.2 Segmentation Based on Super Voxel Clustering Method

Based on the super voxel clustering, the individual trees are segmented as super voxels. As evident from Figure 5.42, the method also successfully extracts the tree trunks and crown points. 3D reconstruction of individual trees was successfully done based on the method and as shown in Figure 5.42. Compared to the min-cut method, the super voxel method detects the trees even when they are closely connected and clumped. However, in some cases, there is a possibility of detection of the crown of the trees having missed trunks.

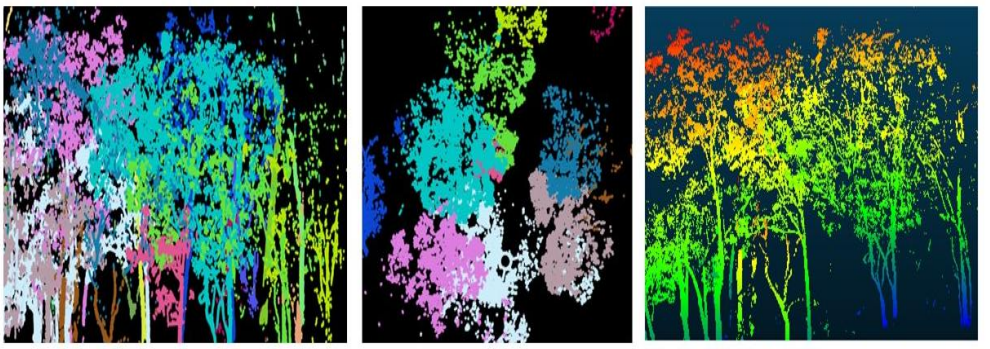

Figure 5.42: Super voxel clustering results-a) side view of trees by super voxel clustering; b) top view; c) Delineation of trees based on height

5.2.3 Estimation of Structural Metrics

Individual tree height was estimated from 3D segmentation of TLS point cloud using hierarchical min-cut segmentation results and super voxel clustering results. The height values are compared with the ground measurements for validating the performance. Figure 5.43 shows a statistical comparison of the detected tree heights with the ground measurements by both the methods.

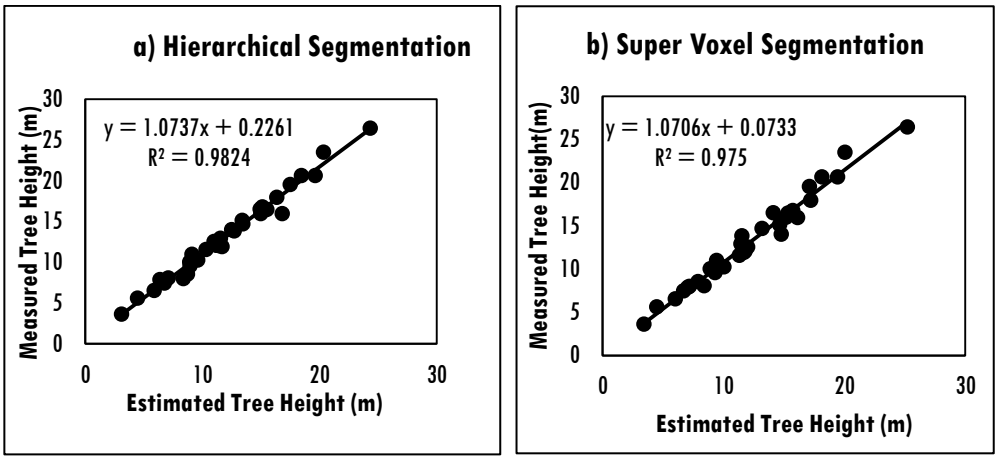

Figure 5.43: Variation of estimated tree height with the measured tree height using a) hierarchical segmentation; b) super voxel segmentation

As evident from Figure 5.43, TLS based individual tree height estimates exhibit a consistent correlation with the in-situ measurements. For the min-cut segmentation method the correlation is R^2=0.98, and for super voxel segmentation, the correlation is R^2=0.97.

5.2.4 Estimation of LAI from TLS

Two methods are used for the estimation of LAI from the TLS point cloud. The first method is the estimation of LAI by the multivariate regression of height and DBH retrieved from the 3D segmentation process. In the second method, a new algorithm is proposed for direct estimation of LAI from TLS point cloud

5.2.5 Estimation of Leaf Area Index by Multivariate Regression

LAI was estimated by multivariate regression from the 3D segmentation results of the structural metrics of both hierarchical min-cut segmentation and super voxel segmentation method. A comparison of estimated LAI and the in situ LAI measurements are shown in Figure 5.44.

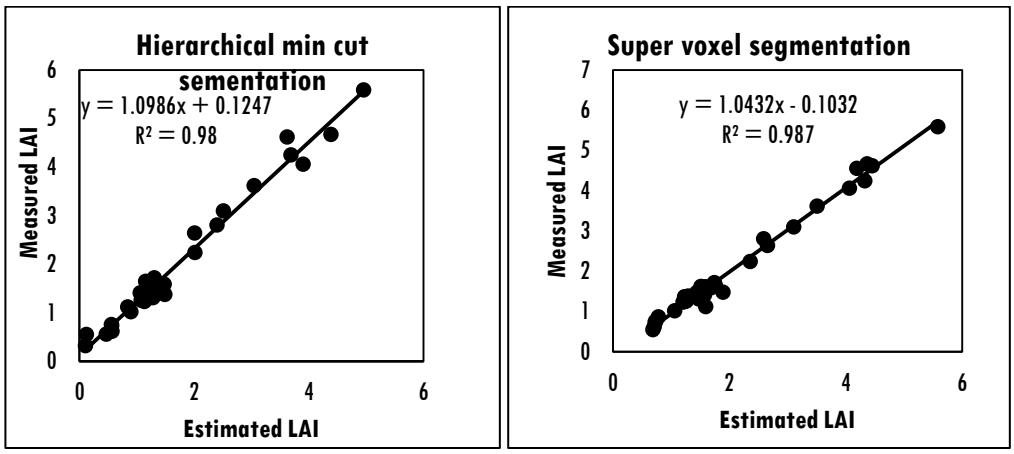

Figure 5.44 Comparison of estimated LAI with in situ LAI

The estimated LAI and the measured LAI show a strong correlation (R^2= 0.98) indicating that both the segmentation method can be used for individual tree segmentation. Three-dimensional reconstruction of trees was accurately done by using TLS point cloud segmentation approach.

5.3 Direct Estimation of LAI using Terrestrial Laser Scanner

The individual trees along with the segmented super voxels are shown in Figure 5.45.

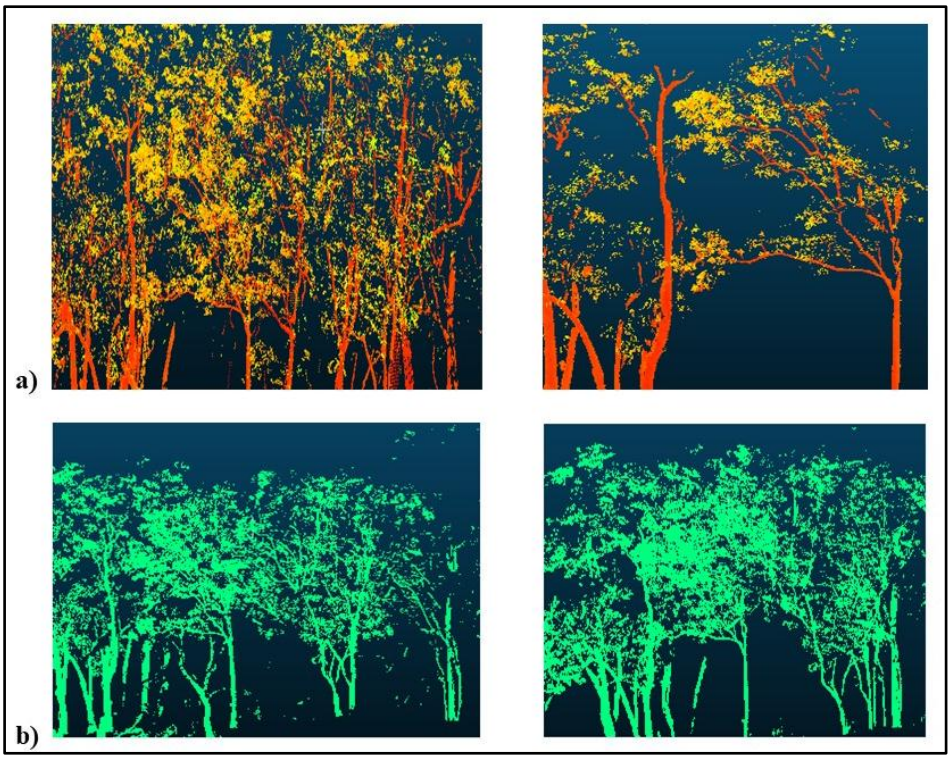

Figure 5.45: a) Segmented and reconstructed trees by hierarchical min-cut method and b) super voxel clustering results

For the present study, the individual trees within a box dimension were segmented, and the proposed PSD algorithm was implemented based on the density of trees. The point spacing of the TLS point cloud is 6 mm. LAI was calculated for all the reconstructed trees in the study area. The performance of the PSD algorithm was tested by comparing the LAI values estimated with in-situ LAI measurements.

5.3.1 Tree Reconstruction

The results of the 3D segmentation reconstruction of trees are shown in Figures 5.46 and 5.47 respectively. Both the algorithms successfully extracted individual trees and reconstructed trees conforming to the typical shapes of trees in the study area.

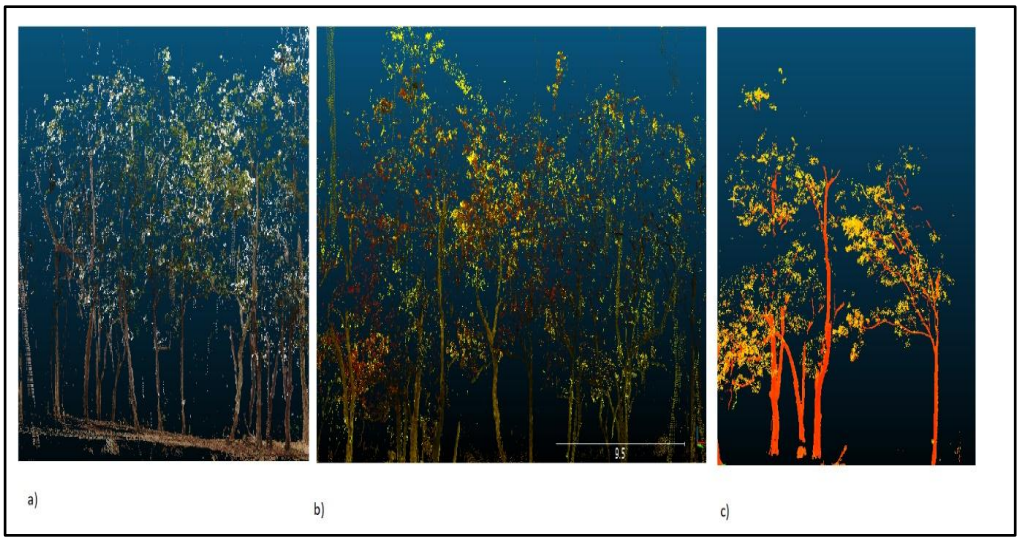

Figure 5.46: a) TLS point cloud, b) point cloud after minimum cut segmentation, c) reconstructed trees

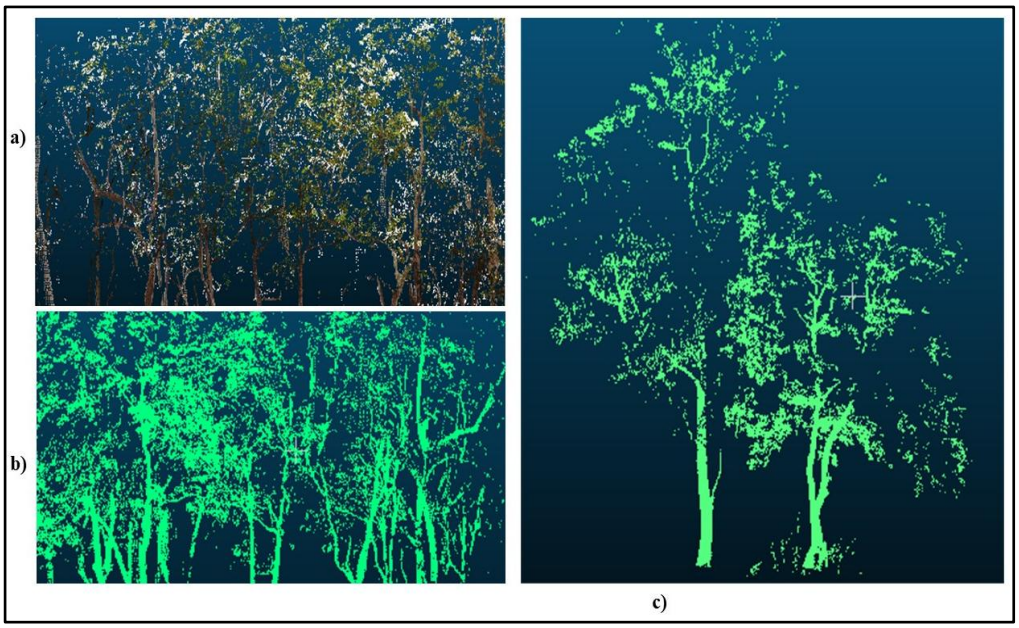

Figure 5.47: a) TLS point cloud, b) segmentation results of super voxel clustering, c) reconstructed trees

A 3D model of the reconstructed trees is shown in Figure 5.48.

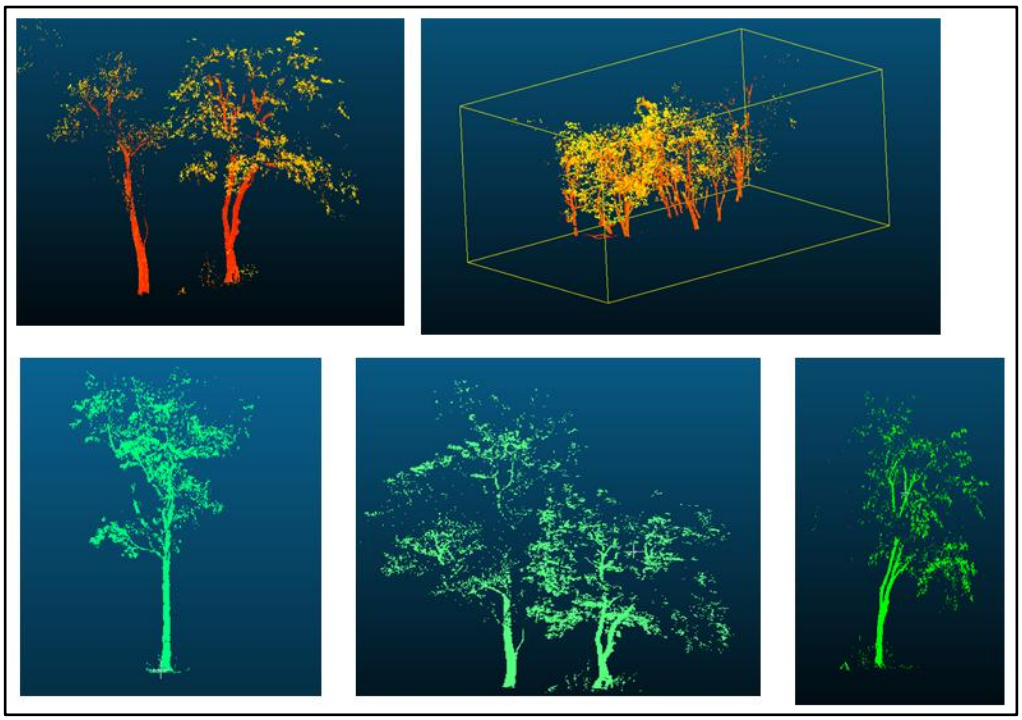

Figure 5.48: 3D model of reconstructed trees

5.3.2 Estimation of LAI by PSD Algorithm

LAI was estimated by the proposed Point Spatial Density algorithm (PSD). LAI values of individual trees are computed. Trees are selected within specific box dimensions, and the number of points for each tree is noted. The selected trees within the box dimensions are shown in Figure 5.49.

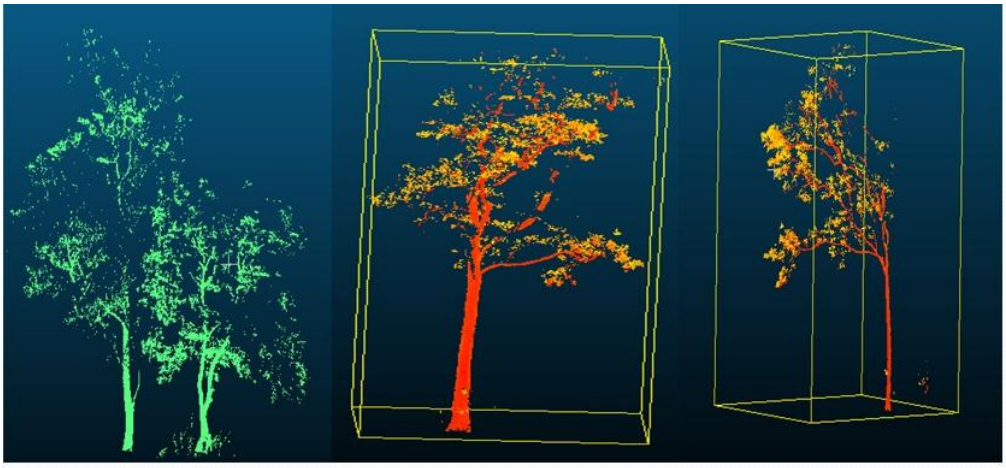

Figure 5.49: Reconstructed trees selected for applying the PSD algorithm

For example, to a selected tree, the number of points for a given area (n_p) = 676, d=6 mm for the given instrument. The LAI estimated from the proposed PSD algorithm is 1.622.

Modelled LAI values of some of the trees estimated by the PSD algorithm for both the segmentation methods are shown in Tables 5.1 and 5.2. The LAI values estimated by PSD algorithm for the individual trees and the corresponding in situ measurements of LAI are compared for performance validation (Figure 5.50).

Table 5.1: Modelled LAI and measured LAI from hierarchical min-cut segmentation

Trees	No of Points (N)	X(m)	Y(m)	Z(m)	Modeled LAI	Ground measured LAI
1	1721	3.811	7.816	4.47	0.901	1.02
2	6456	13.442	10.573	11.437	0.572	0.62
3	15576	10.104	15.201	11.541	1.334	1.51
4	15323	8.114	7.570	11.662	2.012	2.64
5	8480	7.097	6.669	5.894	2.510	3.1
6	11613	3.463	5.208	6.761	4.954	5.59
7	91378	20.349	16.333	15.505	3.902	4.06
8	30833	7.153	14.356	12.708	3.048	3.62
9	676	7.962	6.744	9.0949	0.122	0.55
10	59221	14.45	14.646	20.341	2.401	2.81
11	66955	11.652	19.337	14.982	3.687	4.25
12	10639	11.75	8.684	10.310	1.239	1.61
13	12080	11.015	9.59	12.487	1.132	1.23
14	1979	5.918	4.355	8.377	0.564	0.74
15	6090	5.597	6.841	11.198	1.059	1.41
16	1423	13.849	14.74	10.993	0.108	0.32
17	35505	14.982	12.271	8.720	3.621	4.62
18	19045	12.919	7.182	18.457	1.341	1.62
19	30808	21.177	16.049	17.505	1.156	1.65
20	21715	12.294	11.178	14.928	1.490	1.38
21	14917	8.348	7.927	16.824	1.308	1.72
22	1250	3.649	3.541	8.918	0.467	0.56
23	23163	16.867	17.163	15.125	1.080	1.26
24	26315	11.4	9.4	15.2	2.016	2.24
25	13678	8.1	7.3	16.8	1.272	1.47
26	14808	7.9	8.8	16.4	1.301	1.48
27	6860	5.1	4.5	13.64	1.262	1.37
28	5494	2	0.92	11.92	4.388	4.67
29	4685	3.96	2.56	12.2	1.481	1.59
30	4491	5.6	4.88	18.48	0.559	0.76
31	12778	5.84	7.6	18.04	1.286	1.31
32	788	0.68	3.44	6.36	1.309	1.45
33	643	9.4	4.8	1.44	0.843	1.12

Table 5.2: Modelled and measured LAI from super voxel segmentation

Trees	No of Points (N)	X (m)	Y (m)	Z(m)	Modeled LAI	Ground measured LAI
1	2035	3.811	7.816	4.48	1.063	1.02
2	8124	13.442	10.573	11.579	0.7112	0.62
3	17321	10.104	15.201	11.441	1.496	1.51
4	20324	8.114	7.570	11.69	2.663	2.64
5	10712	7.097	6.669	6.013	3.108	3.1
6	12978	3.463	5.208	6.7	5.587	5.59
7	94123	20.349	16.333	15.325	4.066	4.06
8	32187	7.153	14.356	11.523	3.510	3.62
9	2992	7.962	6.744	9.449	0.520	0.55
10	62989	14.45	14.646	20.041	2.592	2.81
11	76623	11.652	19.337	15.182	4.164	4.25
12	14978	11.75	8.684	11.310	1.591	1.61
13	15246	11.015	9.59	14.787	1.206	1.23
14	2188	5.918	4.355	7.177	0.728	0.74
15	9541	5.597	6.841	11.779	1.578	1.41
16	11688	13.849	14.74	11.993	0.818	0.87
17	39645	14.982	12.271	7.909	4.458	4.62
18	21153	12.919	7.182	18.157	1.514	1.62
19	45889	21.177	16.049	17.120	1.761	1.65
20	18899	12.294	11.178	14.128	1.370	1.38
21	19109	8.348	7.927	16.124	1.748	1.72
22	11201	3.649	3.541	8.918	4.192	4.56
23	28127	16.867	17.163	15.725	1.261	1.26
24	51173	11.4	9.4	25.2	2.364	2.24
25	15923	8.1	7.3	17.23	1.444	1.47
26	14808	10.9	11.4	8.4	1.898	1.48
27	7899	5.1	4.5	14.64	1.354	1.37
28	25345	6.7	4	19.45	3.121	4.67
29	5785	3.96	2.56	13.2	1.691	1.59
30	3001	5.6	4.88	9.31	0.741	0.76
31	6778	5.84	6.6	10.04	1.307	1.31
32	1004	0.68	3.44	7.06	1.502	1.45
33	1943	9.4	4.8	3.44	1.066	1.12

From Tables 5.1 and 5.2, it is clear that the proposed PSD algorithm estimates LAI, consistently and are reasonably accurate. A strong correlation

of about R^2= 0.96 and R^2 = 0.95 are obtained for hierarchical and super voxel segmentation used respectively.

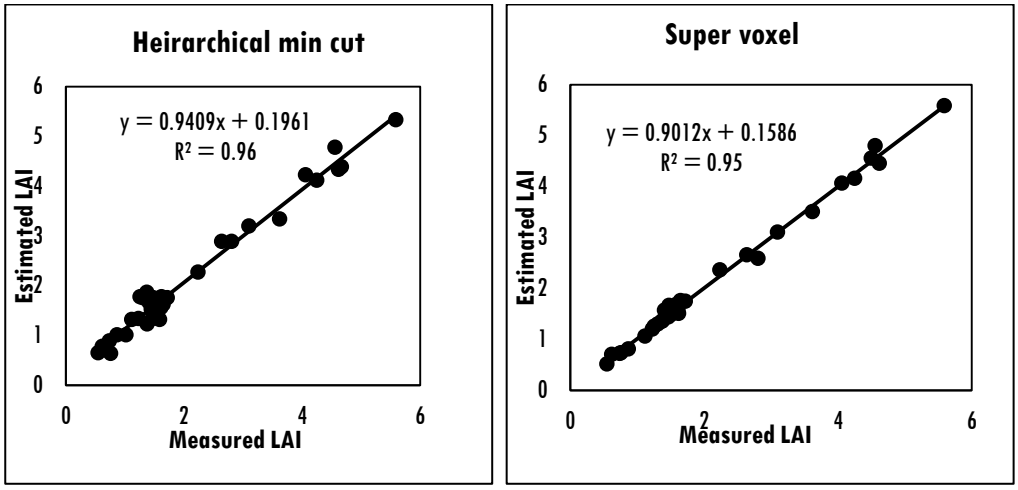

Figure 5.50: Variation of estimated and measured LAI from the PSD algorithm

This method thus seems to be applicable in estimating the LAI values of complex heterogeneous forests which consists of tropical deciduous trees with a thick understory. The method can mitigate the challenges in the LAI estimation of existing methods including the voxel size, sampling resolution problems, noise and occlusion effects. There are no extreme cases of overestimation and underestimation problems. The PSD algorithm depends only on the point spacing which is scanner dependant, point density of the individual trees which depends on the effectiveness and accuracy of the segmentation results.

5.4 Estimation of Biophysical Parameters using Hyperspectral and LiDAR Point Cloud

The pre-processed AVIRIS-NG imagery data is integrated with the GLAS point cloud data and the parameters such as LAI and biomass were estimated.

5.4.1 Estimated Leaf Area Index and Biomass of Mudumalai Forest

LAI estimated for Mudumalai forest is shown in Figure 5.51. The maximum value of LAI for the Mudumalai forest is 5.79. From the figure, portions marked in white color has lower LAI values which are low vegetation areas. The other portions indicate higher values of LAI. Higher values of LAI are found in the regions with thick understory and canopy cover with a wide variety of trees. In the regions with lower values of LAI, canopy cover is less.

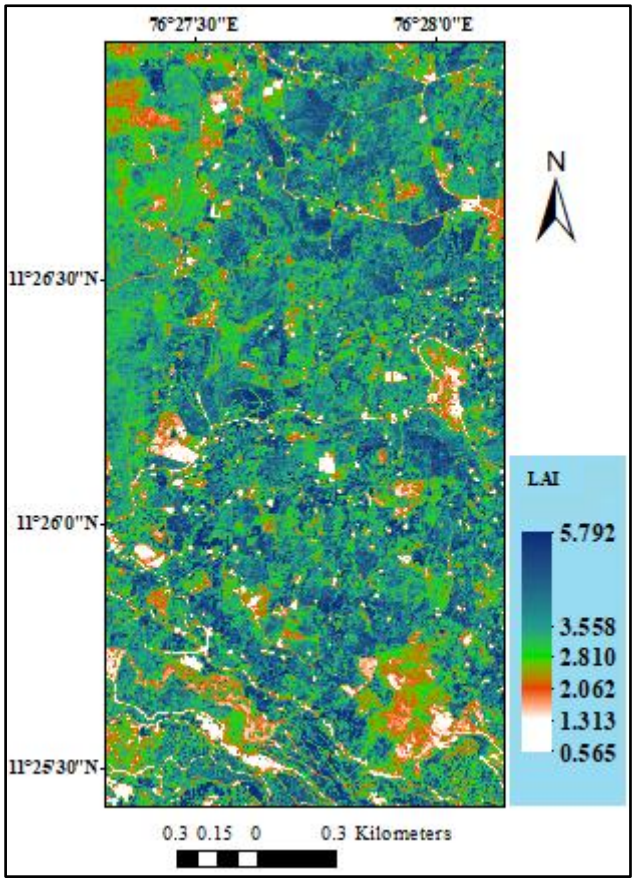

Figure 5.51: LAI of Mudumalai forest using AVIRIS-NG imagery

Biomass estimated by SVM regression for Mudumalai forest is indicated in Figure 5.52. The maximum value of the biomass of Mudumalai forest is 389.5 Ton/Ha.

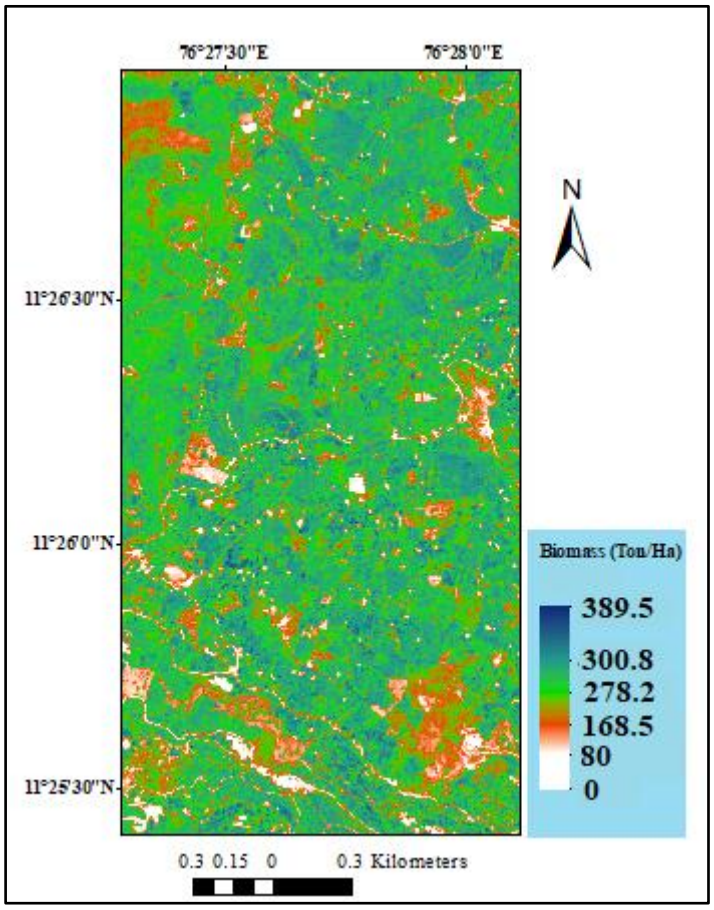

Figure 5.52: Biomass of Mudumalai forest using AVIRIS-NG imagery

From the figure, regions in white color indicate non-vegetation areas. Other regions with red color indicate a substantial gradient of biomass. The regions indicated in green color show substantially higher values of biomass. Regions with higher values of biomass have a wide variety of tree species with height values 5 to 50 m as evident from the CHM of Mudumalai forest. Thick understory vegetation can also be found with values ranging from 1 m to 5 m.

5.4.2 Estimated LAI and Biomass of Sholayar Forests

For the Sholayar forest region, the estimated biomass and LAI using AVIRIS imagery are shown in Figures 5.53 and 5.54 respectively.

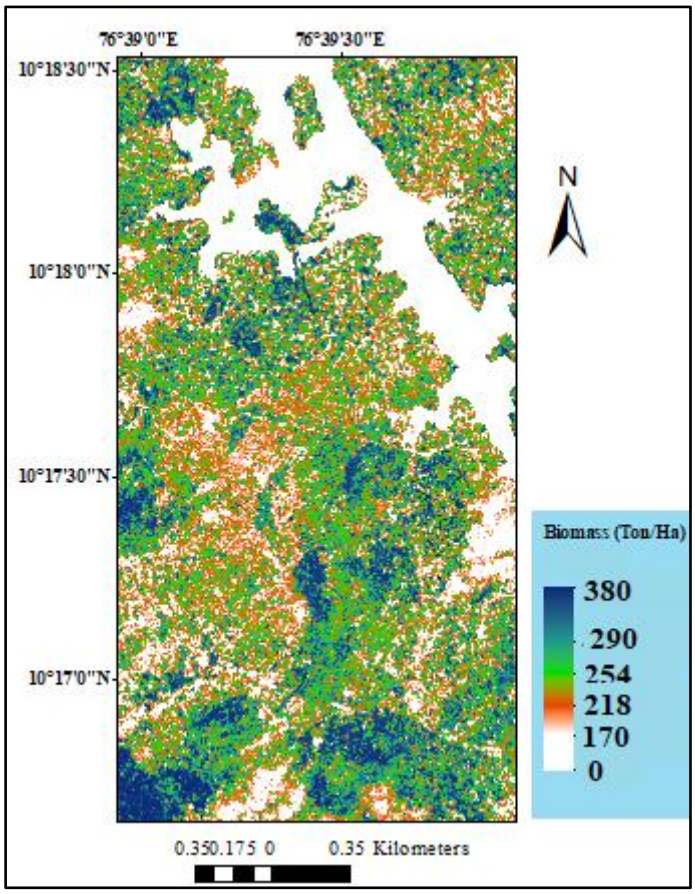

Figure 5.53: Biomass of Sholayar forest using AVIRIS -NG

Estimated LAI for Sholayar forest has a maximum value of 3.8. The estimated biomass has a maximum value of 380 Ton/Ha. The regions with lower biomass values are represented using a white color which shows the degradation of the forest/ non- vegetation areas. There is a substantial variation of biomass in other portions with values from 218 Ton/Ha to 380 Ton/Ha.

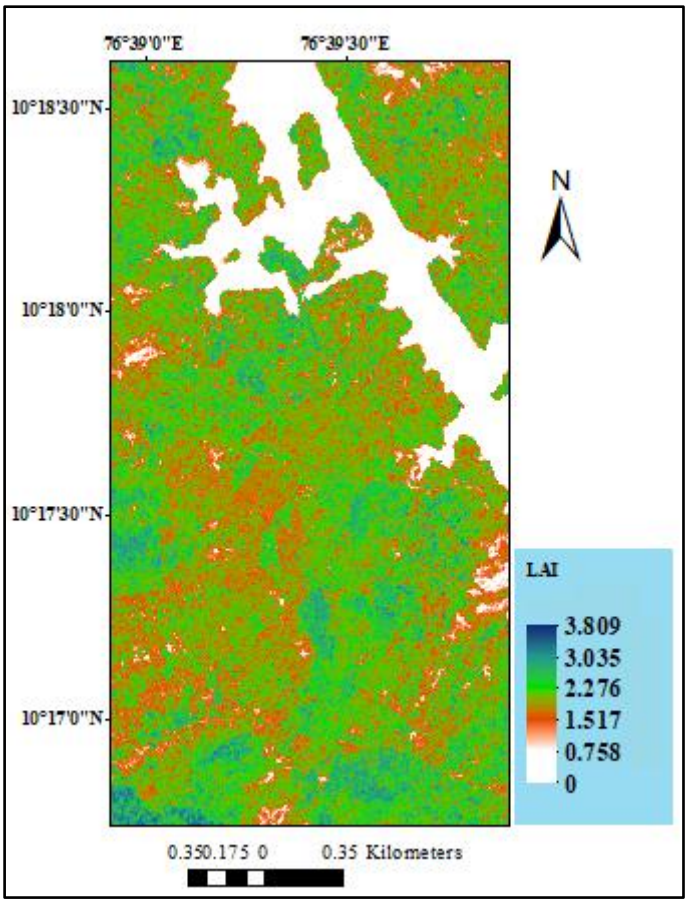

Figure 5.54: LAI of Sholayar forest using AVIRIS-NG

In the figure at the topmost portion, a region with lower LAI values is a water body. The other portions indicate higher values of LAI with a wide variety of thick canopy and understory vegetation, and less degradation.

5.4.3 Statistical Analysis

The biomass of Mudumalai forest and Sholayar forest estimated were validated with the reference measurements. The scatter plot showing the variation of estimated biomass with the reference biomass of Mudumalai forest, and Sholayar forest is shown in Figure 5.55.

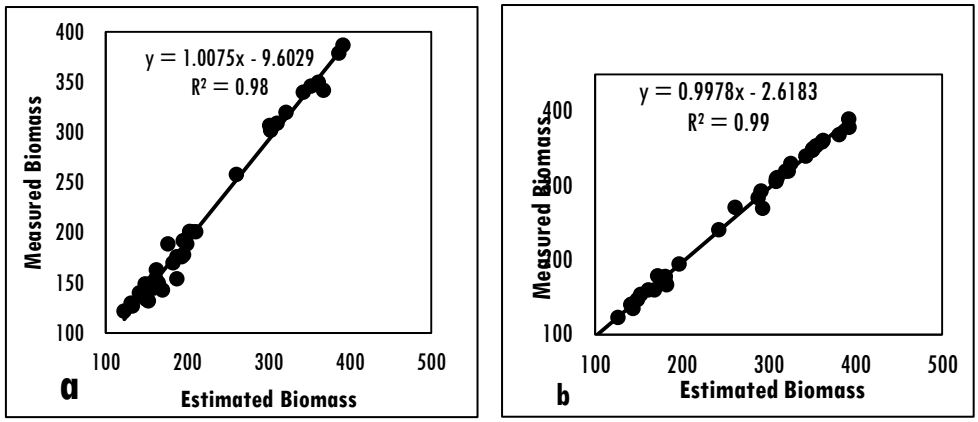

Figure 5.55: Variation of estimated biomass using AVIRIS-NG with reference biomass for a) in Mudumalai forest, and b) in Sholayar forest

The scatter plot showing the variation of estimated LAI with the measured LAI for both Mudumalai forest and Sholayar forest is shown in Figure 5.56.

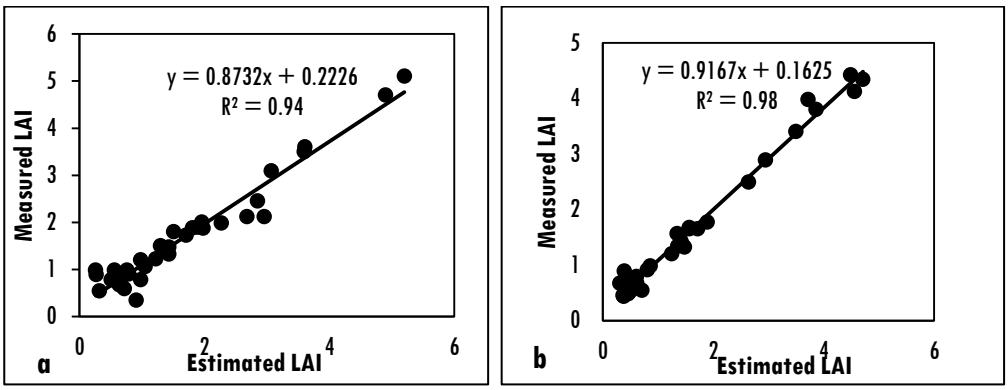

Figure 5.56: Variation of estimated LAI using AVIRIS-NG with measured LAI for a) Mudumalai forest, and b) Sholayar forest

From the validation of results, consistent correlation is seen for the biomass and LAI estimated by the integration of AVIRIS-NG with GLAS point cloud.

The estimated biomass by the integration of Landsat imagery and GLAS point cloud ranges from 34 Ton/Ha to 385.4 Ton/Ha for Mudumalai forest and 65.7 Ton/Ha to 389.5 Ton/Ha for Sholayar forest. By integration of Sentinel-2 imagery with GLAS point cloud, the biomass values are found to range from 71 Ton/Ha to 394.3 Ton/Ha for Mudumalai forest and 62 Ton/Ha to 388.1 Ton/Ha for Sholayar forest. On the integration of AVIRIS-NG with GLAS point cloud, estimated biomass for Mudumalai forest is in between 80 Ton/Ha to 389.5 Ton/Ha and for Sholayar forest, they are within 170 Ton/Ha to 380 Ton/Ha. LAI for Mudumalai forest and Sholayar forest has a maximum value of 3.005 and 2.38 respectively on the integration of Landsat imagery with GLAS point cloud. On the integration of Sentinel-2 with GLAS point cloud, estimated LAI has the maximum value of 5.67 and 5.34 (R^2=0.98, R^2=0.97 with reference measurements) for Mudumalai and Sholayar forest respectively. Correlation with the in-situ LAI for Mudumalai is R^2=0.98 and R^2=0.95 by super voxel segmentation method and R^2=0.98, R^2=0.96 for min-cut segmentation method. On the integration of AVIRIS-NG with GLAS point cloud, estimated LAI obtained a correlation of R^2=0.94 and R^2=0.98 when compared with reference LAI values for Mudumalai and Sholayar forests respectively. Similarly, canopy heights obtained from GLAS point cloud has strong correlation R^2=0.98, and R^2=0.972 for Mudumalai and Sholayar forest respectively when compared with reference measurements. Tree height estimated by TLS point cloud by both segmentation method has strong correlation R^2=0.98 and R^2=0.97 with reference values. The results indicate the effective performance of the methods employed for the estimation of biophysical parameters in Sholayar and Mudumalai forests respectively.

5.5 Chapter Conclusion

The biophysical parameters extracted by the integration of multispectral imagery with LiDAR point cloud indicate consistent correlation with the in situ measurements. Given, the highly diverse and spatially extensive nature of the Western Ghats in India, LiDAR-based modeling of forest parameters greatly benefits from the fusion of multispectral imagery and applying non-parametric approaches for retrieving the parameters. The methodology developed in this study significantly contributes to forest parameters' estimation using spaceborne LiDAR point cloud and a thorough understanding of Western Ghats by providing estimates of forest structural parameters. The application of terrestrial laser scanned data for direct estimation of LAI and by the SVM based regression indicate the potential of remote estimation of LAI accurately. TLS also accurately estimates the structural parameters of individual trees in Mudumalai forests and show consistent correlation with the field measurements. TLS seems a viable general tool for replacing the various standard practices of ground truth measurements. The integration of AVIRIS-NG imagery with LiDAR point cloud successfully estimated the biomass and LAI close to in situ measurements.

******

Chapter 6

SUMMARY AND CONCLUSION

Contents

This chapter summarizes the major outcome of this thesis based on a critical analysis of the observations and validations of the estimated biophysical parameters. The relative merits and demerits of the integration methods, the algorithmic approaches as well as the validation with the field measurements are presented. The chapter ends with major conclusions and the relevant outlook for the future scope of the study.

Major conclusions of this study are specified below.

- The study has successfully estimated biophysical parameters: canopy height, biomass, understory vegetation height and canopy density in the dense heterogeneous tropical forests of the Western Ghats, India.
- Both the structural parameters and spectral parameters are necessary for estimation of multiple biophysical parameters which characterize vertical and horizontal components of tree stands.
- The height of forest undergrowth vegetation can be estimated with GLAS point cloud. Airborne hyperspectral imagery (AVIRIS-NG imagery in this case), will not be suitable for tree height estimations;

biomass can be estimated with moderate accuracy using the LAI as surrogate variable from hyperspectral imagery.

Estimates of biophysical parameters using GLAS point cloud and multispectral imagery correlate well with the field measurements compared to multispectral or hyperspectral imagery alone.

- Three-dimensional modeling of the individual trees in the Western Ghats region can be done using TLS point cloud, and some important structural parameters -individual tree height, DBH, and LAI can be retrieved accurately from TLS based 3D tree modeling. This reduces the need for an extensive manual collection of field measurements using traditional instruments and enhances periodic and effective management of forests.
- Results reaffirm the potential of airborne hyperspectral remote sensing images in retrieving some essential biophysical variables which can be related to forest ecosystem processes, health as well as in detecting vegetation stress.

6.1 Chapter Summary

The thesis starts with an introduction chapter which outlines the significance of the research, the characteristics and application of multispectral imagery in heterogeneous forest, need for LiDAR remote sensing, need for the integration of LIDAR with multispectral as well as hyperspectral imagery and the importance of terrestrial laser scanner in tropical forest for the estimation various ground measurements simultaneously. The second chapter elucidates and reviews various literature regarding traditional measurements in the forestry, the application of optical remote sensing, the need for LIDAR remote sensing, integration of LiDAR and optical imagery, and the significance of

terrestrial Laser scanner in forest mensuration. Description of forests in the Western Ghats, as well as the details of each study area (Mudumalai forest and Sholayar forest), are described in chapter 3. The data set used for the study area including optical imageries like Landsat and AVIRIS -NG hyperspectral imagery are detailed. Both spaceborne and terrestrial LiDAR point cloud and, the field measurements which are used for the validation of the results are presented in chapter 3. In chapter 4, the methodology of the research which includes the pre-processing steps, a method for integration of the optical and LiDAR point cloud and the methodology for the analysis of TLS point cloud are given in detail. In Chapter 5, the results are presented and analyzed. The summary of work related to each objective is given below

6.1.1 Biophysical Characterisation by the Integration of Spaceborne LiDAR Point Cloud and Multispectral Imagery

Summary of the first objective is given as the following. The study estimated the biophysical parameters of Mudumalai and Sholayar forests of the Western Ghats of India by the integrated analysis of spaceborne LiDAR point cloud with multispectral imagery and the biophysical parameters estimated are canopy height, understory vegetation height, canopy density, and biomass. Consistent correlation of about R^2= 0.98 and R^2 = 0.97 (Mudumalai and Sholayar respectively) is obtained when comparing the heights estimated from canopy height models and the ground measurement heights. Biomass estimated also has a strong correlation (R^2 = 0.97 and R^2 = 0.96) with in situ measurements. The canopy height models from the GLAS LiDAR point cloud facilitate the possibility of estimation of understory vegetation height. The study also estimated the heights of the understory vegetation which reflects the growth of a lot of invasive species in the Western Ghats forest region. There are no studies in India for the estimation of the height of the understory

vegetation using remote sensing. This study, for the first time, has attempted to estimate the spatial distribution of understory using spaceborne LiDAR point cloud.

6.1.2 3-D Tree Reconstruction and Biophysical Parameter Estimation using Terrestrial Laser Scanner (TLS)

The summary of the work related to the second objective is as follows. The study proposes a novel method of the three-dimensional reconstruction of individual trees in Mudumalai forests of Western Ghats by implementing hierarchical min-cut algorithm and super voxel clustering algorithm. The study has estimated the structural metrics of individual trees with consistent correlation with the ground measurements. The estimated structure metrics are the height of the trees and the diameter at breast height (DBH). The study also accurately estimated LAI of the Mudumalai forest region by the multivariate regression analysis of DBH and height. A consistent correlation with the in-situ measurement is obtained for LAI estimated. Both the segmentation algorithms implemented in the study achieved good balance between the over-segmentation and the under-segmentation of the tree point clouds from the TLS point cloud. Three- dimensional reconstruction of trees and the individual tree detection helps to estimate the tree structural metrics such as LAI determined in this study at a higher level of accuracy by proposing a new algorithm called Point Spatial Density algorithm (PSD) for direct estimation of LAI. The study also implemented two segmentation methods for the individual three-dimensional tree reconstruction and segmentation of trees very effectively which enables the successful detection of tree crowns, trunks, and the branch details. A strong correlation is obtained when the estimated LAI values are compared with the ground measurements. The novelty of the method is the estimation of LAI with a method which depends only on the

point density, point spacing, and height of the trees, which can significantly contribute to mitigate the challenges faced by the forest inventory methods and practices for LAI estimation in the heterogeneous complex forest ecosystems.

6.1.3 Estimation of Biophysical Parameters from Airborne Hyperspectral Imagery by Integration with LiDAR Point Cloud

About the third objective, the integration of LiDAR point cloud with the hyperspectral imagery in the Western Ghats regions of India had successfully estimated the biophysical parameters. The important biophysical parameters estimated are canopy height, biomass, and LAI. Also, the approach developed in this study throws light on the forest health conditions.

The LAI retrieved by two different segmentation methods and by the direct estimation using the proposed PSD algorithm show a strong correlation with reference measurements. The biomass estimated by the integration of LiDAR point cloud, the multispectral imagery, and the hyperspectral imagery also shows a strong correlation with reference measurements. The approach reveals that the integration method used in the study leads to meaningful extraction of the biophysical parameters. The study represents an important step towards future tasks of remote sensing based biomass and carbon budget estimation of heterogeneous forests in India.

6.2 Future Recommendations

The spaceborne full waveform LiDAR point cloud used in this thesis has lots of gaps in the areal coverage; being an experimental spaceborne LiDAR satellite GLAS sensor has had acquired point cloud globally with discrete footprints which are separated by hundreds of meters. These discrete

footprints are insufficient for effectively modeling the variation in forest biomass. Therefore, it is suggested that there should be a continuous acquisition of footprints instead of discrete footprints. For the effective and accurate modeling of the highly complex forests such as the Western Ghats, it is required that both the LiDAR point cloud and spectral data should be acquired simultaneously and preferably from the same type of platform – satellite or airborne. It should also be in correlation with the spatial resolution of optical sensors. This thesis has integrated the point cloud and spectral data at the primary data level. Future studies may enable the integration of point cloud and spectral data at the feature/decision level for ease of computation and visualization.

******

REFERENCES

[1] Abdel-Rahman, E. M., Landmann, T., Kyalo, R., Ong'amo, G., Mwalusepo, S., Sulieman, S., & Le Ru, B. (2017). Predicting stem borer density in maize using RapidEye data and generalized linear models. *International journal of applied earth observation and geoinformation*, *57*, 61-74.

[2] Aboal, J. R., Arévalo, J. R., & Fernández, Á. (2005). Allometric relationships of different tree species and stand above ground biomass in the Gomera laurel forest (Canary Islands). *Flora-Morphology, Distribution, Functional Ecology of Plants*, 200(3), 264-274.

[3] Abshire, J. B., Sun, X., Riris, H., Sirota, J. M., McGarry, J. F., Palm, S., ... & Liiva, P. (2005). Geoscience laser altimeter system (GLAS) on the ICESat mission: on-orbit measurement performance. *Geophysical Research Letters*, *32*(21).

[4] Adan, M. S. (2017). *Integrating Sentinel-2 Derived Vegetation Indices and Terrestrial Laser Scanner to Estimate Above-Ground Biomass/Carbon in Ayer Hitam Tropical Forest Malaysia* (Doctoral dissertation, Master's Thesis, The University of Twente, Enschede, The Netherlands).

[5] Adler-Golden, S., Berk, A., Bernstein, L. S., Richtsmeier, S., Acharya, P. K., Matthew, M. W., ... & Chetwynd, J. H. (1998, December). FLAASH, a MODTRAN4 atmospheric correction package for hyperspectral data retrievals and simulations. In *Proc. 7th Ann. JPL Airborne Earth Science Workshop* (Vol. 97, pp. 9-14). Pasadena, CA: JPL Publication.

[6] Aijazi, A. K., Checchin, P., & Trassoudaine, L. (2013). Segmentation based classification of 3D urban point clouds: A super-voxel based approach with evaluation. *Remote Sensing*, *5*(4), 1624-1650.

[7] Alam, M. B., Shahi, C., & Pulkki, R. (2014). Economic impact of enhanced forest inventory information and merchandizing yards in the forest product industry supply chain. *Socio-Economic Planning Sciences*, *48*(3), 189-197.

[8] Andersen, H. E., McGaughey, R. J., & Reutebuch, S. E. (2005). Estimating forest canopy fuel parameters using LIDAR data. *Remote sensing of Environment*, *94*(4), 441-449.

[9] Andersen, H. E., Reutebuch, S. E., & McGaughey, R. J. (2006). A rigorous assessment of tree height measurements obtained using airborne-LiDAR and conventional field methods. *Canadian Journal of Remote Sensing*, *32*(5), 355-366.

[10] Anderson, J. E., Plourde, L. C., Martin, M. E., Braswell, B. H., Smith, M. L., Dubayah, R. O., ... & Blair, J. B. (2008). Integrating waveform lidar with hyperspectral imagery for inventory of a northern temperate forest. *Remote Sensing of Environment*, *112*(4), 1856-1870.

[11] Antonarakis, A. S., Richards, K. S., Brasington, J., & Muller, E. (2010). Determining leaf area index and leafy tree roughness using terrestrial laser scanning. *Water Resources Research*, *46*(6).

[12] Bachman, C. G. (1979). Laser radar systems and techniques. *Dedham, Mass., Artech House, Inc., 1979. 203 p.*

[13] Bae, S., &Schutz, B. E. (2002). Precision attitude determination (PAD). *Algorithm Theoretical Basis Documents (ATBD)*.

[14] Baghdadi, N., Le Maire, G., Fayad, I., Bailly, J. S., Nouvellon, Y., Lemos, C., & Hakamada, R. (2014). Testing different methods of forest height and aboveground biomass estimations from ICESat/GLAS data in Eucalyptus plantations in Brazil. *IEEE Journal of Selected Topics in Applied Earth Observations and Remote Sensing*, *7*(1), 290-299.

[15] Baltsavias, E. P. (1999). A comparison between photogrammetry and laser scanning. *ISPRS Journal of photogrammetry and Remote Sensing*, *54*(2), 83-94.

[16] Bassier, M., Bonduel, M., Van Genechten, B., & Vergauwen, M. (2017, November). Segmentation of Large Unstructured Point Clouds Using Octree-Based Region Growing and Conditional Random Fields. In *The International Archives of the Photogrammetry, Remote Sensing and Spatial Information Sciences* (Vol. 42, pp. 25-30).

[17] Belgiu, M., & Drăguţ, L. (2016). Random forest in remote sensing: A review of applications and future directions. *ISPRS Journal of Photogrammetry and Remote Sensing*, *114*, 24-31.

[18] Binot, J. M., Pothier, D., & Lebel, J. (1995). Comparison of relative accuracy and time requirement between the caliper, the diameter tape and an electronic tree measuring fork. *The Forestry Chronicle*, 71(2), 197-200.

[19] Blair, J. B., Rabine, D. L., & Hofton, M. A. (1999). The Laser Vegetation Imaging Sensor: a medium-altitude, digitisation-only, airborne laser altimeter for mapping vegetation and topography. *ISPRS Journal of Photogrammetry and Remote Sensing*, *54*(2), 115-122.

[20] Boegh, E., Soegaard, H., Broge, N., Hasager, C. B., Jensen, N. O., Schelde, K., & Thomsen, A. (2002). Airborne multispectral data for quantifying leaf area index, nitrogen concentration, and photosynthetic efficiency in agriculture. *Remote sensing of Environment*, *81*(2-3), 179-193.

[21] Bonham, C.D., 1989. Measurements for Terrestrial Vegetation. *John Wiley &Sons*, New York.

[22] Boudreau, J., Nelson, R. F., Margolis, H. A., Beaudoin, A., Guindon, L., & Kimes, D. S. (2008). Regional aboveground forest biomass using airborne and spaceborne LiDAR in Québec. *Remote Sensing of Environment*, *112*(10), 3876-3890.

[23] Bournez, E., Landes, T., Saudreau, M., Kastendeuch, P., & Najjar, G. (2017). From TLS point clouds to 3D models of trees: a comparison of existing algorithms for 3D tree reconstruction. *The International Archives of Photogrammetry, Remote Sensing and Spatial Information Sciences*, *42*, 113.

[24] Brosofske, K. D., Froese, R. E., Falkowski, M. J., & Banskota, A. (2014). A review of methods for mapping and prediction of inventory attributes for operational forest management. *Forest Science*, *60*(4), 733-756.

[25] Brown, S., Schroeder, P., & Birdsey, R. (1997). Aboveground biomass distribution of US eastern hardwood forests and the use of large trees as an indicator of forest development. *Forest Ecology and Management*, 96(1-2), 37-47.

[26] Brummer, J. E., Nichols, J. T., Engel, R. K., & Eskridge, K. M. (1994). Efficiency of different quadrat sizes and shapes for sampling standing crop. *Journal of Range management*, 84-89.

[27] Cao, Q., Miao, Y., Shen, J., Yu, W., Yuan, F., Cheng, S., ... & Liu, F. (2016). Improving in-season estimation of rice yield potential and responsiveness to topdressing nitrogen application with Crop Circle active crop canopy sensor. *Precision agriculture*, *17*(2), 136-154.

[28] Carlson, T. N., & Ripley, D. A. (1997). On the relation between NDVI, fractional vegetation cover, and leaf area index. *Remote sensing of Environment*, *62*(3), 241-252.

[29] Ceccato, P., Flasse, S., Tarantola, S., Jacquemoud, S., & Grégoire, J. M. (2001). Detecting vegetation leaf water content using reflectance in the optical domain. *Remote sensing of environment*, *77*(1), 22-33.

[30] Champion, S. H., & Seth, S. K. (1968). A revised survey of the forest types of India. *A revised survey of the forest types of India.*

[31] Chandran, M. D. S., & Mesta, D. K. (2001). On the conservation of the Myristica swamps of the Western Ghats. *Forest genetic resources: status, threats, and conservation strategies*, 1-19.

[32] Chauve, A., Durrieu, S., Bretar, F., Pierrot-Deseilligny, M., & Puech, W. (2008, July). Processing full-waveform lidar data to extract forest parameters and digital terrain model: Validation in an alpine coniferous forest. In *ForestSat Conference'07* (p. 5).

[33] Chave, J., Andalo, C., Brown, S., Cairns, M. A., Chambers, J. Q., Eamus, D., ... & Lescure, J. P. (2005). Tree allometry and improved estimation of carbon stocks and balance in tropical forests. *Oecologia*, *145*(1), 87-99.

[34] Chen, J. C., Yang, C. M., Wu, S. T., Chung, Y. L., Charles, A. L., & Chen, C. T. (2007). Leaf chlorophyll content and surface spectral reflectance of tree species along a terrain gradient in Taiwan's Kenting National Park. *Stud*, *48*, 71-77.

[35] Chen, J. M., & Black, T. A. (1992). Defining leaf area index for non-flat leaves. *Plant, Cell & Environment*, *15*(4), 421-429.

[36] Chen, K. S., Huang, W. P., Tsay, D. H., & Amar, F. (1996). Classification of multifrequency polarimetric SAR imagery using a dynamic learning neural network. *IEEE Transactions on Geoscience and Remote Sensing*, *34*(3), 814-820.

[37] Chen, Q. (2010). Retrieving vegetation height of forests and woodlands over mountainous areas in the Pacific Coast region using satellite laser altimetry. *Remote Sensing of Environment*, *114*(7), 1610-1627.

[38] Chi, H., Sun, G., Huang, J., Li, R., Ren, X., Ni, W., & Fu, A. (2017). Estimation of Forest Aboveground Biomass in Changbai Mountain Region Using ICESat/GLAS and Landsat/TM Data. *Remote Sensing*, *9*(7), 707.

[39] Cifuentes, R., Van der Zande, D., Farifteh, J., Salas, C., & Coppin, P. (2014). Effects of voxel size and sampling setup on the estimation of forest canopy gap fraction from terrestrial laser scanning data. *Agricultural and forest meteorology*, *194*, 230-240.

[40] Clark, D. A., & Clark, D. B. (2001). Getting to the canopy: tree height growth in a neotropical rain forest. *Ecology*, 82(5), 1460-1472.

[41] Clark, M. L., Clark, D. B., & Roberts, D. A. (2004). Small-footprint lidar estimation of sub-canopy elevation and tree height in a tropical rain forest landscape. *Remote Sensing of Environment*, *91*(1), 68-89.

[42] Clark, M. L., Roberts, D. A., & Clark, D. B. (2005). Hyperspectral discrimination of tropical rain forest tree species at leaf to crown scales. *Remote sensing of environment*, *96*(3-4), 375-398.

[43] Clawges, R., Vierling, L., Calhoon, M., & Toomey, M. (2007). Use of a ground-based scanning lidar for estimation of biophysical properties of western larch (Larix occidentalis). *International Journal of Remote Sensing*, *28*(19), 4331-4344.

[44] Cohen, W. B., & Goward, S. N. (2004). Landsat's role in ecological applications of remote sensing. *AIBS Bulletin*, 54(6), 535-545.

[45] Cohen, W. B., Maiersperger, T. K., Spies, T. A., & Oetter, D. R. (2001). Modelling forest cover attributes as continuous variables in a regional context with Thematic Mapper data. *International Journal of Remote Sensing*, *22*(12), 2279-2310.

[46] Cortes, C., & Vapnik, V. (1995). Support-vector networks. *Machine learning*, *20*(3), 273-297.

[47] Côté, J. F., Fournier, R. A., & Egli, R. (2011). An architectural model of trees to estimate forest structural attributes using terrestrial LiDAR. *Environmental Modelling & Software*, *26*(6), 761-777.

[48] Danson, F. M., Gaulton, R., Armitage, R. P., Disney, M., Gunawan, O., Lewis, P., ... & Ramirez, A. F. (2014). Developing a dual-wavelength full-waveform terrestrial laser scanner to characterize forest canopy structure. *Agricultural and Forest Meteorology*, *198*, 7-14.

[49] Danson, F. M., Hetherington, D., Morsdorf, F., Koetz, B., &Allgower, B. (2007). Forest canopy gap fraction from terrestrial laser scanning. *IEEE Geoscience and Remote Sensing Letters*, *4*(1), 157-160.

[50] Darvishzadeh, R., Atzberger, C., Skidmore, A., & Schlerf, M. (2011). Mapping grassland leaf area index with airborne hyperspectral imagery: A comparison study of statistical approaches and inversion of radiative transfer models. *ISPRS Journal of Photogrammetry and Remote Sensing*, *66*(6), 894-906.

[51] Dean, T. J., Roberts, S., Gilmore, D., Maguire, D. A., Long, J. N., O'hara, K. L., & Seymour, R. S. (2002). An evaluation of the uniform stress hypothesis based on stem geometry in selected North American conifers. *Trees*, *16*(8), 559-568.

[52] Devi, L. S., & Yadava, P. S. (2009). Aboveground biomass and net primary production of semi-evergreen tropical forest of Manipur, north-eastern India. *Journal of Forestry Research*, 20(2), 151-155.

[53] Dimri, Suchita, Pratibha Baluni, and Chandra Mohan Sharma. "GROWING STOCK OF VARIOUS PURE CONIFER FOREST TYPES OF CENTRAL (GARHWAL) HIMALAYA, INDIA." *International Journal of Current Research and Review* 6.22 (2014): 45.

[54] Dornbusch, T., Wernecke, P., & Diepenbrock, W. (2007). A method to extract morphological traits of plant organs from 3D point clouds as a database for an architectural plant model. *Ecological Modelling*, *200*(1-2), 119-129.

[55] Dubayah, R. O., & Drake, J. B. (2000). Lidar remote sensing for forestry. *Journal of Forestry*, *98*(6), 44-46.

[56] Dube, T., & Mutanga, O. (2015). Evaluating the utility of the medium-spatial resolution Landsat 8 multispectral sensor in quantifying aboveground biomass in uMgeni catchment, South Africa. *ISPRS Journal of Photogrammetry and Remote Sensing*, *101*, 36-46.

[57] Duncanson, L. I., Niemann, K. O., & Wulder, M. A. (2010). Estimating forest canopy height and terrain relief from GLAS waveform metrics. *Remote Sensing of Environment*, *114*(1), 138-154.

[58] Dymond, C. C., Mladenoff, D. J., & Radeloff, V. C. (2002). Phenological differences in Tasseled Cap indices improve deciduous forest classification. *Remote Sensing of Environment*, *80*(3), 460-472.

[59] Eggleston, N. (2001). Tree and terrain measurements from a small-footprint multiple-return airborne LIDAR. *Master Thesis, Mississippi State University*.

[60] Erfanifard, Y., Stereńczak, K., Kraszewski, B., & Kamińska, A. (2018). Development of a robust canopy height model derived from ALS point clouds for predicting individual crown attributes at the species level. *International Journal of Remote Sensing*, *39*(23), 9206-9227.

[61] Evans, J. S., Hudak, A. T., Faux, R., & Smith, A. (2009). Discrete return lidar in natural resources: Recommendations for project planning, data processing, and deliverables. *Remote Sensing*, *1*(4), 776-794.

[62] Flood, M., & Gutelius, B. (1997). Commercial implications of topographic terrain mapping using scanningairborne laser radar. *Photogrammetric Engineering and Remote Sensing*, *63*(4), 327-332

[63] Foody, G. M., Cutler, M. E., Mcmorrow, J., Pelz, D., Tangki, H., Boyd, D. S., & Douglas, I. (2001). Mapping the biomass of Bornean tropical rain forest from remotely sensed data. *Global Ecology and Biogeography*, 10(4), 379-387.

[64] FSI (2017) India state of forest report 2017. Forest Survey of India, Ministry of Environment, Forest and Climate Change. Government of India, Dehradun.

[65] Franklin, J. F., Spies, T., Perry, D., Harmon, M., & McKee, A. (1986). Modifying Douglas-fir management regimes for nontimber objectives. *Modifying Douglas-fir management regimes for non-timber objectives*, 373-379.

[66] Fujisaki, I. (2005).LiDAR-based Forest Visualization. *PhD Dissertation, Mississippi State University.*

[67] Fujisaki, I., M.J. Mohammadi-Aragh, D. Irby, R.J. Moorhead, D.L. Evans and S.D. Roberts. (2003).LiDAR based forest visualization: modeling forest stands and cognitive issues. *Proceedings of the American Society for Photogrammetry and Remote Sensing*. May 5–9. Anchorage, AK.

[68] Gao, B. C. (1995, June). Normalized difference water index for remote sensing of vegetation liquid water from space. In *Imaging Spectrometry* (Vol. 2480, pp. 225-237). International Society for Optics and Photonics.

[69] Gao, H., Wang, L., Jing, L., & Xu, J. (2016, April). An effective modified water extraction method for Landsat-8 OLI imagery of mountainous plateau regions. In *IOP Conference Series: Earth and Environmental Science* (Vol. 34, No. 1, p. 012010). IOP Publishing.

[70] Geist, H. J., &Lambin, E. F. (2001). What drives tropical deforestation. *LUCC Report series*, *4*, 116.

[71] Ghassemian, H. (2016). A review of remote sensing image fusion methods. *Information Fusion*, *32*, 75-89.

[72] Gillis, M. D., & Leckie, D. G. (1996). Forest inventory update in Canada. *The Forestry Chronicle*, *72*(2), 138-156.

[73] Gitelson, A. A., & Merzlyak, M. N. (1998). Remote sensing of chlorophyll concentration in higher plant leaves. *Advances in Space Research*, *22*(5), 689-692.

[74] Goetz, A. F., & Landauer Jr, F. P. (1979). *U.S. Patent No. 4,134,683*. Washington, DC: U.S. Patent and Trademark Office.

[75] Golovinskiy, A., & Funkhouser, T. (2009, September). Min-cut based segmentation of point clouds. In *Computer Vision Workshops (ICCV Workshops), 2009 IEEE 12th International Conference on* (pp. 39-46). IEEE.

[76] Goodwin, A. N. (2004). Measuring tall tree heights from the ground. *TASFORESTS-HOBART-*, 15, 85-98.

[77] Goodwin, N. R., Coops, N. C., & Culvenor, D. S. (2006). Assessment of forest structure with airborne LiDAR and the effects of platform altitude. *Remote Sensing of Environment*, *103*(2), 140-152.

[78] Govender, M., Chetty, K., & Bulcock, H. (2007). A review of hyperspectral remote sensing and its application in vegetation and water resource studies. *Water Sa*, *33*(2).

[79] Hajj, M. E., Baghdadi, N., Fayad, I., Vieilledent, G., Bailly, J. S., & Minh, D. H. T. (2017). Interest of integrating spaceborneLiDAR data to improve the estimation of biomass in high biomass forested areas. *Remote Sensing*, *9*(3), 213.

[80] Hamraz, H., & Contreras, M. A. (2017). Remote sensing of forests using discrete return airborne LiDAR. *arXiv preprint arXiv:1707.09865*.

[81] Hansen, A. J., Rasker, R., Maxwell, B., Rotella, J. J., Johnson, J. D., Parmenter, A. W., ... & Kraska, M. P. (2002). Ecological Causes and Consequences of Demographic Change in the New West: As natural amenities attract people and commerce to the rural west, the resulting land-use changes threaten biodiversity, even in protected areas, and challenge efforts to sustain local communities and ecosystems. *AIBS Bulletin*, *52*(2), 151-162.

[82] Harding, D. J., & Carabajal, C. C. (2005). ICESat waveform measurements of within-footprint topographic relief and vegetation vertical structure. *Geophysical research letters*, *32*(21).

[83] Harding, D. J., Blair, J., Garvin, J. B., & Lawrence, W. T. (1994, August). Laser altimetry waveform measurement of vegetation

canopy structure. In *Geoscience and Remote Sensing Symposium, 1994. IGARSS'94. Surface and Atmospheric Remote Sensing: Technologies, Data Analysis and Interpretation., International* (Vol. 2, pp. 1251-1253). IEEE.

[84] Harding, D. J., Lefsky, M. A., Parker, G. G., & Blair, J. B. (2001). Laser altimeter canopy height profiles: Methods and validation for closed-canopy, broadleaf forests. *Remote Sensing of Environment*, *76*(3), 283-297.

[85] Hashimotio, T., Kojima, K., Tange, T., & Sasaki, S. (2000). Changes in carbon storage in fallow forests in the tropical lowlands of Borneo. *Forest Ecology and Management*, *126*(3), 331-337.

[86] Hayashi, M., Saigusa, N., Oguma, H., & Yamagata, Y. (2013). Forest canopy height estimation using ICESat/GLAS data and error factor analysis in Hokkaido, Japan. *ISPRS journal of photogrammetry and remote sensing*, *81*, 12-18.

[87] Hiremath, A. J., & Sundaram, B. (2013). Invasive plant species in Indian protected areas: conserving biodiversity in cultural landscapes. In *Plant invasions in protected areas* (pp. 241-266). Springer, Dordrecht.

[88] Hopkinson, C., & Chasmer, L. E. (2007, September). Modelling canopy gap fraction from lidar intensity. In *ISPRS Workshop on Laser Scanning 2007 and SilviLaser 2007* (pp. 190-194). IAPRS Espoo, Finland.

[89] Hopkinson, C., Chasmer, L. E., Sass, G., Creed, I. F., Sitar, M., Kalbfleisch, W., & Treitz, P. (2005). Vegetation class dependent errors in LiDAR ground elevation and canopy height estimates in a

boreal wetland environment. *Canadian Journal of Remote Sensing*, *31*(2), 191-206.

[90] Hosoi, F., & Omasa, K. (2006). Voxel-based 3-D modeling of individual trees for estimating leaf area density using high-resolution portable scanning lidar. *IEEE transactions on geoscience and remote sensing*, *44*(12), 3610-3618.

[91] Hu, T., Su, Y., Xue, B., Liu, J., Zhao, X., Fang, J., & Guo, Q. (2016). Mapping global forest aboveground biomass with spaceborne LiDAR, optical imagery, and forest inventory data. *Remote Sensing*, *8*(7), 565.

[92] Huang, H., Li, Z., Gong, P., Cheng, X., Clinton, N., Cao, C., ... & Wang, L. (2011). Automated methods for measuring DBH and tree heights with a commercial scanning lidar. *Photogrammetric Engineering & Remote Sensing*, *77*(3), 219-227.

[93] Hudak, A. T., Lefsky, M. A., Cohen, W. B., & Berterretche, M. (2002). Integration of lidar and Landsat ETM+ data for estimating and mapping forest canopy height. *Remote sensing of Environment*, *82*(2-3), 397-416.

[94] Hudak, A. T., Strand, E. K., Vierling, L. A., Byrne, J. C., Eitel, J. U., Martinuzzi, S., & Falkowski, M. J. (2012). Quantifying aboveground forest carbon pools and fluxes from repeat LiDAR surveys. *Remote Sensing of Environment*, *123*, 25-40.

[95] Huete, A. R. (1988). A soil-adjusted vegetation index (SAVI). *Remote sensing of environment*, *25*(3), 295-309.

[96] Huete, A. R., Liu, H., & van Leeuwen, W. J. (1997, August). The use of vegetation indices in forested regions: issues of linearity and

saturation. In *IGARSS'97. 1997 IEEE International Geoscience and Remote Sensing Symposium Proceedings. Remote Sensing-A Scientific Vision for Sustainable Development* (Vol. 4, pp. 1966-1968). IEEE.

[97] Huete, A., Didan, K., Miura, T., Rodriguez, E. P., Gao, X., & Ferreira, L. G. (2002). Overview of the radiometric and biophysical performance of the MODIS vegetation indices. *Remote sensing of environment*, *83*(1-2), 195-213.

[98] Hughes, R. F., Kauffman, J. B., & Jaramillo, V. J. (1999). Biomass, carbon, and nutrient dynamics of secondary forests in a humid tropical region of Mexico. *Ecology*, 80(6), 1892-1907.

[99] Hussin, Y. A., & Sha, K. (1996). Monitoring forest cover changes using remotely sensed data and geographical information systems in sub-tropical environment.

[100] Jackson, R. D., & Huete, A. R. (1991). Interpreting vegetation indices. *Preventive veterinary medicine*, *11*(3-4), 185-200.

[101] Jupp, D. L., Culvenor, D. S., Lovell, J. L., Newnham, G. J., Strahler, A. H., & Woodcock, C. E. (2009). Estimating forest LAI profiles and structural parameters using a ground-based laser called 'Echidna®. *Tree physiology*, *29*(2), 171-181.

[102] Karlson, M., Ostwald, M., Reese, H., Sanou, J., Tankoano, B., & Mattsson, E. (2015). Mapping tree canopy cover and aboveground biomass in Sudano-Sahelian woodlands using Landsat 8 and random forest. *Remote Sensing*, 7(8), 10017-10041.

[103] Kasturirangan, K., Babu, C. R., Mauskar, J. M., Chopra, K., Kishwan, J., Shankar, D., ... & Chandrasekharan, I. (2013). Report

of the high level working group on Western Ghats. *submitted to the Ministry of Environment and Forests, Government of India*.

[104] Kosaka, N., Akiyama, T., Tsai, B., & Kojima, T. (2005, July). Forest type classification using data fusion of multispectral and panchromatic high-resolution satellite imageries. In *Geoscience and Remote Sensing Symposium, 2005. IGARSS'05. Proceedings. 2005 IEEE International* (Vol. 4, pp. 2980-2983). IEEE.

[105] Kretschmer, U., Kirchner, N., Morhart, C., & Spiecker, H. (2013). A new approach to assessing tree stem quality characteristics using terrestrial laser scans. *Silva Fenn*, *47*(5), 1071.

[106] Lang, A. R. G. (1991). Application of some of Cauchy's theorems to estimation of surface areas of leaves, needles and branches of plants, and light transmittance. *Agricultural and Forest Meteorology*, *55*(3-4), 191-212.

[107] Larjavaara, M., & Muller-Landau, H. C. (2013). Measuring tree height: a quantitative comparison of two common field methods in a moist tropical forest. *Methods in Ecology and Evolution*, 4(9), 793-801.

[108] Latifi, H., Fassnacht, F., & Koch, B. (2012). Forest structure modeling with combined airborne hyperspectral and LiDAR data. *Remote Sensing of Environment*, *121*, 10-25.

[109] Latifi, H., Hill, S., Schumann, B., Heurich, M., & Dech, S. (2017). Multi-model estimation of understorey shrub, herb and moss cover in temperate forest stands by laser scanner data. *Forestry: An International Journal of Forest Research*, *90*(4), 496-514.

[110] Leblanc, S. G. (2002). Correction to the plant canopy gap-size analysis theory used by the tracing radiation and architecture of canopies instrument. *Applied Optics*, *41*(36), 7667-7670.

[111] Lefsky, M. A. (2010). A global forest canopy height map from the Moderate Resolution Imaging Spectroradiometer and the Geoscience Laser Altimeter System. *Geophysical Research Letters*, *37*(15).

[112] Lefsky, M. A., Cohen, W. B., & Spies, T. A. (2001). An evaluation of alternate remote sensing products for forest inventory, monitoring, and mapping of Douglas-fir forests in western Oregon. *Canadian journal of forest research*, 31(1), 78-87.

[113] Lefsky, M. A., Cohen, W. B., Acker, S. A., Parker, G. G., Spies, T. A., & Harding, D. (1999). Lidar remote sensing of the canopy structure and biophysical properties of Douglas-fir western hemlock forests. *Remote sensing of environment*, *70*(3), 339-361.

[114] Lefsky, M. A., Cohen, W. B., Acker, S. A., Spies, T. A., Parker, G. G., & Harding, D. (1998, July). Lidar remote sensing of forest canopy structure and related biophysical parameters at HJ Andrews experimental forest, Oregon, USA. In *Geoscience and Remote Sensing Symposium Proceedings, 1998. IGARSS'98. 1998 IEEE International* (Vol. 3, pp. 1252-1254). IEEE.

[115] Lefsky, M. A., Cohen, W. B., Harding, D. J., Parker, G. G., Acker, S. A., & Gower, S. T. (2002b). Lidar remote sensing of above-ground biomass in three biomes. *Global ecology and biogeography*, *11*(5), 393-399.

[116] Lefsky, M. A., Cohen, W. B., Parker, G. G., & Harding, D. J. (2002a). Lidar remote sensing for ecosystem studies: Lidar, an emerging remote sensing technology that directly measures the three-dimensional distribution of plant canopies, can accurately estimate vegetation structural attributes and should be of particular interest to forest, landscape, and global ecologists. *AIBS Bulletin*, *52*(1), 19-30.

[117] Lefsky, M. A., Harding, D. J., Keller, M., Cohen, W. B., Carabajal, C. C., Del BomEspirito-Santo, F., Maria O. Hunter & de Oliveira, R. (2005). Estimates of forest canopy height and aboveground biomass using ICESat. *Geophysical research letters*, *32*(22).

[118] Lefsky, M. A., Keller, M., Pang, Y., De Camargo, P. B., & Hunter, M. O. (2007). Revised method for forest canopy height estimation from Geoscience Laser Altimeter System waveforms. *Journal of Applied Remote Sensing*, *1*(1), 013537.

[119] Liang, X., & Hyyppä, J. (2013). Automatic stem mapping by merging several terrestrial laser scans at the feature and decision levels. *Sensors*, *13*(2), 1614-1634.

[120] Liang, X., Kankare, V., Hyyppä, J., Wang, Y., Kukko, A., Haggrén, H., ... & Holopainen, M. (2016). Terrestrial laser scanning in forest inventories. *ISPRS Journal of Photogrammetry and Remote Sensing*, *115*, 63-77.

[121] Lillesand, T., Kiefer, R. W., & Chipman, J. (2014). *Remote sensing and image interpretation*. John Wiley & Sons.

[122] Lim, K., Treitz, P., Wulder, M., St-Onge, B., & Flood, M. (2003). LiDAR remote sensing of forest structure. *Progress in physical geography*, *27*(1), 88-106.

[123] Lindberg, E., Holmgren, J., Olofsson, K., & Olsson, H. (2012). Estimation of stem attributes using a combination of terrestrial and airborne laser scanning. *European Journal of Forest Research*, *131*(6), 1917-1931.

[124] Listopad, C. M., Masters, R. E., Drake, J., Weishampel, J., & Branquinho, C. (2015). Structural diversity indices based on airborne LiDAR as ecological indicators for managing highly dynamic landscapes. *Ecological indicators*, *57*, 268-279.

[125] Liu, K., Wang, J., Zeng, W., & Song, J. (2017). Comparison and Evaluation of Three Methods for Estimating Forest above Ground Biomass Using TM and GLAS Data. *Remote Sensing*, *9*(4), 341.

[126] Liu, S., Lv, Y., Tong, X., Xie, H., Liu, J., & Chen, L. (2016). An Alternative Approach for Registration of High-Resolution Satellite Optical Imagery and ICESat Laser Altimetry Data. *Sensors*, *16*(12), 2008.

[127] Lodhiyal, N., & Lodhiyal, L. S. (2003). Biomass and net primary productivity of Bhabar Shisham forests in central Himalaya, India. *Forest Ecology and Management*, 176(1-3), 217-235.

[128] Lovell, J. L., Jupp, D. L., Culvenor, D. S., & Coops, N. C. (2003). Using airborne and ground-based ranging lidar to measure canopy structure in Australian forests. *Canadian Journal of Remote Sensing*, *29*(5), 607-622.

[129] Lu, D. (2006). The potential and challenge of remote sensing-based biomass estimation. *International journal of remote sensing*, *27*(7), 1297-1328.

[130] Luo, S., Wang, C., Li, G., & Xi, X. (2013). Retrieving leaf area index using ICESat/GLAS full-waveform data. *Remote sensing letters*, *4*(8), 745-753.

[131] Maclean, G. A., & Martin, G. L. (1984). Merchantable timber volume estimation using cross-sectional photogrammetric and densitometric methods. *Canadian Journal of Forest Research*, 14(6), 803-810.

[132] Magnusson, M., Fransson, J. E., & Holmgren, J. (2007). Effects on estimation accuracy of forest variables using different pulse density of laser data. *Forest Science*, *53*(6), 619-626.

[133] Mahoney, C., Hopkinson, C., Held, A., Kljun, N., & Van Gorsel, E. (2016). ICESat/GLAS Canopy Height Sensitivity Inferred from Airborne Lidar. *Photogrammetric Engineering & Remote Sensing*, *82*(5), 351-363.

[134] Maltamo, M., & Packalen, P. (2014). Species-specific management inventory in Finland. In *Forestry applications of airborne laser scanning* (pp. 241-252). Springer Netherlands.

[135] Martin, M. E., Newman, S. D., Aber, J. D., & Congalton, R. G. (1998). Determining forest species composition using high spectral resolution remote sensing data. *Remote Sensing of Environment*, *65*(3), 249-254.

[136] Masemola, C., Cho, M. A., & Ramoelo, A. (2016). Comparison of Landsat 8 OLI and Landsat 7 ETM+ for estimating grassland LAI using model inversion and spectral indices: case study of Mpumalanga, South Africa. *International Journal of Remote Sensing*, *37*(18), 4401-4419.

[137] Matthew, M. W., Adler-Golden, S. M., Berk, A., Felde, G., Anderson, G. P., Gorodetzky, D., ... & Shippert, M. (2002, October). Atmospheric correction of spectral imagery: evaluation of the FLAASH algorithm with AVIRIS data. In *Applied Imagery Pattern Recognition Workshop, 2002. Proceedings.* (pp. 157-163). IEEE.

[138] McCombs, J. W., Roberts, S. D., & Evans, D. L. (2003). Influence of fusing lidar and multispectral imagery on remotely sensed estimates of stand density and mean tree height in a managed loblolly pine plantation. *Forest Science*, *49*(3), 457-466.

[139] McElhinny, C., Gibbons, P., Brack, C., & Bauhus, J. (2005). Forest and woodland stand structural complexity: its definition and measurement. *Forest Ecology and Management*, *218*(1-3), 1-24.

[140] McInerney, D. O., Suarez-Minguez, J., Valbuena, R., & Nieuwenhuis, M. (2010). Forest canopy height retrieval using LiDAR data, medium-resolution satellite imagery and k NN estimation in Aberfoyle, Scotland. *Forestry*, *83*(2), 195-206.

[141] Means, J. E., Acker, S. A., Fitt, B. J., Renslow, M., Emerson, L., & Hendrix, C. J. (2000). Predicting forest stand characteristics with airborne scanning lidar. *Photogrammetric Engineering and Remote Sensing*, *66*(11), 1367-1372.

[142] Meng, X., Wang, L., Silván-Cárdenas, J. L., & Currit, N. (2009). A multi-directional ground filtering algorithm for airborne LIDAR. *ISPRS Journal of Photogrammetry and Remote Sensing*, *64*(1), 117-124.

[143] Meng, J., Li, S., Wang, W., Liu, Q., Xie, S., & Ma, W. (2016). Estimation of forest structural diversity using the spectral and textural information derived from SPOT-5 satellite images. *Remote Sensing*, *8*(2), 125.

[144] Miller, J. R., Wu, J., Boyer, M. G., Belanger, M., & Hare, E. W. (1991). Seasonal patterns in leaf reflectance red-edge characteristics. *International Journal of Remote Sensing*, *12*(7), 1509-1523.

[145] Mitchell, A. L. (2004). *Forest Inventory System with Multispectral Imaging and LiDAR* (Doctoral dissertation, Mississippi State University. Department of Forestry).

[146] Mongus, D., & Žalik, B. (2012). Parameter-free ground filtering of LiDAR data for automatic DTM generation. *ISPRS Journal of Photogrammetry and Remote Sensing*, *67*, 1-12.

[147] Mutanga, O., & Skidmore, A. K. (2004). Narrow band vegetation indices overcome the saturation problem in biomass estimation. *International journal of remote sensing*, *25*(19), 3999-4014.

[148] Muthuramkumar, S., Ayyappan, N., Parthasarathy, N., Mudappa, D., Raman, T. S., Selwyn, M. A., & Pragasan, L. A. (2006). Plant Community Structure in Tropical Rain Forest Fragments of the Western Ghats, India 1. *Biotropica: The Journal of Biology and Conservation*, *38*(2), 143-160.

[149] Naesset, E. (1997a). Determination of mean tree height of forest stands using airborne laser scanner data. *ISPRS Journal of Photogrammetry and Remote Sensing*, *52*(2), 49-56.

[150] Naesset, E. (1997b). Estimating timber volume of forest stands using airborne laser scanner data. *Remote Sensing of Environment*, *61*(2), 246-253.

[151] Næsset, E., Gobakken, T., Holmgren, J., Hyyppä, H., Hyyppä, J., Maltamo, M., ... &Söderman, U. (2004). Laser scanning of forest resources: the Nordic experience. *Scandinavian Journal of Forest Research*, *19*(6), 482-499.

[152] Nair, N.G; Sasidharan, N (1985). Distribution of important forest tree species in Kerala (Central Circle). (*KFRI Research Report* No: 28: 31p).

[153] Nelson, B. W., Mesquita, R., Pereira, J. L., De Souza, S. G. A., Batista, G. T., & Couto, L. B. (1999). Allometric regressions for improved estimate of secondary forest biomass in the central Amazon. *Forest ecology and management*, 117(1-3), 149-167.

[154] Olsoy, P. J., Glenn, N. F., Clark, P. E., & Derryberry, D. R. (2014). Above ground total and green biomass of dryland shrub derived from terrestrial laser scanning. *ISPRS Journal of Photogrammetry and Remote Sensing*, *88*, 166-173.

[155] Omasa, K., Hosoi, F., Uenishi, T. M., Shimizu, Y., & Akiyama, Y. (2008). Three-dimensional modeling of an urban park and trees by combined airborne and portable on-ground scanning LIDAR remote sensing. *Environmental modeling & assessment*, *13*(4), 473-481.

[156] Ørka, H. O. (2011). Improving forest inventory and monitoring by combining remotely sensed three-dimensional and spectral information.

[157] Panel, W. G. E. E., & Gadgil Commission. (2011). Report of the Western Ghats Ecology Expert Panel. *The Ministry of Environment and Forests, Government of India, New Delhi*.

[158] Park, T., Kennedy, R. E., Choi, S., Wu, J., Lefsky, M. A., Bi, J., ... &Knyazikhin, Y. (2014). Application of physically-based slope correction for maximum forest canopy height estimation using waveform LiDAR across different footprint sizes and locations: Tests on LVIS and GLAS. *Remote Sensing*, *6*(7), 6566-6586.

[159] Parker, G. G., Lefsky, M. A., & Harding, D. J. (2001). Light transmittance in forest canopies determined using airborne laser altimetry and in-canopy quantum measurements. *Remote Sensing of Environment*, *76*(3), 298-309.

[160] Parker, R. C., & Evans, D. L. (2004). An application of LiDAR in a double-sample forest inventory. *Western Journal of Applied Forestry*, *19*(2), 95-101.

[161] Parker, R. C., & Matney, T. G. (1999). Comparison of optical dendrometers for prediction of standing tree volume. *Southern Journal of Applied Forestry*, 23(2), 100-107.

[162] Peterson, B., & Nelson, K. J. (2014). Mapping forest height in Alaska using GLAS, Landsat composites, and airborne LiDAR. *Remote Sensing*, *6*(12), 12409-12426.

[163] Peterson, D. J., Resetar, S., Brower, J., & Diver, R. (1999). Forest monitoring and remote sensing. *White House Office of Science and Technology Policy*.

[164] Pirotti, F., Guarnieri, A., Masiero, A., Vettore, A., & Lingua, E. (2014). Processing lidar waveform data for 3D visual assessment of forest environments. *The International Archives of Photogrammetry, Remote Sensing and Spatial Information Sciences*, *40*(5), 493.

[165] Pithon, S., Jubelin, G., Guitet, S., & Gond, V. (2013). A statistical method for detecting logging-related canopy gaps using high-resolution optical remote sensing. *International Journal of Remote Sensing*, *34*(2), 700-711.

[166] Popescu, S. C., & Wynne, R. H. (2004). Seeing the trees in the forest. *Photogrammetric Engineering & Remote Sensing*, *70*(5), 589-604.

[167] Popescu, S. C., & Zhao, K. (2008). A voxel-based lidar method for estimating crown base height for deciduous and pine trees. *Remote sensing of environment*, *112*(3), 767-781.

[168] Popescu, S. C., Wynne, R. H., & Scrivani, J. A. (2004). Fusion of small-footprint lidar and multispectral data to estimate plot-level volume and biomass in deciduous and pine forests in Virginia, USA. *Forest Science*, *50*(4), 551-565.

[169] Prasad, A. E. (2010). Effects of an exotic plant invasion on native understory plants in a tropical dry forest. *Conservation Biology*, *24*(3), 747-757.

[170] Quan, X., He, B., Yebra, M., Yin, C., Liao, Z., Zhang, X., & Li, X. (2017). A radiative transfer model-based method for the estimation of grassland aboveground biomass. *International journal of applied earth observation and geoinformation*, *54*, 159-168.

[171] Ramaswami, G., & Sukumar, R. (2011). Woody plant seedling distribution under invasive Lantana camara thickets in a dry-forest plot in Mudumalai, southern India. *Journal of Tropical Ecology*, *27*(4), 365-373.

[172] Raumonen, P., Kaasalainen, M., Åkerblom, M., Kaasalainen, S., Kaartinen, H., Vastaranta, M., ... & Lewis, P. (2013). Fast automatic precision tree models from terrestrial laser scanner data. *Remote Sensing*, *5*(2), 491-520.

[173] Ravindranath, N. H., & Ostwald, M. (2008). *Generic Methods for Inventory of Carbon Pools* (pp. 99-111). Springer Netherlands.

[174] Reddy, C. S., Jha, C. S., Diwakar, P. G., & Dadhwal, V. K. (2015). Nationwide classification of forest types of India using remote sensing and GIS. *Environmental monitoring and assessment*, *187*(12), 777.

[175] Reddy, C. S., Ugle, P., Murthy, M. S. R., & Sudhakar, S. (2008). Quantitative structure and composition of tropical forests of Mudumalai Wildlife Sanctuary, Western Ghats, India. *Taiwania*, *53*(2), 150-156.

[176] Reese, H., Nilsson, M., Sandström, P., & Olsson, H. (2002). Applications using estimates of forest parameters derived from satellite and forest inventory data. *Computers and Electronics in Agriculture*, 37(1-3), 37-55.

[177] Reitberger, J., Krzystek, P., & Stilla, U. (2008). Analysis of full waveform LIDAR data for the classification of deciduous and coniferous trees. *International journal of remote sensing*, *29*(5), 1407-1431.

[178] Reitberger, J., Krzystek, P., & Stilla, U. (2009, March). Benefit of airborne full waveform lidar for 3D segmentation and classification of single trees. In *ASPRS 2009 Annual Conference* (pp. 1-9).

[179] Renslow M, Greenfield P, Guay T. *Evaluation of Multi-Return LIDAR for Forestry Applications. RSAC-2060/4810-LSP-0001-RPT1*. 2000. USDA Forest Service - Engineering. Remote Sensing Applications Center.

[180] Rhody, B. (1975). A new approach to terrestrial and photographic forest sampling: The use of a panoramic lens. *Photogrammetria,* 30(2), 75-85.

[181] Richter, K., Vuolo, F., & D'Urso, G. (2008, July). Leaf area index and surface albedo estimation: comparative analysis from vegetation indexes to radiative transfer models. In *IGARSS 2008-2008 IEEE International Geoscience and Remote Sensing Symposium* (Vol. 3, pp. III-736). IEEE.

[182] Roberts, J. W., Tesfamichael, S., Gebreslasie, M., Van Aardt, J., & Ahmed, F. B. (2007). Forest structural assessment using remote sensing technologies: an overview of the current state of the art. *Southern Hemisphere Forestry Journal*, *69*(3), 183-203.

[183] Rock, B. N., Hoshizaki, T., & Miller, J. R. (1988). Comparison of in situ and airborne spectral measurements of the blue shift associated with forest decline. *Remote Sensing of Environment*, *24*(1), 109-127.

[184] Rosell, J. R., Llorens, J., Sanz, R., Arno, J., Ribes-Dasi, M., Masip, J., ... & Gil, E. (2009). Obtaining the three-dimensional structure of tree orchards from remote 2D terrestrial LIDAR scanning. *Agricultural and Forest Meteorology*, *149*(9), 1505-1515.

[185] Rosette, J. A. B., North, P. R. J., & Suarez, J. C. (2008). Vegetation height estimates for a mixed temperate forest using satellite laser altimetry. *International Journal of Remote Sensing*, *29*(5), 1475-1493.

[186] Rouse Jr, J., Haas, R. H., Schell, J. A., & Deering, D. W. (1974). Monitoring vegetation systems in the Great Plains with ERTS.

[187] Rowe, J. (2013). Ground Classification and Below Ground Response Assessment of Forested Regions using Full-Waveform LiDAR.

[188] Roy, P. S., & Ravan, S. A. (1996). Biomass estimation using satellite remote sensing data—an investigation on possible approaches for natural forest. *Journal of biosciences*, *21*(4), 535-561.

[189] Saatchi, S. S., Harris, N. L., Brown, S., Lefsky, M., Mitchard, E. T., Salas, W., ...&Petrova, S. (2011). Benchmark map of forest carbon stocks in tropical regions across three continents. *Proceedings of the National Academy of Sciences*, *108*(24), 9899-9904.

[190] Sampson, P. H., Zarco-Tejada, P. J., Mohammed, G. H., Miller, J. R., & Noland, T. L. (2003). Hyperspectral remote sensing of forest condition: Estimating chlorophyll content in tolerant hardwoods. *Forest science*, *49*(3), 381-391.

[191] Schutz, B. E., Zwally, H. J., Shuman, C. A., Hancock, D., & DiMarzio, J. P. (2005). Overview of the ICESat mission. *Geophysical Research Letters*, *32*(21).

[192] Seidel, D., Fleck, S., & Leuschner, C. (2012). Analyzing forest canopies with ground-based laser scanning: a comparison with hemispherical photography. *Agricultural and Forest Meteorology*, *154*, 1-8.

[193] Simard, M., Pinto, N., Fisher, J. B., & Baccini, A. (2011). Mapping forest canopy height globally with spaceborne lidar. *Journal of Geophysical Research: Biogeosciences*, *116*(G4).

[194] Singh, J. S., Lauenroth, W. K., & Steinhorst, R. K. (1975). Review and assessment of various techniques for estimating net aerial primary production in grasslands from harvest data. *The Botanical Review*, 41(2), 181-232.

[195] Sripada, R. P. (2005). Determining In-Season Nitrogen Requirements for Corn Using Aerial Color-Infrared Photography.

[196] Sripada, R. P., Heiniger, R. W., White, J. G., & Meijer, A. D. (2006). Aerial color infrared photography for determining early in-season nitrogen requirements in corn. *Agronomy Journal*, *98*(4), 968-977.

[197] Sukumar, R., Dattaraja, H. S., Suresh, H. S., Radhakrishnan, J., Vasudeva, R., & Nirmala, S. (1992). Long-term monitoring of vegetation in a tropical. *Current Science*, *62*(9), 608-616.

[198] Sukumar, R., Suresh, H. S., Dattaraja, H. S., John, R., & Joshi, N. V. (2004). Mudumalai forest dynamics plot, India.

[199] Sullivan, M. J., Lewis, S. L., Hubau, W., Qie, L., Baker, T. R., Banin, L. F., ... & Arets, E. (2018). Field methods for sampling tree height for tropical forest biomass estimation. *Methods in Ecology and Evolution*, 9(5), 1179-1189.

[200] Sun, G., Ranson, K. J., Kimes, D. S., Blair, J. B., & Kovacs, K. (2008). Forest vertical structure from GLAS: An evaluation using LVIS and SRTM data. *Remote Sensing of Environment*, *112*(1), 107-117.

[201] Sun, X., Abshire, J. B., Riris, H., McGarry, J., & Sirota, M. (2004, December). Geoscience Laser Altimeter System (GLAS) on the ICESat Mission: Science measurement performance since launch. In *AGU Fall Meeting Abstracts*.

[202] Suresh, H. S., Dattaraja, H. S., & Sukumar, R. (1996). Tree flora of Mudumalai Sanctuary, Tamil Nadu, Southern India. *Indian Forester*, *122*(6), 507-519.

[203] Suresh, H. S., Dattaraja, H. S., & Sukumar, R. (2010). Relationship between annual rainfall and tree mortality in a tropical dry forest: results of a 19-year study at Mudumalai, southern India. *Forest Ecology and Management*, *259*(4), 762-769.

[204] Takeda, T., Oguma, H., Sano, T., Yone, Y., & Fujinuma, Y. (2008). Estimating the plant area density of a Japanese larch (Larix kaempferi Sarg.) plantation using a ground-based laser scanner. *Agricultural and Forest Meteorology*, *148*(3), 428-438.

[205] Tao, S., Guo, Q., Li, C., Wang, Z., & Fang, J. (2016). Global patterns and determinants of forest canopy height. *Ecology*, *97*(12), 3265-3270.

[206] Timothy, D., Onisimo, M., & Riyad, I. (2016). Quantifying aboveground biomass in African environments: A review of the trade-offs between sensor estimation accuracy and costs. *Tropical Ecology*, *57*(3), 393-405.

[207] Tomppo, E., Gschwantner, T., Lawrence, M., McRoberts, R. E., Gabler, K., Schadauer, K., ... & Cienciala, E. (2010). National forest inventories. *Pathways for Common Reporting. European Science Foundation*, 541-553.

[208] Tong, Q., Xue, Y., & Zhang, L. (2014). Progress in hyperspectral remote sensing science and technology in China over the past three decades. *IEEE Journal of Selected Topics in Applied Earth Observations and Remote Sensing*, *7*(1), 70-91.

[209] Townsend, P. A., Foster, J. R., Chastain, R. A., & Currie, W. S. (2003). Application of imaging spectroscopy to mapping canopy nitrogen in the forests of the central Appalachian Mountains using Hyperion and AVIRIS. *IEEE Transactions on Geoscience and Remote Sensing*, *41*(6), 1347-1354.

[210] Trochta, J., Krůček, M., Vrška, T., & Král, K. (2017). 3D Forest: An application for descriptions of three-dimensional forest structures using terrestrial LiDAR. *PloS one*, *12*(5), e0176871.

[211] Tucker, C. J. (1979). Red and photographic infrared linear combinations for monitoring vegetation. *Remote sensing of Environment*, *8*(2), 127-150.

[212] Turner, D. P., Cohen, W. B., Kennedy, R. E., Fassnacht, K. S., & Briggs, J. M. (1999). Relationships between leaf area index and Landsat TM spectral vegetation indices across three temperate zone sites. *Remote sensing of environment*, 70(1), 52-68.

[213] Van Laar, A., & Akça, A. (2007). *Forest mensuration* (Vol. 13). Springer Science & Business Media.

[214] Vandermeer, J. (1995). The ecological basis of alternative agriculture. *Annual Review of Ecology and Systematics*, *26*(1), 201-224.

[215] Vashum, K. T., & Jayakumar, S. (2012). Methods to estimate above-ground biomass and carbon stock in natural forests-A review. *J. Ecosyst. Ecogr*, *2*(4), 1-7.

[216] Wang, Q., Adiku, S., Tenhunen, J., & Granier, A. (2005). On the relationship of NDVI with leaf area index in a deciduous forest site. *Remote sensing of environment*, *94*(2), 244-255.

[217] Wang, L., & Dessler, A. E. (2006). Instantaneous cloud overlap statistics in the tropical area revealed by ICESat/GLAS data. *Geophysical research letters*, *33*(15).

[218] Wang, L., Hunt Jr, E. R., Qu, J. J., Hao, X., & Daughtry, C. S. (2013). Remote sensing of fuel moisture content from ratios of narrow-band vegetation water and dry-matter indices. *Remote Sensing of Environment*, *129*, 103-110.

[219] Wang, L., Sousa, W. P., & Gong, P. (2004). Integration of object-based and pixel-based classification for mapping mangroves with

IKONOS imagery. *International Journal of Remote Sensing*, *25*(24), 5655-5668.

[220] Wang, W., Zhao, W., Huang, L., Vimarlund, V., & Wang, Z. (2014). Applications of terrestrial laser scanning for tunnels: a review. *Journal of Traffic and Transportation Engineering (English Edition)*, *1*(5), 325-337.

[221] Wang, X., Cheng, X., Gong, P., Huang, H., Li, Z., & Li, X. (2011). Earth science applications of ICESat/GLAS: a review. *International Journal of Remote Sensing*, *32*(23), 8837-8864.

[222] Wang, Y., Li, G., Ding, J., Guo, Z., Tang, S., Wang, C., ... & Chen, J. M. (2016). A combined GLAS and MODIS estimation of the global distribution of mean forest canopy height. *Remote Sensing of Environment*, *174*, 24-43.

[223] Wang, Z., Skidmore, A. K., Darvishzadeh, R., & Wang, T. (2018). Mapping forest canopy nitrogen content by inversion of coupled leaf-canopy radiative transfer models from airborne hyperspectral imagery. *Agricultural and forest meteorology*, *253*, 247-260.

[224] Waring, R. H., Way, J., Hunt, E. R., Morrissey, L., Ranson, K. J., Weishampel, J. F., ... & Franklin, S. E. (1995). Imaging radar for ecosystem studies. *BioScience*, *45*(10), 715-723.

[225] Watson, D. J. (1947). Comparative physiological studies on the growth of field crops: I. Variation in net assimilation rate and leaf area between species and varieties, and within and between years. *Annals of botany*, *11*(41), 41-76.

[226] Weaver, S. A., Ucar, Z., Bettinger, P., Merry, K., Faw, K., & Cieszewski, C. J. (2015). Assessing the accuracy of tree diameter measurements collected at a distance. Croatian Journal of Forest Engineering: *Journal for Theory and Application of Forestry Engineering*, 36(1), 73-83.

[227] Wehr, A., & Lohr, U. (1999). Airborne laser scanning—an introduction and overview. *ISPRS Journal of photogrammetry and remote sensing*, *54*(2), 68-82.

[228] Weiss, M., Baret, F., Smith, G. J., Jonckheere, I., & Coppin, P. (2004). Review of methods for in situ leaf area index (LAI) determination: Part II. Estimation of LAI, errors and sampling. *Agricultural and forest meteorology*, *121*(1-2), 37-53.

[229] White, J. C., Coops, N. C., Wulder, M. A., Vastaranta, M., Hilker, T., & Tompalski, P. (2016). Remote sensing technologies for enhancing forest inventories: A review. *Canadian Journal of Remote Sensing*, 42(5), 619-641.

[230] Wilson, J. W. (1965). Stand structure and light penetration. I. Analysis by point quadrats. *Journal of applied Ecology*, 383-390.

[231] Wu, Z., Dye, D., Vogel, J., & Middleton, B. (2016). Estimating forest and woodland aboveground biomass using active and passive remote sensing. *Photogrammetric Engineering & Remote Sensing*, *82*(4), 271-281.

[232] Wulder, M. (1998). Optical remote-sensing techniques for the assessment of forest inventory and biophysical parameters. *Progress in physical Geography*, 22(4), 449-476.

[233] Wulder, M. A., & Seemann, D. (2003). Forest inventory height update through the integration of lidar data with segmented Landsat imagery. *Canadian journal of remote sensing*, *29*(5), 536-543.

[234] Wulder, M. A., Bater, C. W., Coops, N. C., Hilker, T., & White, J. C. (2008). The role of LiDAR in sustainable forest management. *The Forestry Chronicle*, *84*(6), 807-826.

[235] Wulder, M. A., Han, T., White, J. C., Sweda, T., & Tsuzuki, H. (2007). Integrating profiling LIDAR with Landsat data for regional boreal forest canopy attribute estimation and change characterization. *Remote Sensing of Environment*, *110*(1), 123-137.

[236] Xu, Y., Hoegner, L., Tuttas, S., & Stilla, U. (2017). VOXEL-AND GRAPH-BASED POINT CLOUD SEGMENTATION OF 3D SCENES USING PERCEPTUAL GROUPING LAWS. *ISPRS Annals of Photogrammetry, Remote Sensing & Spatial Information Sciences*, *4*.

[237] Yang, B., Dai, W., Dong, Z., & Liu, Y. (2016). Automatic forest mapping at individual tree levels from terrestrial laser scanning point clouds with a hierarchical minimum cut method. *Remote Sensing*, *8*(5), 372.

[238] Yoda, K., Suzuki, M., & Suzuki, H. (2000). Development and evaluation of a new type of opto-electronic dendrometer. *IAWA Journal*, *21*(4), 425-434.

[239] Young, B., Evans, D. L., & Parker, R. C. (2000, January). Methods for comparison of lidar and field measurements of loblolly pine. In *Proceedings of the Second International Conference: Geospatial Information in Agriculture and Forestry* (pp. 10-12).

[240] Young, M. (1986). Optics and lasers: Including fiber optics and optical waveguides.

[241] Yu, Y., Yang, X., & Fan, W. (2015). Estimates of forest structure parameters from GLAS data and multi-angle imaging spectrometer data. *International Journal of Applied Earth Observation and Geoinformation*, *38*, 65-71.

[242] Zarco-Tejada, P. J., Miller, J. R., Mohammed, G. H., Noland, T. L., & Sampson, P. H. (1999). Canopy optical indices from infinite reflectance and canopy reflectance models for forest condition monitoring: Application to hyperspectral CASI data. In *Geoscience and Remote Sensing Symposium, 1999. IGARSS'99 Proceedings. IEEE 1999 International* (Vol. 3, pp. 1878-1881). IEEE.

[243] Zhang, K., Chen, S. C., Whitman, D., Shyu, M. L., Yan, J., & Zhang, C. (2003). A progressive morphological filter for removing nonground measurements from airborne LIDAR data. *IEEE transactions on geoscience and remote sensing*, *41*(4), 872-882.

[244] Zhang, W., Qi, J., Wan, P., Wang, H., Xie, D., Wang, X., & Yan, G. (2016). An easy-to-use airborne LiDAR data filtering method based on cloth simulation. *Remote Sensing*, *8*(6), 501.

[245] Zhang, Z., Ni, W., Fu, A., Guo, Z., Sun, G., & Wang, D. (2008). Estimation of forest structural parameters from Lidar and SAR data. *Int Arch Photogramm, Remote Sens Spat Inf Sci*, *37*, 1121-1126.

[246] Zheng, G., & Moskal, L. M. (2012). Leaf orientation retrieval from terrestrial laser scanning (TLS) data. *IEEE Transactions on Geoscience and Remote Sensing*, *50*(10), 3970-3979.

[247] Zheng, G., Moskal, L. M., & Kim, S. H. (2013). Retrieval of Effective Leaf Area Index in Heterogeneous Forests With Terrestrial Laser Scanning. *IEEE Trans. Geoscience and Remote Sensing*, *51*(2), 777-786.

[248] Zimble, D. A., Evans, D. L., Carlson, G. C., Parker, R. C., Grado, S. C., & Gerard, P. D. (2003). Characterizing vertical forest structure using small-footprint airborne LiDAR. *Remote sensing of Environment*, *87*(2-3), 171-182.

[249] Zwally, H. J., Schutz, B., Abdalati, W., Abshire, J., Bentley, C., Brenner, A., ... & Herring, T. (2002). ICESat's laser measurements of polar ice, atmosphere, ocean, and land. *Journal of Geodynamics*, *34*(3), 405-445.

[250] Zwally, H. J., Schutz, R., Bentley, C., Bufton, J., Herring, T., Minster, J., ... & Thomas, R. (2010). GLAS/ICESat L2 Antarctic and Greenland ice sheet altimetry data V031. *National Snow and Ice Data Center, Boulder, Colorado*.

******

LIST OF PUBLICATION

[1] Indu Indirabai, M V Harindranathan Nair, Jaishankar R. Nair, and Rama Rao Nidamanuri, "Estimation of Biomass and Leaf Area Index in the Western Ghats Forest Ecosystem by the Integrated Analysis of Hyperspectral Data and Space Borne LiDAR Data", *Journal of Geography, Environment and Earth Science International*, Vol.19 No.4 (2019), pp. 1-12.

[2] Indu Indirabai, M V Harindranathan Nair, Jaishankar R. Nair, and Rama Rao Nidamanuri, "Estimation of Vegetation Indices and Biomass by the Fusion of LiDAR Data and Landsat Images in Mudumalai Forests of the Western Ghats, India", *International Journal of Applied Engineering Research*, Volume 13, Number 3 (2018) Spl, pp. 56-62.

[3] Indu Indirabai, M V Harindranathan Nair, Jaishankar R. Nair, and Rama Rao Nidamanuri, "Biophysical Characterisation of Heterogeneous Forest and Phenological Study In Western Ghats of India by the Integration of Sentinel-2 Data with Space Borne Lidar Data", *Journal of Emerging Technologies and Innovative Research* Vol.6, Issue 3, (2019), pp.768-777.

[4] Indu Indirabai, M V Harindranathan Nair, Jaishankar R. Nair, and Rama Rao Nidamanuri, "Optical Remote Sensing for Biophysical Characterisation in Forests: A Review", *International Journal of Applied Engineering Research*, ISSN 0973-4562, Volume 14, Number 2 (2019) pp. 344-354

[5] Indu Indirabai, M V Harindranathan Nair, Jaishankar R. Nair, and Rama Rao Nidamanuri, "Forest Measurements Using ICESat-Geoscience Laser Altimeter System- A Review", *International Journal of Research in Advent Technology*, Vol.6, No.12 (2018), pp. 3700-3776.

Papers Currently Under Peer Review

[1] Terrestrial Laser Scanner based 3D Reconstruction of Trees and Retrieval of Leaf Area Index in a Forest Environment. *(Ecological informatics by Elsevier Publications).*

[2] Biophysical Characterization of Forests in Western Ghats of India by Integration of Space-borne LiDAR and Multispectral Remote Sensing *(Egyptian journal of remote sensing by Elsevier Publications).*

[3] Estimation of Forest Canopy Height using ICESat/GLAS-Space Borne Laser Altimetry Data in the Western Ghats Region of India *(Journal of Geovisualization and Spatial Analysis by Springer Publications).*

[4] Direct Estimation of Leaf Area Index of Tropical Forests using Terrestrial Laser Scanner LiDAR Point Cloud *(Remote sensing of Environment by Elsevier Publications).*

Paper Presentation in Conferences:

[1] Estimation of Vegetation Indices and Biomass by the fusion of LiDAR data and Landsat Images in Mudumalai Forest of Western Ghats, India", at *International Conference on Science and Technology (ICST 2018), 23-25 April 2018, Cochin University of Science and Technology, Kochi, Kerala, India*.

[2] Three-Dimensional Reconstruction of Trees and Direct Estimation of Leaf Area Index of a Tropical Forest Using Terrestrial Laser Scanner LiDAR Point Cloud" in *31st Kerala Science Congress, 02-03 February 2019, Fatima Mata National College, Kollam, Kerala, India.* (Shortlisted for the Best Paper Award Category in Environmental Science, Forestry & Wildlife).

[3] "Three-Dimensional Urban Building Detection using LiDAR data" using point cloud library and visual studio C++" in *Imaging & Geospatial Technology Forum (IGTF) 2016 American Society for Photogrammetry & Remote Sensing (ASPRS) Conference and Co-Located JACIE Workshop, 11-15 April 2016, Fort Worth, Texas, USA.*

Paper published in Conference Proceedings:

[1] Full paper entitled "Three Dimensional Urban Building Detection using Lidar data" using point cloud library and visual studio C++" in the *Proceedings of the Imaging & Geospatial Technology Forum (IGTF) 2016 American Society for Photogrammetry & Remote Sensing (ASPRS) Conference and Co-Located JACIE Workshop, 11-15 April 2016, Fort Worth, Texas, USA.*

[2] Abstract of the paper entitled" Three-Dimensional Reconstruction of Trees And Direct Estimation of Leaf Area Index of A Tropical Forest Using Terrestrial Laser Scanner Lidar Point Cloud" published in the *Proceedings of the 31st Kerala Science Congress, 02-03 February, 2019, pp.108-109.*

******